ORIGIN AND FATE OF RADIUM IN FLOWBACK AND PRODUCED WATER FROM MARCELLUS SHALE GAS EXPLORATION

by

Tieyuan Zhang

Bachelor of Engineering in Environmental Engineering, Guangzhou University, 2010

Master of Science in Civil Engineering, University of Pittsburgh, 2012

Submitted to the Graduate Faculty of

Swanson School of Engineering in partial fulfillment

of the requirements for the degree of

Doctor of Philosophy

University of Pittsburgh

2015

UNIVERSITY OF PITTSBURGH

SWANSON SCHOOL OF ENGINEERING

This dissertation was presented

by

Tieyuan Zhang

It was defended on

April 1, 2015

and approved by

Radisav D. Vidic, Ph.D., Professor, Civil and Environmental Engineering Department

Kyle J. Bibby, Ph.D., Assistant Professor, Civil and Environmental Engineering Department

Leonard W. Casson, Ph.D., Associate Professor, Civil and Environmental Engineering Department

Kelvin B. Gregory, Ph.D., Associate professor, Civil and Environmental Engineering Department (CMU)

Daniel J. Bain, Ph.D., Assistant Professor, Geology and Planetary Science Department

Dissertation Director: Radisav D. Vidic, Ph.D., Professor

ORIGIN AND FATE OF RADIUM IN FLOWBACK AND PRODUCED WATER FROM MARCELLUS SHALE GAS EXPLORATION

Tieyuan Zhang, Ph.D.

University of Pittsburgh, 2015

Marcellus Shale is one of the world's largest unconventional gas resources. Recent developments in horizontal drilling and hydraulic fracturing enabled efficient and economical extraction of natural gas from unconventional (shale) resources and have led to rapid expansion of natural gas production in the United States. Hydrofracturing generates large volume of flowback and produced water that contains high concentrations of total dissolved solids (TDS), heavy metals, and naturally occurring radioactive materials (NORMs) resulting in significant environmental and public concerns and challenging waste management issues. Ra-226 is the dominant form of NORM and is one of the key challenges for sustainable management of Marcellus Shale wastewater.

This study is focused on the life cycle of NORMs during natural gas extraction from Marcellus Shale. A rapid method for Ra-226 analysis by inductively coupled plasma mass spectrometry (ICP-MS) was developed to overcome some of the shortcomings of current analytical techniques (e.g., long detection time). The fate of Ra-226 under different scenarios associated with the shale gas extraction, including origin of Ra-226, partitioning in flowback water storage and treatment facilities, and associated solid waste disposal issues were evaluated in this study. This study showed that radium mainly originates from relative rapid shale leaching. High concentration of radium in the Marcellus Shale wastewater can be managed by proper

treatment (e.g., sulfate precipitation). However, solid waste generated from treatment facilities or impoundments containing elevated radium concentrations far exceed the limits for disposal in the Resource Conservation and Recovery Act Subtitle D (RCRA-D) landfills. Current practice in landfill management allows the disposal of this solid waste by controlling the Allowed Source Term Loading (ALST) on annual basis. However, if the landfill capacity to accept all the NORM generated from Marcellus Shale gas extraction becomes insufficient, other disposal or beneficial use options for solid waste should be developed. Reuse of radium enriched barite as weighting agent in drilling mud might be a sustainable strategy to reduce the mass of NORM that has to be disposed in the landfills.

Health risks associated with NORMs were evaluated for several typical scenarios associated with Marcellus Shale gas extraction. Total effective dose equivalent (TEDE) at drilling pads, storage impoundments and landfills are well below the Nuclear Regulatory Commission (NRC) limit for the general public of 100 mrem/yr even under the worst-case scenario assumptions. Workers in the centralized waste treatment facilities might receive excessive TEDE and appropriate measures recommended by NRC should be applied. For example, a safe distance of 5 m is recommended to reduce TEDE to acceptable level. Hence, the key environmental and public health risks associated with NORM brought to the surface by natural gas extraction from Marcellus Shale are from the spills that may contaminate surface and groundwater.

Overall, this study contributes to the understanding of the fate of NORMs associated with Marcellus Shale gas wastewater management and expands the ability to resolve the environmental concerns associate with NORMs. A novel rapid analytical for Ra-226 measurement by ICP-MS offers an alternative for researchers to quickly analyze environmental

samples. The fate of Ra-226 in centralized treatment facilities and storage facilities is important for operators to choose proper management strategy for liquid and solid waste disposal/reuse. The health risk associated with NORM that is assessed in this study will help to resolve the public concern stemming from the high NORM extracted from Marcellus Shale play and provides several options to further reduced its risks.

TABLE OF CONTENTS

LIST OF TABLES

LIST OF FIGURES

PREFACE

This work was performed as part of the National Energy Technology Laboratory's Regional University Alliance (NETL-RUA), a collaborative initiative of the NETL, under the RES contract RES1000027 156. I am very grateful to all the sponsors.

I would like to express my sincere gratitude to my advisor and mentor, Professor Radisav Vidic, for giving me the opportunity to work on such an exciting and profoundly important research project. His enthusiasm, innovative ideas and immense knowledge provided the foundation of this research. My doctoral studies under his direction have been an unforgettable experience and will be priceless assets for me to guide my future professional career and personal life.

I would also like to thank my Ph.D. committee members: Professor Kyle J. Bibby, Leonard W. Casson, Kelvin B. Gregory, and Daniel J. Bain, who shared their precious knowledge and insights regarding the academic research and personal professional development. Professor Bibby and professor Casson have urged me to think about how to fit my study in a boarder field of engineering application. It has been very useful in enhance the quality of this study. Professor Gregory is experienced in treatment of radionuclides and provided very valuable opinions about the methodologies of research. Professor Bain is experienced in trace element analysis and provided helps on radionuclides measurements and element purification techniques.

I am grateful to work with my inspired and diligent colleagues: Dr. Wenshi Liu, Dr. Shi-Hsisang Chien, Dr. Elise Barbot, Can He, Yang Li, Li Chen, Xin Zhao, Meng Li, Xuan Zheng, and Wenjing Cheng. I won't forget the days and nights we spent together to pursue the truth.

I want to give special thanks to my friends Dun Mao, Heng Tang, Ziqi Liu, Xiaozhuo Lv, Xiaotian Chen, Guoqing Liu, Peixiao Liu, Huiqi Deng, Zichang Li, Cheng Fang, Siyu Li, Nian Tong, Lu Tan, Huacheng Wang and Jingjing Duan. They make my life colorful and remind me to hold my aspiration and make a difference.

Finally, I would like to thank my parents Lin Zhang and Yulian Song. Their unconditional love, care and support are the most important asset to me.

To Them I dedicate

The Ones who helped me

My Parents, Lin Zhang and Yulian Song

1.0 INTRODUCTION

The increased energy consumption along with demand for cleaner energy drives markets towards natural gas. Due to its abundance and relatively low cost, natural gas is an attractive fuel for new electricity generation and transportation. The US Energy Information Administration (US EIA) predicts that natural gas would surpass coal as the nation's largest source of energy for electricity generation.[1] The growth of domestic natural gas production is one of the key factors reshaping the U.S. energy picture that will boost industrial production.

Natural gas exists in both conventional and unconventional geological formations. Conventional oil and gas reservoirs are stratigraphic traps that are caused by folding and/or faulting of sedimentary layers. Natural gas, crude oil, and water or brines are preserved inside the arch in different layers.[2] In the unconventional gas reservoirs, however, a geological folding and/or faulting of sedimentary layers are not necessary. Natural gas is stored inside the source rock (e.g., shale), which is essentially impermeable and, as a consequence, more difficult to produce gas from.[3] Due to the low permeabilities of reservoir formation, natural gas stored in unconventional formations was considered uneconomical to produce.[4] In early 21th century, the breakthroughs in directional well drilling and reservoir stimulation enabled profitable extraction of natural gas from unconventional reservoirs. The US EIA estimated the technically recoverable unconventional gas resources in the continental US at 750 trillion cubic feet (Tcf). Shale gas production is projected to increase from 9.7 Tcf in 2012 to 19.8 Tcf in 2040, which accounts for

40% and 53% of total US natural gas production, respectively.[1] Marcellus Shale is one of the largest unconventional gas reservoirs in the US containing 141 Tcf of unproved technically recoverable natural gas.[5]

The directional drilling and hydraulic fracturing are the two key technologies to allow economical recovery of natural gas from tight shale formations. Hydraulic fracturing or fracking of a typical horizontal shale gas wells requires between 4-6 million gallons of water that is mixed with proppant (commonly, sand) and chemicals before injection into the well under high pressure (7,000-12,000 psi) to open the existing fractures or initiate new fractures. After hydraulic fracturing is completed, approximately 10% to 30% of the fracturing fluid can be recovered as flowback water in the first 2-3 weeks following well completion. Once the well is connected to the gas pipeline, produced water continues to be generated at a rate of 200-1,000 gal/day throughout the life of the well.[6,7] The flowback and produced water generated from Marcellus Shale gas exploration contain high concentrations of salts, heavy metals, and Naturally Occurring Radioactive Materials (NORM).[6-8]

1.1 PROBLEM IDENTIFICATION

Stratigraphically, Marcellus Shale is the lowest unit of the Devonian age Hamilton Group and is mainly composed of black shale, which has a relatively high content of organic matter.[8] Black shales typically contain much more uranium (U) than other common sedimentary rocks because uranium is retained and even concentrated in the organic matter and iron sulfide in the black shale.[9] The dominant uranium forms that are stable in geologic environment are the uranous (U^{4+}) and uranyl (U^{6+}, UO_2^{2+}) ions; the former is significantly less soluble than the latter,

whereas the latter can form numerous complexes.[10] Thus, in the reduced state, such as in deep shales, U^{4+} is the main form of uranium, which is essentially insoluble in water. Thorium (Th) is a particle reactive element and tends to adsorb on particulate matter, such as the sedimentary rock (e.g., shale).[11]

Ra-226 and Ra-228 are formed by natural decay of U-238 and Th-232, respectively, and may remain within the original host mineral or other solid phases or may be released into the adjacent pore water and into the flowback and produced water. Ra-226 is the predominant radium isotope with a long half-life (1,600 years), yielding extended activity when brought to the surface. Therefore, Ra-226 is an important proxy for the radioactivity of waste streams produced during unconventional gas production. Ra-226 activity in Marcellus Shale produced water ranges from several hundred to tens of thousands pCi/L with a median of 5,350 pCi/L and generally shows positive correlation with total dissolved solid (TDS) and barium content despite the differences in reservoir lithologies.[7,12] In comparison, Ra-226 limit for drinking water and industrial effluent is 5 and 60 pCi/L, respectively.[13] Oral radium uptakes can cause calcium substitution in bones and continuous alpha and gamma emissions, resulting in increased long-term human health risks.[14,15]

Fate of Ra-226 in different scenarios relevant to Marcellus Shale gas extraction was studied because of its potential environmental and public health impacts. Those scenarios include the underground shale gas reservoir, flowback water storage facilities, flowback water treatment facilities, and solid waste disposal facilities. Furthermore, the radiation health risk associated with NORMs, which is expressed as Total Effective Dose Equivalent (TEDE), was evaluated for several typical scenarios associated with Marcellus Shale gas exploration. This study contributes to informed decision making for flowback/produced water management strategies and

radioactive solid waste management. The extrapolation of this work is relevant to the environmental concerns regarding radium during hydraulic fracturing.

1.2 RESEARCH OBJECTIVES

This study aims to investigate the life cycle of Naturally Occurring Radioactive Materials during Marcellus Shale gas extraction. Fate of Ra-226, which is the dominant radionuclide in Marcellus shale flowback and produced water, in different scenarios associated with the shale gas exploration was studied. Those scenarios include the underground shale gas reservoir, flowback water storage facilities, flowback water treatment facilities, and solid waste disposal facilities. Radium-226 is a trace element, and its concentration in flowback water ranges from several hundred to several thousand pCi/L (i.e., 1 - 10 ppt). Traditional methods for Ra-226 determination require either a long sample holding time or a long detection time and are frequently unavailable in environmental laboratories. Thus a rapid method for determination of Ra-226 by ICP-MS was developed in this study. In addition, the health risks associated with NORMs, which is expressed as Total Effective Dose Equivalent (TEDE), was evaluated for several typical scenarios associated with Marcellus Shale gas exploration. This dissertation incorporates four journal manuscripts and is presented in seven chapters. The objectives of this study are accomplished through five specific tasks.

Task 1 (Chapter 2): Understand the origin of key ions, including Ra-226, in flowback and produced water

This task is focused on elucidating the geochemical process that contribute the elevated salinity, divalent cations, and naturally occurring radioactive materials (NORMs) in Marcellus Shale flowback and produced water. It has been argued that there are two possible pathways towards elevated TDS in Marcellus Shale flowback and produced water: One possible source of dissolved solids are the formation brines that exist in target (Marcellus Shale) or adjacent formations (e.g., Onondaga Limestone) and the other one is the dissolution of the shale itself. In order to answer this question, characteristics of Marcellus Shale flowback and produced waters are compared with the concentrated seawater to interpret whether the target ions originated from concentrated seawater. In addition, a novel isotopic tracing with a combination of Ra-228:Ra-226 and Th-228:Ra-228 ratios was developed to estimate the residence time of radium isotopes in the liquid phase, which can indicate whether the shale leaching or dissolution is the source of NORM.

Task 2 (Chapter 3): Develop a rapid method for Ra-226 measurement by ICP-MS

Measurement of trace amounts of radionuclide is one of the biggest challenges for this study. Traditional methods for Ra-226 determination require either a long sample holding time or a long detection time. Recent developments in the ICP-MS or TIMS enables direct measurement of mass to charge ratio and could be used for rapid Ra-226 measurement. Produced water samples cannot be analyzed directly by ICP-MS due to high ionic strength (1 to 3 M) and high concentration of matrix elements (e.g., Ba^{2+}, Sr^{2+}) that would interfere with the ICP-MS measurement for Ra-226. To minimize signal drift and matrix suppression, Radium needs to be purified prior to measurement. A purification method was developed in this study for accurate and robust measurement of Ra-226 by ICP-MS.

Task 3 (Chapter 4): Investigate the fate of Ra-226 in flowback water treatment facilities

The objective of this task is to investigate the fate of Radium during sulfate precipitation, which is a common method for flowback water treatment in either mobile or centralized treatment facilities. During sulfate precipitation, it is less likely to observe pure $RaSO_4$ precipitates because Ra^{2+} concentrations are too low to reach saturation limit ($K_{sp,RaSO4} = 10^{-10.38}$). However, it is common for Ra^{2+} to co-precipitate with carrier metals. Radium removal in Ba-Sr-SO_4 co-precipitation system at different ionic strength was evaluated, and the main carrier for Radium during sulfate precipitation was identified. The outcome of this work provides fundamental understanding of the co-precipitation of Ra with $BaSO_4$ and $SrSO_4$ with implications for sustainable management of flowback water. Potential risk associated with the solid waste containing elevated Ra levels generated by these treatment facilities was also discussed in this study.

Task 4 (Chapter 5): Investigate the fate of Ra-226 in centralized storage facilities

This task is aimed to evaluate the fate of Ra-226 during flowback water storage in centralized facilities. Ra-226 content in both wastewater and sludge phase was tracked over a 2.5-year period. Results of Sequential Extraction Procedure and sludge chemical composition analysis were compared to understand the partition of Ra-226 into the solid phase. Toxicity Characteristic Leaching Procedure (TCLP) was conducted to determine the fate of radioactive sludge in the solid waste landfills. The outcome of this task provides information about the fate of Ra-226 during flowback water storage and potential hazards associated with solid waste management.

Task 5 (Chapter 6): Evaluate the health risks associated with NORMs generated by Marcellus Shale gas extraction

This chapter investigates the health risks from NORM for on-site workers under typical scenarios associated with Marcellus Shale gas extraction. Total Effective Dose Equivalent (TEDE), with a unit of Roentgen equivalent man (REM), representing the stochastic biological effects of ionizing radiation, was used to quantify the health risks in unconventional gas industry. The calculations were performed using the RESidual RADioactivity (RESRAD) model and typical conditions relevant to gas extraction from Marcellus Shale. The outcome of this task addresses the public health concern related to NORMs generated by unconventional gas industry and provides realistic information about TEDE for on-site workers in different scenarios. Several cost-effective alternatives that minimize TEDE were recommended.

2.0 ORIGIN OF KEY COMPONENTS AND RADIOACTIVITY AND FATE OF RA-226 IN FLOWBACK AND PRODUCED WATER

This chapter, written by Tieyuan Zhang and coauthored by Can He, Richard W. Hammack, and Radisav D. Vidic, will be submitted for publication.

Development of unconventional shale gas in Marcellus Shale region has generated large quantities of high salinity wastewater. While the wastewater treatment technologies for the Marcellus produced water have been intensively studied, the origin of elevated salinity and its key components (e.g., Cl^-, Ca^{2+}, Ba^{2+} and Ra^{2+}) is still not clear. This study summarizes current debate about the origin of salinity in produced water and focuses on elucidating the geochemical processes that contribute major monovalent and divalent cations, and naturally occurring radioactive materials (NORMs) in Marcellus Shale produced water. Results show that the major monovalent (e.g., Cl, Na) and divalent ions (e.g., Ca, Mg) in the produced water originated from the mixing of the fracking fluid with ancient connate water. A novel isotopic tracing based on Ra-228:Ra-226 and Th-228:Ra-228 ratios was developed to estimate the residence time of NORM in the liquid phase. This study shows that the mean residence time of radium in liquid phase is between 0.4-6 years. The relatively short residence time of Ra isotopes in the Marcellus Shale produced water suggests that shale core leaching is the dominant source over mixing with connate water.

2.1 INTRODUCTION

Conventional oil and gas reservoirs are stratigraphic traps that are caused by folding and/or faulting of sedimentary layers. Natural gas, crude oil, and water or brines are preserved inside the arch in different layers. In the unconventional gas reservoir; however, a geological folding and/or faulting of sedimentary layers are not necessary. Natural gas is stored inside the source rock (e.g., shale), which has since become impermeable and, as a consequence, more difficult to produce.[1] The hydrocarbon reserves inside the source rock (or in the unconventional gas reservoir) are economically recovered because of the development of the combination of horizontal drilling and hydraulic fracturing. During the hydraulic fracturing, large quantities of produced water are generated, raising significant environmental concerns. The key issues with the produced water are elevated salinity, alkaline earth metals and NORM.[2-5]

A clear understanding of the origin of those key components would help to predict the brine composition at the later stages of gas production and may help to develop economic methods of brine disposal and optimize hydraulic-fracturing process (e.g., modify the fracturing fluid composition to alleviate the shale leaching and shale and pipe scaling). In this study, we summarize the current debate on the origin of salinity in Marcellus Shale produced water and focus on elucidating the geochemical processes that contribute salinity, including divalent cations and radioactive material, to Marcellus Shale produced water. In addition, isotopic dating based on Ra-228:Ra-226 and Th-228:Ra-228 ratios was applied to interpret the mean residence time of Ra in the liquid phase and understand the impact of shale leaching on the quality of produced water.

2.2 METHODS AND DATA SOURCES

Marcellus Shale flowback water samples from three well sites (A, B, and C) in three counties across southwest Pennsylvania have been collected at various times from day 1 to day 30 of the flowback period. One sample of produced water from each well was collected after 2 - 3.5 years of gas production. Wells at Sites A and C were completed with fresh water while the well at Site B was completed with reused flowback water. Samples of flowback and produced water were filtered through a 0.45 μm mixed cellulose ester membrane (MF-Millipore, HAWP) prior to analysis. Bromide, chloride and sulfate measurement were performed using Ion Chromatography System (DIONEX ICS-1100). Major cation analysis was performed using atomic absorption spectrometry (Perkin-Elmer 1000 AAS). Ra-226 activity was measured by Canberra broad energy germanium gamma detector at 186 KeV peak.[6] Th-228 activity was measured by quantifying the activity of Pb-212 after sample was sealed for at least 26 days to build the secular equilibrium while Ra-228 activity was determine based on the activity of Ac-228 after the sample was sealed for at least 1 day.[7] Since the actual sample analysis was performed 1-3 years after sample collection, Ra-228 activity at the time of sample collection ($A_{Ra228,0}$) was determined based on the decay model as described below:

$$A_{Ra228,0} = \frac{A_{Ra228,t}}{e^{-\lambda_{Ra228} \times t}} \quad (2\text{-}1)$$

Where, $A_{Ra228,t}$ is the measured Ra-228 activity, λ is the decay constant, t is the time between sample collection and measurement.

Concentrations of radionuclides collected from two other data sources, including the New York State Department of Environmental Conservation (NYSDEC) analysis of produced water samples from vertical Marcellus wells in southwest New York State[8] and PADEP Bureau of Oil

and Gas management analysis of produced water samples from horizontal Marcellus wells collected across Pennsylvania[9] were used in this study. Two data points showing distinctively low Ra concentration (Ra-226< 1pCi/L) that is not representative of Marcellus Shale produced water were discarded from the analysis.

2.3 RESULTS AND DISCUSSION

2.3.1 Correlation between Marcellus Shale produced water and evaporated seawater

Marcellus shale is the lower part of the middle Devonian black shale, which is formed by marine sedimentation and deposition in the Devonian age (400 million years ago). The warm climate and high sea levels in the Devonian age helped to accumulate massive deposits of organic-rich sediments at the bottom of lakes or oceans. Since the anaerobic bacteria are less efficient consumers of organic matter than aerobic bacteria, the sediments retained much of their organic content.[1,10] Under high temperature and pressure, the organic sediments are converted to oil and gas while the seawater evaporates and the dissolved solids are preserved inside the shale core. The connate water, which is the liquid that is trapped in the pores of sedimentary rocks, is essentially concentrated seawater.[11]

Composition of the connate water is mainly affected by evaporation and mineral precipitation. Evaporation would result in increased salinity of connate water while mineral precipitation would result in a reduced concentration of dissolved solids. Some elements are not involves in precipitation of evaporite minerals and are considered “conservative parameters”. [4, 11-14] Thus, by interpreting the correlations between target ions and conservative parameters in

comparison to the correlations that would be observed during seawater evaporation, it is possible to determine whether the ions of interest originated from the dilution of concentration seawater (i.e., connate water) or from other mechanisms (e.g., sedimentary rock leaching). Since Br is unlikely to precipitate even at high degree of seawater evaporation and would not be incorporated into other minerals, it is conserved during seawater evaporation and has been used as a conservative parameter in this study.

2.3.2 Origin of monovalent ions (Na^+ and Cl^-)

Chloride and sodium are the major monovalent ions in Marcellus Shale produced water (Table 2.1). During the seawater evaporation, both Cl and Br are enriched and the concentration of Cl and Na are proportional with the Br concentration until the saturation of halite (NaCl) is achieved (i.e., slope of Cl:Br during seawater evaporation is equal to 1 until halite starts to precipitate) as shown by the seawater evaporation line in Figure 2.1. When the connate water mixes with fracturing fluid, the concentration of both Cl and Br decreases and their relationship would be parallel with the seawater evaporation line. On the other hand, if the shale leaching, such as dissolution of halite occurs, the Cl:Br ratio would decrease, as shown by the arrow in Figure 2.1. The relationship of Log (Cl) versus conservative Log (Br) for Marcellus produced water samples is compared with seawater evaporation line to examine the origin of chloride (Figure 2.1).[4,15] Results show that Log (Cl) versus Log (Br) for Marcellus Shale produced water samples is parallel with the seawater evaporation with a slope that is close to 1, suggesting that concentrated seawater (i.e., connate water) is a common source of Cl and Br. Correlation of Log (Cl) versus Log (Br) for Marcellus Shale flowback and produced water follows the fresh water dilution line, which suggests that chloride in the produced water is mainly contributed by mixing

of highly concentrated seawater with fracturing fluid.[15, 16] Consequently, dissolution of halite is not likely the dominant source of chloride since the deviation from the seawater line is not observed.

The connate water composition can be further estimated from the correlation between Br and Cl. During seawater concentration, the Br:Cl ratio in connate water follows the seawater evaporation line. In addition, since the Marcellus Shale produced water is a mixture of fracturing fluid and connate water, the Br:Cl ratio in connate water also lies on the frac fluid dilution line. Thus, the intersection of the fresh water dilution line and seawater evaporation line (large hexagon in Figure 2.1) represents the composition of connate water. The intersection derived in this study indicates that the Br concentration in connate water is around 2,000 ppm (50 meq/L), which suggests that seawater was concentrated almost 1,300 times.

Table 2.1 Typical Marcellus Shale produced water characteristics[4]

	Minimum	Maximum	Average	Number of samples
Total dissolved solids (mg/L)	680	345,000	106,390	129
Total suspended solids (mg/L)	4	7,600	352	156
Chemical oxygen demand (mg/L)	195	36,600	15,358	89
Total organic carbon (mg/L)	1.2	1530	160	55
pH	5.1	8.42	6.56	156
Cl (mg/L)	64.2	196,000	57,447	154
Br (mg/L)	0.2	1,990	511	95
Alkalinity (mg/L as $CaCO_3$)	7.5	577	165	144
SO_4 (mg/L)	0	763	71	113
Na (mg/L)	69.2	117,000	24,123	157
Ca (mg/L)	37.8	41,000	7,220	159
Mg (mg/L)	17.3	2,550	632	157
Ba (mg/L)	0.24	13,800	2,224	159
Sr (mg/L)	0.59	8,460	1,695	151
Ra-228 (pCi/L)	0	1,360	120	46
Ra-226 (pCi/L)	2.75	9,280	623	46
U-235 (pCi/L)	0	20	1	14
U-238 (pCi/L)	0	497	42	14

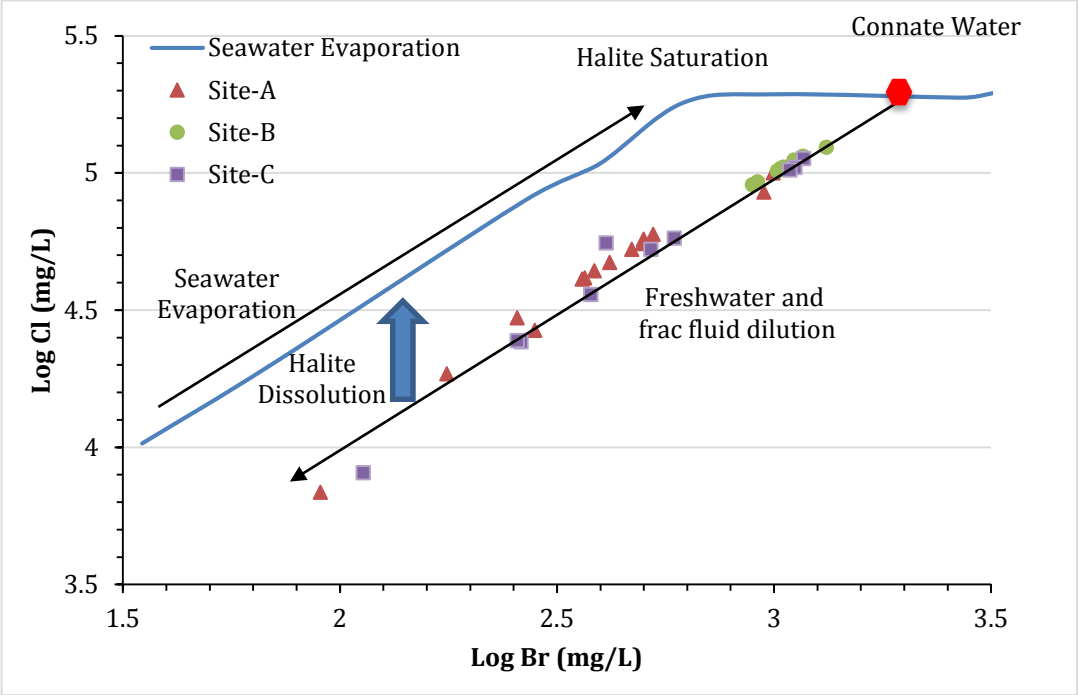

Figure 2.1 Correlation of Log (Cl) versus Log (Br) for Marcellus Shale produced water

2.3.3 Origin of divalent ions (M^{2+}, SO_4^{2-} and CO_3^{2-})

The majority of the wastewater generated from the conventional oil and gas industry is disposed by deep well injection.[17] However, the limited number of underground injection wells in Pennsylvania and the high cost of transporting the wastewater to Ohio or West Virginia limits the disposal of this wastewater by underground injection. As a result, 90% of the produced water generated from Marcellus Shale gas extraction is currently reused for subsequent hydraulic fracturing. The major concern with produced water reuse is its high mineral scaling potential, which is mainly contributed by the divalent ions (i.e., Ca^{2+}, Mg^{2+}, Sr^{2+} and Ba^{2+}). [18] Even though

the divalent ions are not a major contributor of salinity, it is crucial to investigate their origin since mineral scaling can impede gas production by plugging the reservoir or the production pipe. Similar to the analysis of monovalent ions, the origin of divalent ions can be assessed by comparing their concentration in produced water with seawater evaporation line.

During the seawater evaporation, precipitation of alkaline earth metals (i.e. Ca^{2+}, Mg^{2+}, Ba^{2+}, Sr^{2+}) consumes equal molarities of sulfate and carbonate. Thus, the quantity of divalent cations associated with chlorides is constant during the evaporation of seawater to the point of precipitation of carnallite ($KMgCl_3 \cdot 6H_2O$). In other words, the precipitation or dissolution of carbonates, sulfates, and halite does not change MCl_2 defined as:

$$MCl_2 = Ca^{2+} + Mg^{2+} + Sr^{2+} + Ba^{2+} - {SO_4}^{2-} - {CO_3}^{2-} \quad (2\text{-}2)$$

The relationship between the two conservative parameters (i.e., Br (mg/L)), MCl_2 (meq/L)) during seawater evaporation is governed by the following equation:

$$Log(MCl_2) = Log(Br) + 0.011 \quad (2\text{-}3)$$

Previous study has developed the relationship of two conservative compounds (i.e., Br and MCl_2) for conventional oil and gas brines and Marcellus Shale produced water samples in Northeast and Southwest Pennsylvania.[4] The trend for the low salinity produced water samples (i.e., water collected in the early flowback stage) shows moderate deviation from the seawater evaporation line, indicating that the early stage Marcellus Shale produced water is either enriched in Br or depleted in MCl_2 compared to seawater evaporation/dilution line (Figure 2.2a).

Since the leaching/dissolution of divalent ions that associated with Cl would increase the MCl_2 concentration and resulting the lower Br:MCl_2 ratio, Log (Br):Log (MCl_2) ratio would move to the right if leaching of divalent ions from depositional salts or shale occurs. However, Log (Br):Log (MCl_2) ratios of all Marcellus Shale produced water samples lies above the

seawater evaporation line, indicating that leaching of divalent ions is not a major source of divalent cations.

To better understand the mixing of frack fluid and connate water, the relationship between Cl and MCl_2 is plotted in Figure 2.2b. The intersection of seawater evaporation line with frac fluid dilution line was determined based on the connate water Br concentration that was determined from Figure 2.1, where the concentration of Br and Cl is 2,040 and 177,827 mg/L, respectively. Results show the water collected in the early stage is depleted in MCl_2 compared to frack fluid dilution of connate water. However, samples collected at the later stages of gas production show regression towards the frack fluid dilution line. This phenomenon can be explained by the relative slow rate of divalent ion diffusion from the capillary bound connate water into frack fluid[19] (i.e., the diffusion of divalent cations may not reach equilibrium at the early stage of gas production). This result is supported by the fact that the diffusion coefficient of divalent cations (e.g., Ba^{2+}, Sr^{2+}, Ca^{2+}) is smaller than that of monovalent cations (e.g., Na^{+}).[20] The kinetics of diffusion might limit the MCl_2 concentration at the early stage of the flowback period. However, the diffusion of MCl_2 would reach equilibrium at the late gas production stage and its concentration would be similar to that resulting from the dilution of connate water.

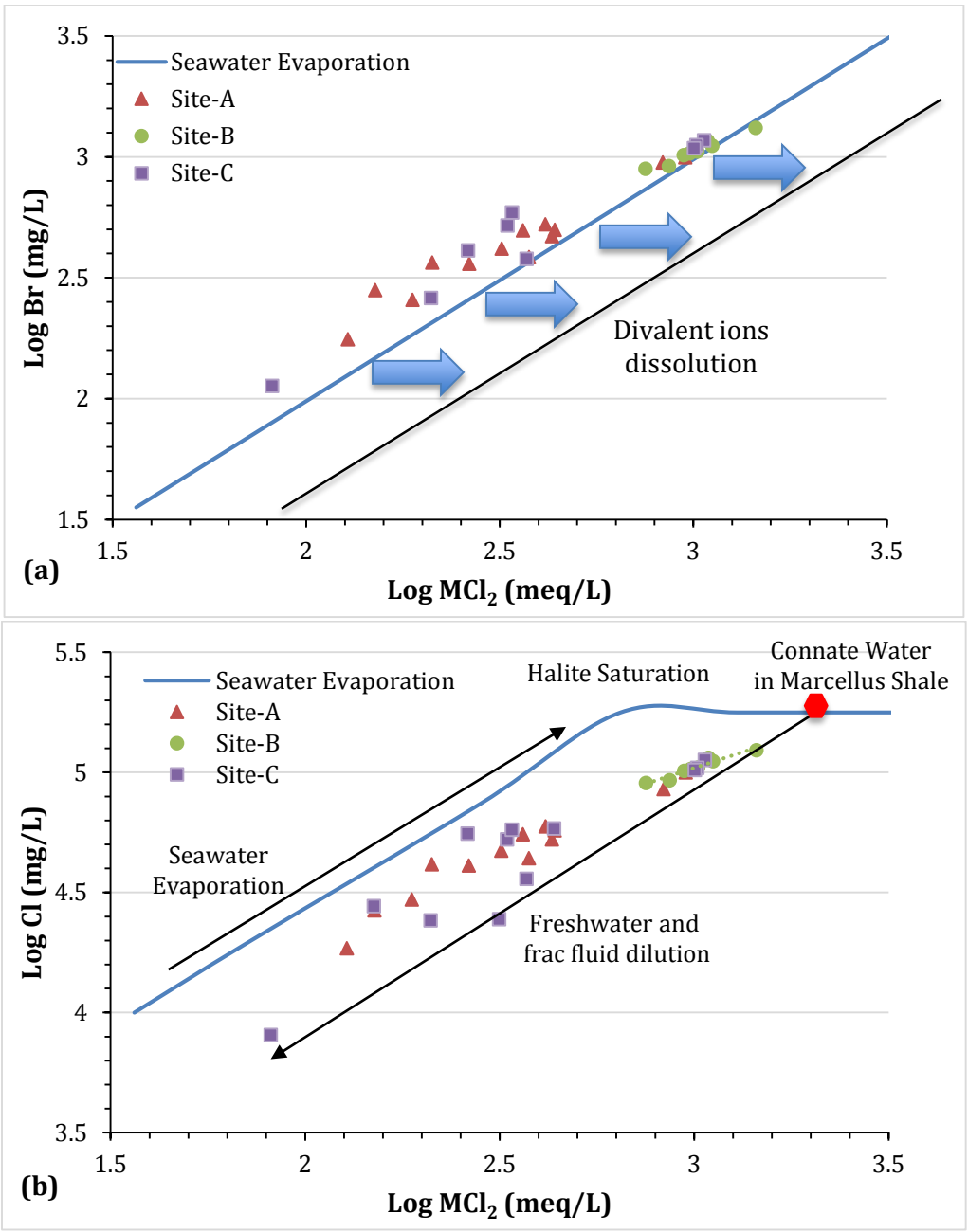

Figure 2.2 Correlation of (a). Log (Br) versus Log (MCl_2) and (b). Log (Cl) versus Log (MCl_2) for Marcellus Shale produced water

In summary, results show that monovalent and divalent ions in the flowback/produced water are contributed by the diffusion of free or capillary bound connate water. The Br concentration in the connate water is around 2,000 ppm (25 meq/L), which suggests the connate

water is 1,300 times concentrated seawater. The corresponding Cl and MCl_2 concentrations in the connate water are 177,800 mg/L and 2,040 meq/L, respectively. In addition, if the volume of connate water or stimulated shale is known, the highest Cl and MCl_2 concentration in produced water can be predicted based on the mixing ratio of frack fluid and connate water.

2.3.4 Fate of radioactive material in Marcellus Shale produced water

Highly mineralized waters generated by oil and gas extraction activities, such as Marcellus Shale produced water, often contain high levels of radioactivity.[5,21] Previous studies found that Ra isotopes are the dominant radionuclides in the oil and gas produced water because Ra is much more soluble in water than other naturally occurring radionuclides (i.e., uranium and thorium).[22,23] Total radium in Marcellus Shale produced water ranges from several hundreds to more than ten thousand pCi/L with a median of 5,350 pCi/L.[5] Radium concentration in the produced water increases with time after hydraulic fracturing and generally shows a linear relationship with salinity.[4]

Concentration profiles of Ra-226 and Ra-228 in Marcellus Shale produced water from three wells in Southwest Pennsylvia are shown in Figure 2.3. Ra-226 concentration in the produced water increased from several hundred pCi/L in the early stage of flowback period (< 10 days) to several thousand pCi/L after the well has been producing gas for more than two years. Ra-228 has a distinctively lower concentration than Ra-226 mainly due to the lower Th content in Marcellus Shale.[5] However, it also increased from less than 400 pCi/L at the early stage to more than 1,000 pCi/L after two years of gas production. Concentration profiles of Ra isotopes are highly dependent on the location and reservoir lithology. The flowback and produced water had similar Ra concentrations tor the two wells close to each other (site A1 and A2). In contrast,

samples collected at site B show distinctively lower Ra-226 and higher Ra-228 concentrations when compared to site A.

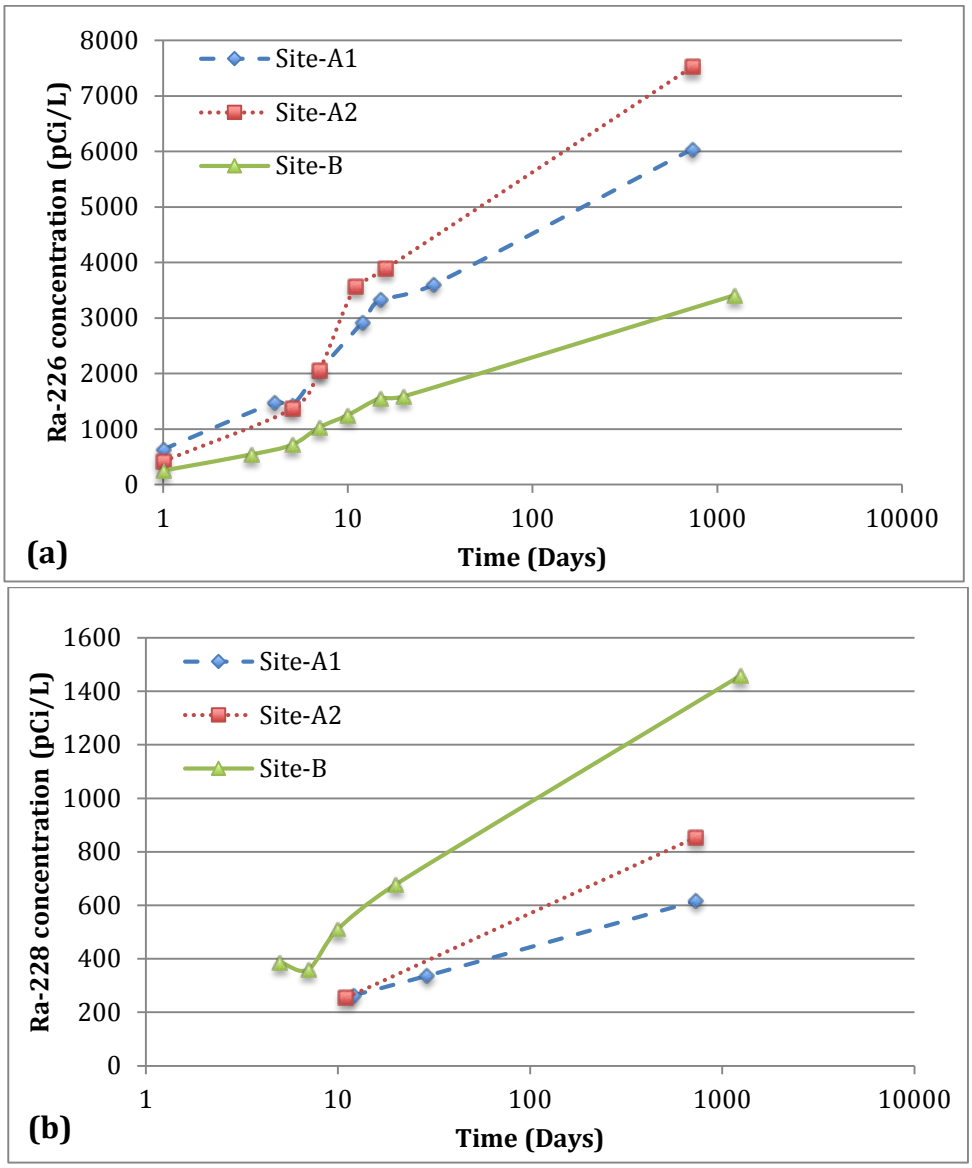

Figure 2.3 Concentration profiles of (a). Ra-226 and (b). Ra-228 as a function of time for three Marcellus Shale wells (Site A1, A2 and B)

Ra has similar chemical properties with Ba and Sr and would co-precipitate with barite and celestite and be deposited in the shale formation.[24] In addition, Ra would also adsorb to

organic materials in the black shales. Due to the natural decay, activity of Ra isotope with the longest half-life (Ra-226) would decrease by 99% after 10,000 years. Considering that the Devonian-age Marcellus Shale was deposited around 400 million years ago, no ancient radium would be observed in the shale or the connate water. Therefore, Ra-226 and Ra-228 that are observed in produced water are essentially contributed by the leaching from the shale core, which is enriched in their parent radionuclide U-238 and Th-232 (Figure 2.3). However, in order to investigate the origin of radionuclides in Marcellus Shale produced water, it is important to determine whether the Ra existed in connate water, which has reached dynamic equilibrium with shale core, or is leached from the shale core into produced water as a consequence of frack fluid injection. In this study, we focus on using isotopic dating to interpret the mean residence time of Ra in the liquid phase.

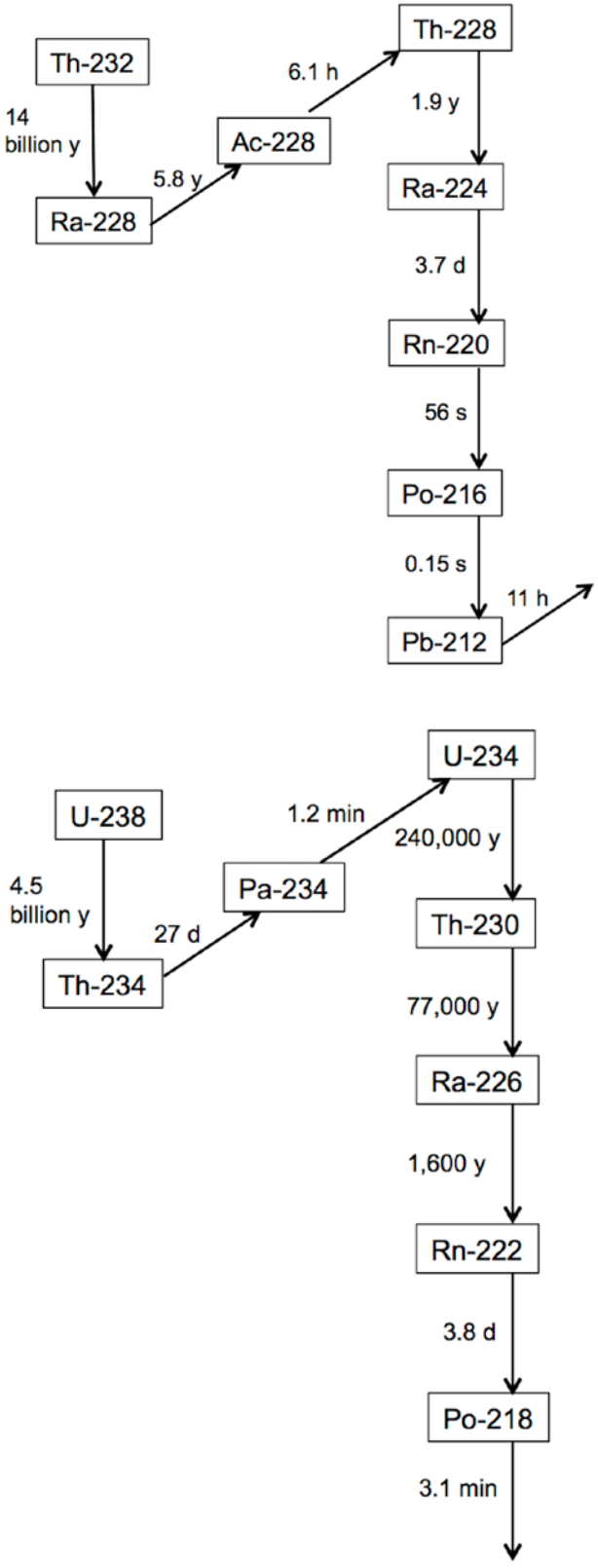

Figure 2.4 Thorium-232 and Uranium-238 natural decay series with associated half-lives

2.3.5 Isotopic dating to identify the origin and mean residence time of radium in produced water

Isotopic dating (or radiometric dating) is a useful tool to date materials, usually based on a comparison between the observed abundance of naturally occurring radioactive isotopes and their decay products. Previous studies used Ra isotopes to determine the origin and age (residence time) of Ra-enriched material.[25-27] In this study, a combination of Ra-228:Ra-226 and Th-228:Ra-228 ratios is used to calculate the mean residence time of Ra in the liquid phase and to determine the origin of Ra in Marcellus Shale produced water. If Ra originated from connate water that has reached dynamic equilibrium with shale core, its the mean residence time would be very long. Otherwise, if Ra originated from relatively rapid shale leaching by the frack fluid, its residence time would be short and its concentration may increase during gas production.

Since Ra-226 and Ra-228 isotopes share the same properties and undergo same processes in the reservoir, the portion of Ra-226 that intruded from the shale into the liquid phase should be equal to that of Ra-228. In other words, Ra-228:Ra-226 ratio in the liquid phase (i.e., connate water) is equal to that in the shale core at the moment when they leached out into the connate water. Ra-226 and Ra-228 have half-lifes of 1600 years and 5.8 years, respectively, indicating the decay rate of Ra-228 is much faster than that of Ra-226. Thus, once the radium isotopes have intruded into the liquid phase, Ra-228:Ra-226 activity ratio would keep decreasing until all Ra-228 was decayed. The residence time of radium in the liquid phase can be estimated by comparing the Ra-228:Ra-226 activity ratio in Marcellus Shale produced water with that in the shale core.

The activities of Ra-226 and Ra-228 in the Marcellus Shale core are obtained using several approaches. First, five Marcellus Shale core samples collected from the depth ranging from 6381-6419 ft from one well in Washington County, PA were analyzed by Gamma-spectrometry and the results are shown in Table 2.2. Second, activity of Ra isotopes can also be calculated based on the concentration of their parent compounds (i.e., U-238 and Th-232). Previous studies reported total uranium concentration in the shale core samples in the range from 10-50 μg/g (ppm), with an average of 28 μg/g, and average total thorium concentration of 8 μg/g.[28] Since the deposition of Devonian-age Marcellus Shale occurred 400 million years ago, the secular equilibrium between parents and their daughter products has been achieved and their activity ratio should be equal to 1.[29] Th-228 is an indirect decay product of Ra-228 and a direct decay product of Ac-228 with a relatively short half-life compared with Ra-228 (Figure 2.3). Transient equilibrium of these radionuclides can be expressed by the Bateman equation[30]:

$$\frac{A_{Th228,,e}}{A_{Ra228,,e}} = \frac{\lambda_{Th228} \cdot \lambda_{Ac228}}{(\lambda_{Ac228} - \lambda_{Ra228}) \cdot (\lambda_{Th228} - \lambda_{Ra228})} = 1.48 \quad (2\text{-}4)$$

where, $A_{\text{Th-228,e}}$ and $A_{\text{Ra-228,e}}$ are activities of the Th-228 and Ra-228 after transient equilibrium has been achieved, λ is the decay constant ($\lambda = 0.693/t_{1/2}$, $t_{1/2}$ is the half-life of the radionuclide).

Activities of radionuclides in the U-238 and Th-232 decay chains can be calculated based on natural decay and equilibrium model (Appendix A) and expressed by the following equations:

$$A_{U238} = A_{Th234} = A_{U234} = A_{Th230} = A_{Ra226} \quad (2\text{-}5)$$

$$A_{Th232} = A_{Ra228} = \frac{1}{1.48} A_{Th228} = \frac{1}{1.48} A_{Ra224} \quad (2\text{-}6)$$

Activity of uranium and thorium isotopes can be calculated based on the mass balance of all naturally occurring uranium and thorium isotopes. (U-235, which is also a natural occurring radionuclide, accounts for 0.72% of total U and can be ignored in the mass balance):

$$A_{U238} \times \frac{2995841g}{Ci} + A_{U234} \times \frac{157g}{Ci} = 28 \times 10^{-6}g \quad (2\text{-}7)$$

$$A_{Th232} \times \frac{9085426g}{Ci} + A_{Th228} \times \frac{0.0012g}{Ci} + A_{Th234} \times \frac{0.00004g}{Ci} + A_{Th230} \times \frac{50.4g}{Ci} = 8 \times 10^{-6}g \quad (2\text{-}8)$$

Table 2.2 Activities of Radionuclides in Marcellus Shale

Decay chain	Radionuclide	Activity to mass ratio (Ci/g)	Theoretical Activity (pCi/g)	Activity measured by Gamma-Spec
U-238 series	U-238	2.99e+6	3.34-16.70 (Avg. 9.35)	1.60-24.50 (Avg. 8.38)
	U-234	1.57e+2		
	Th-234	4.30e-5		
	Ra-226	1.00		
Th-232 series	Th-232	9.09e+6	0.88	0.50-1.27 (Avg. 0.77)
	Th-228	1.21e-2		
	Ra-228	3.70e-3		

Calculated and measured activities of radionuclides in the Marcellus Shale core are summarized in Table A.2 in the Appendix A. Ra-228:Ra-226 ratios measured in this study range from 0.02-0.41, with an average of 0.16 and median of 0.11. Theoretical Ra-228:Ra-226 ratio in the shale core calculated based on U and Th content ranges from 0.05-0.26, with an average of 0.09. Thus, it is reasonable to assume the average Ra-228:Ra-226 ratio in the Marcellus Shale is 0.10.

Assuming that the system remained chemically closed once the Ra leached into the liquid phase, which means that the initial Ra-228 and Ra-226 activity is constant, the activity ratio of Ra-228:Ra-226 as a function of mean residence time can be calculated by the following equation:

$$\frac{A_{Ra228,t}}{A_{Ra226,\mathrm{t}}} = \frac{A_{Ra228,0}}{A_{Ra226,0}} e^{(\lambda_{Ra226} - \lambda_{Ra228}) \cdot t} \quad (2\text{-}9)$$

Where $A_{Ra228,t}$ and $A_{Ra226,t}$ are the activities of Ra-228 and Ra-226 at time t, $A_{Ra228,0}$ and $A_{Ra226,0}$ are the activities of Ra-228 and Ra-226 at time 0, λ is the decay constant ($\lambda_{Ra226} = 0.000433$, $\lambda_{Ra228} = 0.119508$) and t is the mean residence time (elapsed time).

Once Ra isotopes entered into the liquid phase, the activity ratio of Ra-228:Ra-226 would decrease with residence time, as shown in the first five columns in Figure 2.5. Considering that the activity ratio of Ra-228:Ra-226 in the shale core is 0.1, Ra-228:Ra226 ratio would be equal to 0.1 when these isotopes entered into the liquid phase by shale leaching and would decrease to less than 0.05 after 6 years.

Ra-228:Ra226 activity ratio in the Marcellus Shale produced water was collected from three different sources and is shown in the last three columns in Figure 2.5. The NYSDEC database shows that Ra-228:Ra-226 ratio ranges from 0.030 to 0.353, with an average of 0.129 and a median of 0.084 (n=11).[8] The PADEP BOGM survey shows that Ra-228:Ra226 ratio in Marcellus Shale produced water ranges from 0.046-0.502, with an average of 0.150 and a median of 0.133.[9] Fourteen Marcellus Shale produced water samples analyzed in this study show that Ra-228:Ra-226 ratio ranges from 0.071-0.539, with an average of 0.221 and a median of 0.121. Even though the Ra-228:Ra-226 ratio varies from site to site and some of the ratios in the produced water are larger than that in Marcellus Shale (Table 2.2), it is clear that most of the Ra-228:Ra-226 ratios in Marcellus Shale produced water are larger than 0.05 and best overlap with a mean residence time between 0-6 years (Figure 2.5).

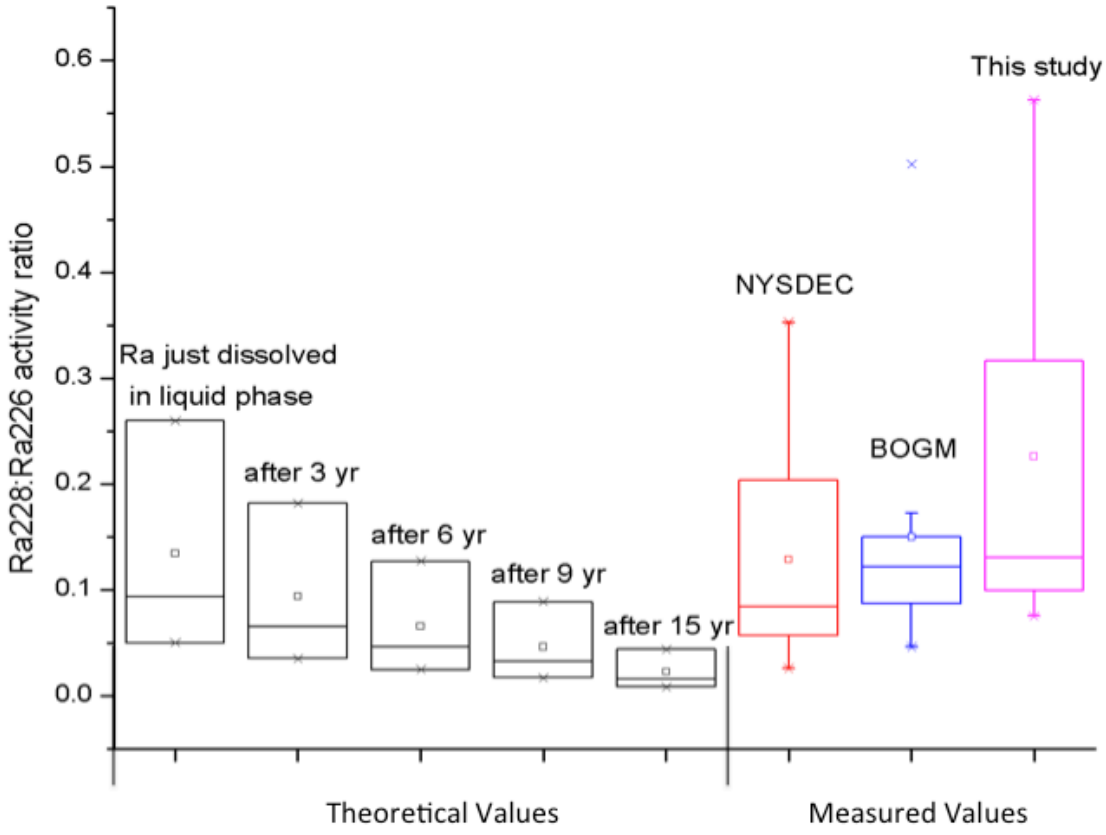

Figure 2.5 Ra-228:Ra-226 activity ratio as a function of Ra residence time in liquid phase (Ra-228:Ra-226 ratio for freshly dissolved sample is calculated based on their activity in the shale core)

The mean residence time of Ra isotopes in the liquid phase may be further used to estimate the rate of Ra leaching from the shale core. If it is assumed that Ra-228 and Ra-226 activities increase due to leaching from shale, their activity ratio with time can be calculated from Equation (2-10):

$$\frac{A_{Ra228,t}}{A_{Ra226,t}} = \frac{A_{Ra228,0}e^{(-\lambda_{Ra228}\cdot t)} + x\cdot A_{Ra228,0}\cdot t\cdot e^{(-\lambda_{Ra228}\cdot t/2)}}{A_{Ra226,0}e^{(-\lambda_{Ra226}\cdot t)} + x\cdot A_{Ra226,0}\cdot t\cdot e^{(-\lambda_{Ra226}\cdot t/2)}} \quad (2\text{-}10)$$

Ra-228:Ra-226 ratio is inevitably decreasing with residence time. However, a higher leaching rate would lower the rate of decrease in Ra-228:Ra-226 ratio with time as shown in Figure 2.6. The comparison of Ra-228:Ra-226 ratio in early flowback and late stage produced

water can be used to estimate the rate of Ra leaching from the shale. If all Ra originated from the connate water, Ra-228:Ra-226 ratio in the late stage produced water would be distinctively lower than that in the flowback water stage, as described in Figure 2.6 (no shale leaching). However, Ra-228:Ra-226 ratios observed in the late stage produced water are similar or even slightly higher than that in the early flowback stage (Table A.1), which suggests that Ra keeps leaching from the shale core during gas well operation.

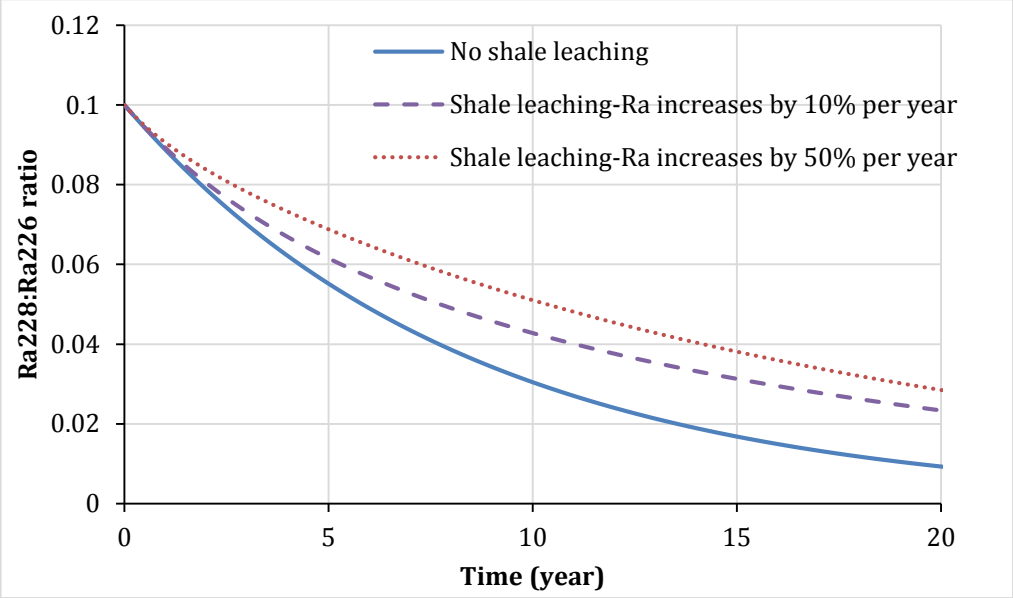

Figure 2.6 Change of Ra-228: Ra-226 ratios as a function of residence time with/out shale leaching

Another isotopic signature that could characterize the residence time of radium in the liquid phase is the ratio of Th-228:Ra-228 (or Ra-224:Ra-228).[32] Ra-228 is a decay product of Th-232 and will subsequently decay into Ac-228, Th-228 and Ra-224. Since uranium and thorium are relatively insoluble under reducing conditions that are typical of oil and gas reservoirs, the concentration of U-238, U-234 and Th-230 in produced water are generally less than 1 pCi/L. However, Th-228 concentration in the produced water is extremely high compared with other thorium isotopes[8] (Figure 2.7), which must be due to Ra-228 decay rather than

leaching of thorium from the shale. Thus, by investigating the Th-228 to Ra-228 ratio and comparing with the theoretical decay model, the mean residence time of radium isotopes in the liquid phase may be predicted.

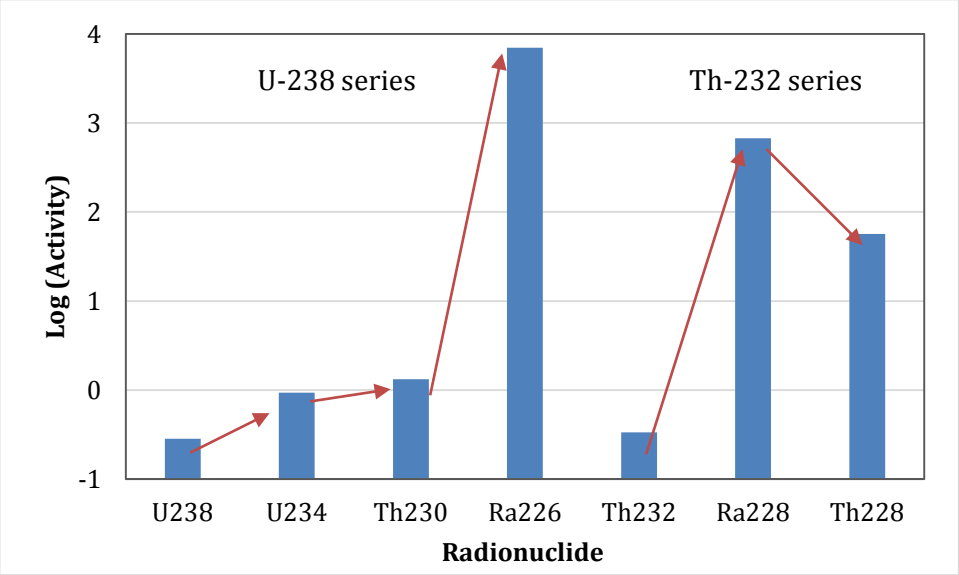

Figure 2.7 Average radionuclides concentration in U-238 and Th-232 decay chain (Marcellus samples from NYSDEC database[8])

After Ra-228 has been released into liquid phase, it would build secular equilibrium with Ac-228 within 2 days and their activity ratio would be 1. Th-228 has a relatively long half-life ($T_{Th-228,1/2} = 1.9 years$) that is comparable with that of Ra-228 ($T_{Ra-228,1/2} = 5.8 years$).[33] Thus, it will take around 13 years (7 half-lives) to build the transient equilibrium between Ra-228 and Th-228.[29,30] The activity ratio of Th-228:Ra-228 can be calculated using Equation 2-11 and will keep increasing until it reaches a value of 1.48, as shown in Figure 2.8.

$$\frac{A_{Th228,t}}{A_{Ra228,t}} = \lambda_{Th228}\left(\frac{\lambda_{Ac228}}{(\lambda_{Ac228}-\lambda_{Ra228})(\lambda_{Th228}-\lambda_{Ra228})} + \frac{\lambda_{Ac228}\cdot e^{(-\lambda_{Ac228}+\lambda_{Ra228})\cdot t}}{(\lambda_{Ra228}-\lambda_{Ac228})(\lambda_{Th228}-\lambda_{Ac228})} + \frac{\lambda_{Ac228}\cdot e^{(-\lambda_{Th228}+\lambda_{Ra228})\cdot t}}{(\lambda_{Ra228}-\lambda_{Th228})(\lambda_{Ac228}-\lambda_{Th228})}\right) \quad (2\text{-}11)$$

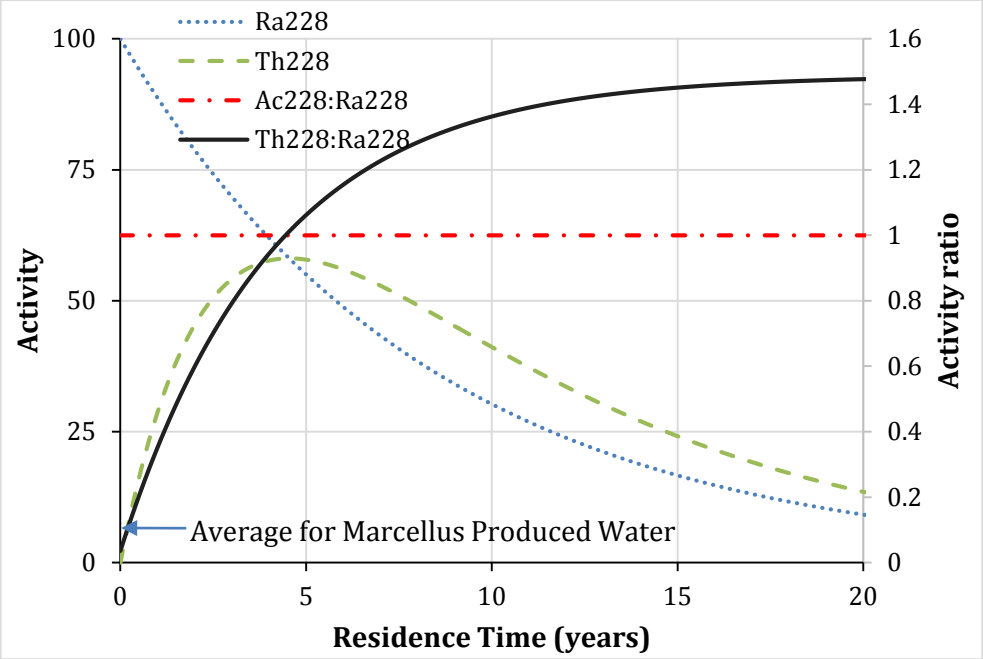

Figure 2.8 Ingrowth of Ac-228, Th-228 and Ra-224 as a function of time. The average value for Th-228 to Ra-228 ratio in Marcellus Shale produced water of 0.13 corresponds to a mean residence time of NORM in the liquid phase of 0.4 years

The NYSDEC database shows that the Th-228:Ra-228 ratio in Marcellus Shale produced water ranges from 0.001-0.68, with an average of 0.13 and a median of 0.062 (n=11).[8] Eight Marcellus Shale produced water samples analyzed in this study show that Th-228:Ra-228 ratio ranges from 0.032-0.553, with an average of 0.181 and a median of 0.143 (Table A.1). Even though significant variance in Th-228:Ra-228 ratios in produced water samples is observed, it can be concluded that the average Th-228:Ra-228 ratio is below 0.15. Such a low activity ratio corresponds to a fairly short residence time of Ra in the liquid phase of around 0.4 years (Figure 2.8). However, it is important to note that thorium tends to absorb on the solid surfaces.[31] Therefore, there is a tendency to underestimate the activity of Th-228 in the liquid phase, which would result in an underestimation of the mean residence time of Ra.

The combination of Ra-228:Ra-226 and Ra-224:Ra-228 isotopic dating for Marcellus Shale produced water shows that the mean residence time of Ra in the liquid phase is between 0.4-6 years (Figure 2.9). The relatively short residence time of Ra isotopes in the Marcellus Shale produced water refutes the hypothesis that Ra existed in connate water, which has reached dynamic equilibrium with shale core and suggests the Ra is mainly contributed by shale core leaching during frack fluid injection.

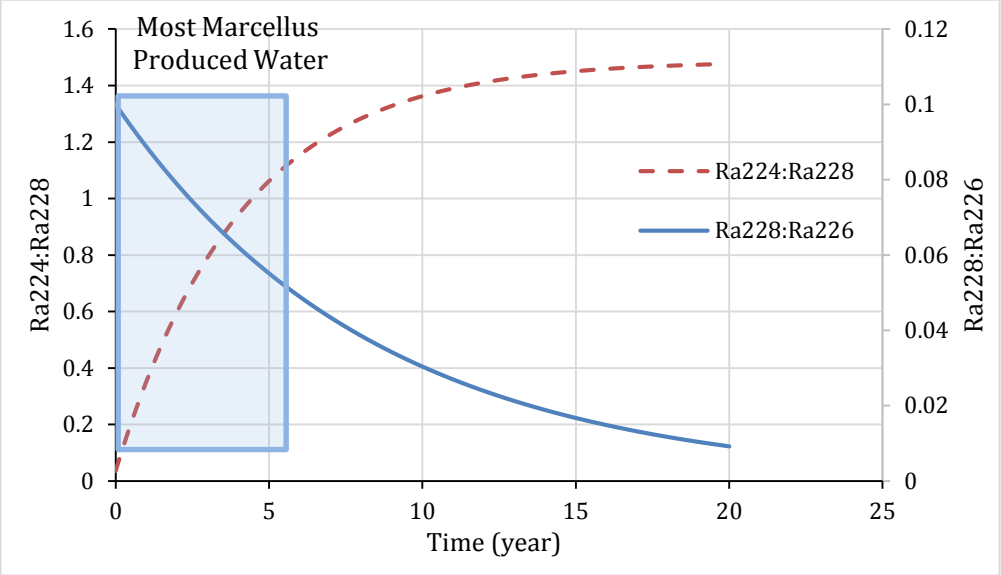

Figure 2.9 Mean residence time of Ra in liquid phase based on isotopic results

2.4 SUMMARY AND CONCLUSION

This study investigated the origin of chloride, which is the major component of salinity, divalent cations, which can potentially cause severe scaling, and radioactive materials, which are a major

concern for public health, in the Marcellus Shale produced water. Results show that the major monovalent (e.g., Cl, Na) and divalent ions (e.g., Ca, Mg) in the produced water originated from the mixing of the fracking fluid with ancient connate water. Results also suggest that the connate water in Marcellus Shale is 1,300 times concentrated seawater, which contains 2,000 mg/L of Br, 177,800 mg/L of Cl, and 2,040 meq/L of MCl_2. If the volume of connate water or the stimulated shale volume is known, the plateau of Cl and MCl_2 concentrations in produced water can be predicted based on the mixing ratio of frac fluid to connate water.

In addition, the isotopic signature of Ra in early and late stage of gas production shows that the mean residence time of Ra isotopes in the liquid phase ranges from 0.4 – 6 years. Relatively short residence time supports the hypothesis that the shale leaching during frack fluid injection is the major source of NORM in produced water and suggests that the radium concentration may increase throughout the lifetime of the well. Further work could quantify the fraction of Ra that originates from shale leaching and estimate the leaching rate. Additional studies are needed to quantify the scaling potential in the shale core and develop modifications of the fracturing fluid composition to alleviate potential impact on the long-term gas production.

3.0 CHALLENGES OF RA-226 MESUREMENT AND DEVELOPMENT OF A RAPID METHOD FOR RA-226 MEASUREMENT BY ICP-MS

This work has been published as:

Zhang, T., Bain, D., Hammack, R. W., & Vidic, R. D. (2015). Analysis of Radium-226 in high salinity wastewater from unconventional gas extraction by Inductively Coupled Plasma-Mass Spectrometry (ICP-MS). Environmental Science & Technology, 49(5), pp. 2969-2976.

Elevated concentration of naturally occurring radioactive material (NORM) in wastewater generated from Marcellus Shale gas extraction is of great concern due to potential environmental and public health impacts. Development of a rapid and robust method for analysis of Ra-226, which is the major NORM component in this water, is critical for the selection of appropriate management approaches to properly address regulatory and public concerns. Traditional methods for Ra-226 determination require long sample holding time or long detection time. A novel method combining Inductively Coupled Mass Spectrometry (ICP-MS) with solid-phase extraction (SPE) to separate and purify radium isotopes from the matrix elements in high salinity solutions is developed in this study. This method reduces analysis time while maintaining requisite precision and detection limit. Radium separation is accomplished using a combination of a strong-acid cation exchange resin to separate barium and radium from other ions in the

solution and a strontium-specific resin to isolate radium from barium and obtain a sample suitable for analysis by ICP-MS. Method optimization achieved high radium recovery (101±6% for standard mode and 97±7% for collision mode) for synthetic Marcellus Shale wastewater (MSW) samples with total dissolved solids as high as 171,000 mg/L. Ra-226 concentration in actual MSW samples with TDS as high as 415,000 mg/L measured using ICP-MS matched very well with the results from gamma spectrometry. The Ra-226 analysis method developed in this study requires several hours for sample preparation and several minutes for analysis with the detection limit of 100 pCi/L with RSD of 45% (standard mode) and 67% (collision mode). The RSD decreased to below 15% when Ra-226 concentration increased over 500 pCi/L.

3.1 INTRODUCTION

Recent developments in horizontal drilling and hydraulic fracturing enabled efficient and economical extraction of natural gas from unconventional resources and has lead to rapid expansion of gas extraction to meet global energy needs.[1] However, hydraulic fracturing generates large volume of wastewater containing high concentrations of total dissolved solids (TDS), heavy metals, and naturally occurring radioactive material (NORM).[1-5] The wastewater generated during the initial period after the well completion (i.e., the first 2 weeks) is typically referred to as “flowback water” and wastewater generated during the well production stage is termed “produced water”. This study refers to both as Marcellus Shale wastewater (MSW).

Radium-226 (i.e., Ra-226) is one of the major components of NORM in Marcellus Shale wastewater and is an important proxy for the radioactivity of waste streams generated during

unconventional gas production.[5] Ra-226 has a very long half-life (1,620 years), resulting in extended period of activity when brought to the surface. Ra-226 activity in wastewater from Marcellus Shale ranges from hundreds to tens of thousands pCi/L and is often strongly correlated with total dissolved solids (TDS) in MSW that can be as high as 350,000 mg/L.[2,4] Several studies investigated the impact of shale gas development on surface water quality in Pennsylvania[1,2,6] and potential treatment options[4,5] for the highly contaminated wastewater generated by this industry. However, the challenging nature of NORM measurement limits our ability to design MSW management strategies to adequately resolve regulatory and public concerns stemming from high NORM content. Hence, the development of a rapid and robust method for NORM analysis in MSW, especially for Ra-226, is critical to advance our understanding of the fate of NORM and to develop best NORM management practice for the unconventional gas industry.

The two approaches that are generally utilized to detect Ra-226 include 1) alpha spectrometry or liquid scintillation counting (LSC) to quantify the emission rates of alpha/beta particles, such as EPA Method 903.0 and 903.1 and 2) gamma spectrometry to quantify the emission rates of gamma rays, such as EPA Method 901.1.[6-14] Alpha spectrometry often relies on Radon-222 (i.e., Rn-222) emanation and requires at least three weeks for the progeny to reach secular equilibrium (ingrowth period) with Ra-226 before sample analysis. Ra-226 can be directly quantified by alpha spectrometry at 4.8 MeV. However, due to the low penetrability of alpha particles, extensive sample preparation is needed to minimize sample thickness.[15,16] Gamma spectrometry utilizes sodium iodide (NaI) scintillation counter or high purity germanium (HPGe) detectors to quantify Ra-226 by analyzing its equilibrium progenies, such as Pb-214 and Bi-214. Indirect measurement of Ra-226 is often necessary in gamma spectrometry due to strong inference from U-235 near the 186 KeV emission of Ra-226. It is possible to measure Ra-226 in

wastewater from shale gas extraction without an ingrowth period because the interfering isotopes (i.e., U-235) are usually present at low concentrations. However, long counting times (24-48 hours) for each sample are required for both alpha and gamma spectrometry to obtain accurate results, thereby limiting the sample throughput.[5, 14]

Techniques using either thermal ionization mass spectrometry (TIMS) or inductively coupled plasma mass spectrometry (ICP-MS) to determine Ra-226 concentration have emerged in recent years.[17-26] These techniques utilize the increasing sensitivity of mass spectrometry. Modern spectrometry has detection limits as low as 0.1 ng/L (part per trillion), corresponding to Ra-226 concentration of 100 pCi/L or Ra-228 concentration of 23,000 pCi/L. In addition, highly efficient sample introduction systems, can increase sensitivity up to ten times.[22]

Previous studies evaluated wet chemical purification procedures for radium extraction from low salinity solutions with reasonable radium recovery (>80%).[17-24] Those techniques include solid-phase extraction using cation exchange resins, co-precipitation with sulfates, manganese dioxide (MnO_2) preconcentration, and 3M Empore^{TM} RAD disks. However, radium recovery efficiencies of these procedures are greatly diminished in high salinity solutions due to high concentrations of competing ions.[24] Several studies successfully separated radium from seawater prior to ICP-MS or TIMS measurement.[25, 26] For example, Hsieh et al. used the MnO_2 for radium adsorption prior to extraction by Sr-Ra-SO_4 co-precipitation, conversion to Sr-Ra-CO_3 and followed by purification with 50W-X8 resin and Sr*spec resin.[25] However, these procedures are not suitable for the MSW, which contains significantly higher concentrations of barium and other matrix components (e.g., calcium, strontium). A recent study evaluated the impact of matrix compounds in MSW on Ra-226 recovery by several wet chemical techniques (e.g., MnO_2 adsorption, Rad Disk) and concluded that the recovery may be as low as 1% due to

very high ionic strength and barium concentration in MSW samples.[9] This study was designed to evaluate an alternative radium extraction/purification procedure for high salinity wastewater from Marcellus Shale in Pennsylvania to enable Ra-226 analysis by ICP-MS. The main focus of this study was to ensure high recovery and accurate detection of Ra-226 while minimizing the analysis time.

3.2 MATERIALS AND METHODS

3.2.1 Reagents and materials

Bio-Rad 50W-X8 (100-230 mesh) cation exchange resin (Bio-Rad Laboratories) was loaded into a 0.8-cm diameter polypropylene column with a 25 ml extension funnel (Eichrom Technologies, Lisle, IL). Sr*Spec (100-150µm) resin (Eichrom Technologies) was purchased in prepackaged 1-mL cartridges. Radium-226 was obtained from the Pennsylvania State University in a Ra-226 stock solution and calibrated using a Canberra gamma spectrometry with broad energy germanium (BeGe) detector (BE2020). Other ACS-grade reagents included barium chloride dihydrate (99.0% min, Mallinckrodt Chemicals), strontium chloride hexahydrate (99.0%, Acros Organics), calcium chloride dihydrate (99.4%, Fisher Scientific), sodium chloride (99.8%, Fisher Scientific), trace metal grade nitric acid, (65-70%, Fisher Scientific), and trace metal grade hydrochloric acid (37.3%, Fisher Scientific). Deionized (DI) water was produced by a laboratory water purification system (Millipore, Billerica, MA, USA). All reagents were found to be free of Ra-226.

3.2.2 Resin preparation

The polypropylene columns were cleaned by soaking in 3 M HNO_3 for 20 minutes prior to loading with 4 mL of 50W-X8 exchange resin. The resin was then conditioned with three bed volumes (12 mL) of 6 M HNO_3 to ensure that it is in the protonated form, washed with 5 bed volumes of DI water and 5 bed volumes of 2% HNO_3 and stored in 2% HNO_3 before use. Spent 50W-X8 resin was also regenerated using this procedure.

The Sr*Spec resin in prepackaged 1-mL cartridges can be regenerated at least once by washing with 10 mL of 6 M heated HCl followed by a rinse with 10 mL of DI water[26, 27].

3.2.3 Marcellus Shale wastewater samples

A synthetic Marcellus Shale wastewater sample containing 5 mM of $BaCl_2$ and $SrCl_2$, 50 mM of $CaCl_2$, 1 M of NaCl and 50,000 pCi/L of Ra-226 was prepared to optimize the radium separation/purification procedure. Seven synthetic samples (S1-S7) that are representative of MSW with varying levels of TDS were prepared to test radium recovery with both new and regenerated Sr*Spec resin. Nine MSW field samples (1-9) containing varying levels of TDS and Ra-226 collected from unconventional gas wells and storage impoundments in southwest and northeast Pennsylvania were analyzed by the ICP-MS method and compared with the reference measurements by gamma spectrometry.

3.2.4 Analytical instruments

The NexION 300x Inductively Coupled Plasma-Mass Spectrometry (Perkin Elmer, Waltham, MA) was used to measure Ra-226 concentration both in standard mode and collision mode using a non-reactive helium gas and Kinetic Energy Discrimination (KED) process. Detection limit was determined to be 0.1 ng/L, which is equal to 100 pCi/L of Ra-226. Details of the instrument components, operating conditions, and data acquisition parameters are summarized in Supplementary Information (Table B.1).

Concentrations of major cations (i.e., Na, Ca, Sr and Ba) in real MSW and their elution profiles were measured by atomic absorption spectrometry (Perkin-Elmer, Model 1000 AAS) with a nitrous oxide-acetylene flame. The eluent samples were diluted with 2% nitric acid and 0.15% KCl solution prior to analysis to limit interferences during metal analysis[2] and the dilution ratios were chosen based on the linear range of the AAS. The reproducibility of this analytical procedure is within 5%.

The elution profile of Ra-226 for synthetic flowback water samples was also analyzed using Packard 2100 Liquid Scintillation Counter (LSC). The eluents from 50W-X8 and Sr*Spec resin were collected in 5 or 0.5 mL volumes, respectively. These samples were evaporated to dryness, redissolved in 5 mL of DI water and 5 mg of Ba^{2+} carrier (i.e., 1.82 mL of 20 mmol $BaCl_2$ solution) and 20 mL of 1M H_2SO_4 were added to ensure complete barium removal by precipitation as barium sulfate (barite). If there was already a significant concentration of barium in the sample, the addition of $BaCl_2$ was adjusted so that the total mass of barium in the sample did not exceed 5 mg to ensure complete dissolution of precipitated barite in EDTA solution as discussed below. The sample was maintained at 80 ^{o}C for 1 hour to ensure that all Ra-226 in

solution is completely co-precipitated with $BaSO_4$.[31] The precipitate was then collected on a 0.45 μm cellulose ester membrane (Millipore, Billerica, MA, USA) and transferred into a scintillation vial by washing with 2 mL of 0.25 M EDTA solution at pH 8-9. The sample was heated at 60 ºC until the solution became transparent to ensure complete dissolution of Ra-$BaSO_4$ in EDTA solution. After the vial is cooled to room temperature, 14 mL of Ultima Gold™ universal LSC-cocktail was added and vigorously mixed with the sample.[7] The sample was then counted on LSC for 60 minutes in 170-230 KeV energy range that is specific to Ra-226.[28, 29]

A Canberra gamma spectrometry system with a broad energy Germanium (BeGe) detector (Be 2020) was used to quantify Ra-226 activity.[4, 8, 14] Ra-226 activity in real Marcellus Shale wastewater samples was quantified by measuring gamma ray emission from the progenies of Ra-226 (Bi-214 and Pb-214) after waiting for at least 21 days to achieve secular equilibrium.

3.3 RESULTS AND DISCUSSION

3.3.1 ICP-MS Calibration

The NexION 300 ICP-MS was calibrated using synthetic Ra-226 standards that were cross-validated by gamma spectrometry. Both standard and collision modes of ICP-MS were evaluated. The standard mode was optimized for maximum ion transmission, resulting in higher Ra-226 intensity (Figure B.1a.). The collision mode with Kinetic Energy Discrimination (KED) used a non-reactive helium gas to remove polyatomic spectral interferences, thereby resulting in lower Ra-226 intensity (Figure B.1b) but lower interferences by matrix elements. Detection limit of Ra-226 was 100 pCi/L (i.e., 0.1 ng/L) with a relative standard deviation (RSD) of 45% and

67% for standard and collision modes, respectively (Figure B.1). The RSD decreased to below 15% in the standard mode and 18% in the collision mode for Ra-226 concentration of 500 pCi/L and decreased even further with an increase in Ra-226 concentration (Figure B.1). The detection limit was always well below the reported Ra-226 concentration in Marcellus Shale wastewater, which ranges from hundreds to tens of thousands pCi/L with a median of 2,460 pCi/L in Pennsylvania or 5,490 pCi/L in New York.[4,5] It is important to note that measurement of Ra-228 in MSW samples by ICP-MS is not feasible without preconcentration because the Ra-228 concentration typically ranges from 100 – 1,000 pCi/L ($4.3x10^{-4}$ – $4.3x10^{-3}$ ng/L)[5], which is far below the detection limit of ICP-MS (0.1 ng/L).

3.3.2 Impact of matrix elements on ICP-MS analysis

Matrix elements can affect the ICP-MS signal for Ra-226 via spectral overlap of polyatomic ions (e.g., $^{88}Sr^{138}Ba$, $^{208}Pb^{18}O$ have an apparent signal with an m/z ratio identical to Ra-226)[22] and/or matrix induced signal intensity changes.[38-40] The latter effect is highly dependent on the ICP-MS operating conditions (e.g., gas flow rate, applied power) that impact the ionization equilibrium of the analyte.[40] Generally, matrix induced signal intensity change would suppress the target analyte signal at higher concentrations of matrix elements and higher plasma power. The increase in concentration of matrix elements decreases the ratio of Ra-226 to the total ions that are introduced into the skimmer orifice. As a result, the space charge effects on the target ion, such as Ra-226, are decreased and the signal is suppressed.[41] To evaluate the interference of matrix elements with Ra-226 measurement by ICP-MS, standard Ra-226 solutions with varying concentrations of matrix elements were prepared and compared with the standard Ra-226 in the background solution (i.e., 2% HNO_3). Results in Table 3.1 show that the

matrix elements have minimal impact on the apparent Ra-226 recovery (ratio of measured to actual Ra-226 concentration) as long as [Ca] < 30 mg/L, [Ba] < 10 mg/L, [Na] < 10 mg/L, and [Sr] < 5 mg/L. Ra-226 recovery obtained using the standard mode and collision mode varied from 93%-109% and 91% - 108%, respectively. Ra-226 recovery decreased below 80% for samples containing more than 20 mg/L of barium.

Table 3.1 Impact of matrix elements on apparent Ra-226 recovery measured by NexION 300 ICP-MS

Interfering elements				**ICP-MS results**			
				Standard Mode		Collision Mode	
Na (mg/L)	Ca (mg/L)	Sr (mg/L)	Ba (mg/L)	Apparent Ra-226 Recovery	RSD	Apparent Ra-226 Recovery	RSD
1	-	-	-	98%	2%	96%	13%
5	-	-	-	101%	3%	98%	15%
10	-	-	-	99%	6%	96%	0%
-	1	-	-	99%	8%	98%	6%
-	10	-	-	93%	4%	91%	4%
-	20	-	-	96%	7%	91%	5%
-	-	1	-	100%	5%	92%	12%
-	-	5	-	101%	6%	95%	2%
-	-	-	1	100%	8%	97%	6%
-	-	-	5	101%	6%	94%	9%
-	-	-	10	105%	7%	94%	8%
-	-	-	20	81%	9%	-	-
-	-	-	40	62%	17%	-	-
1	1	1	1	104%	3%	91%	9%
1	5	0.1	2.5	109%	8%	107%	14%
5	10	0.1	5	101%	4%	94%	9%
5	10	0.1	10	106%	4%	108%	5%
5	15	0.1	10	104%	9%	103%	4%
10	30	0.1	10	106%	6%	95%	8%

3.3.3 Method development for Ra-226 separation and purification

Radium can be easily separated from monovalent and divalent cations that have small hydrated ionic radii, but it is difficult to separate it from barium because of similarities in chemical properties.[17, 21] The radium separation protocol developed in this study addresses these challenges by using two steps: 1) separation of radium, barium, and strontium from other cations and 2) separation of radium from the remaining barium and strontium. In this study, two methods, namely co-precipitation and solid-phase extraction were evaluated in the first step while solid-phase extraction was used to separate radium from barium and strontium in the second step.

3.3.3.1 Separation of Ra/Ba from other cations using co-precipitation

Radium has similar chemical properties to barium and strontium and tends to co-precipitate with $BaSO_4$ or $SrSO_4$ even when solution is not saturated with respect to $RaSO_4$.[31] The co-precipitation of Ra-$BaSO_4$ has been used to separate radium and barium from other matrix elements in a variety of environmental samples.[7, 28, 32, 33] Those studies employed alpha spectrometry or liquid scintillation counting to analyze radium because they did not require further separation of radium and barium. As indicated earlier, the key drawback of alpha spectrometry is that it requires long detection time (i.e., several days) while liquid scintillation typically requires attainment of secular equilibrium, which takes about 3 weeks.[32,33]

Analysis of Ra-226 by ICP-MS requires separation of radium from barium to eliminate barium interference. Previous study converted $BaSO_4$ into $BaCO_3$ by boiling in saturated K_2CO_3 solution[34] so that the carbonate mineral can be separated and dissolved in HNO_3 prior to further purification. A trial experiment with synthetic MSW was conducted to validate the effectiveness of this approach for high salinity solutions. 20 mL of 1M H_2SO_4 was added to 2 mL of synthetic MSW and heated at 80 ^oC for 1 hour to ensure complete co-precipitation of radium with $BaSO_4$. Precipitate was then separated by filtration, washed with 20 mL DI water, transferred into 15 mL of saturated K_2CO_3 (i.e., 8.12 M) and boiled for 3 hours. The resulting precipitate, which should be comprised mostly of $BaCO_3$, was filtered, washed with DI water and dissolved in 1M HNO_3. Concentrations of barium and radium in the solution were then measured to evaluate the chemical yield of $BaCO_3$ from $BaSO_4$ and associated radium recovery. Results showed that the chemical yield of $BaCO_3$ was 42.3% (n=3), indicating incomplete transformation of $BaSO_4$ to $BaCO_3$. As a consequence, radium recovery using this procedure was only 54.9% (n=3). Therefore, this method for the separation of radium and barium does not seem effective for the high salinity samples including wastewater from unconventional gas extraction.

3.3.3.2 Separation of Ra/Ba from other cations using solid-phase extraction

A strong-acid cation exchange resin with high capacity and physical stability along with low eluent flow rate are desirable when trying to enhance the effectiveness and reproducibility of radium separation.[30] Thus, a highly cross-linked resin (Bio Rad AG 50W-X8, 8% divinylbenzene) with relatively small spherical particles (100-230 U.S. Mesh) and gravity driven eluent flow (average flow rate of 0.33 mL/min) were widely used for separation of Ra/Ba from other cations[21,25] and were chosen for this study. Selectivity coefficients for different cations and

hydrogen-form 50W-X8 resin in HCl solution are listed in Table 3.2. Selectivity coefficient for radium is not reported but should be close to or slightly higher than that for barium because of similar chemical properties and a slightly larger ionic radius of radium.

Table 3.2 Selectivity coefficient (K) for AG50W-X8 in HCl[30]

Selectivity coefficient	**HCl**			
	0.1 M	0.5 M	1M	2 M
Ba^{2+}	$>10^4$	590	126.9	36
Sr^{2+}	4700	217	60.2	17.8
Ca^{2+}	3200	151	42.29	12.2
Na^{+}	52	12	5.59	3.6
Selectivity ratio K_H^{Ba}/K_H^{Na}	>192	49	22.7	10

Based on the results shown in Table 3.2, it is expected that most of the radium and barium and some of the strontium can be effectively separated from other cations by this resin. Previous studies used 50W-X8 resin to separate radium and barium from other cations in groundwater with very high radium recoveries (e.g., 97%).[16,21] In order to validate the effectiveness of Ba/Ra separation for the dramatically more saline MSW sample, elution profiles of major cations and Ra-226 were developed in this study when 2 mL of acidified synthetic MSW was loaded on 4 mL of preconditioned 50W-X8 resin. The loaded resin was first washed with 100 mL of 1.7M or 2.2M HCl followed by 25 mL of 6M HNO_3. The major cations and Ra-226 were measured in every 10 mL of the eluent. Results in Figure 3.1 indicate that either 80 mL of 1.7M HCl (Figure 3.1a) or 40 mL of 2.2M HCl (Figure 3.1b) will elute most of the sodium, magnesium, calcium, strontium and some of the barium from the resin. Barium and radium remaining on the resin were then eluted with 25 mL of 6M HNO_3. The lower molarity eluent

(i.e., 1.7M HCl) was selected for further validation to maximize separation of radium from other cations and minimize radium loss.

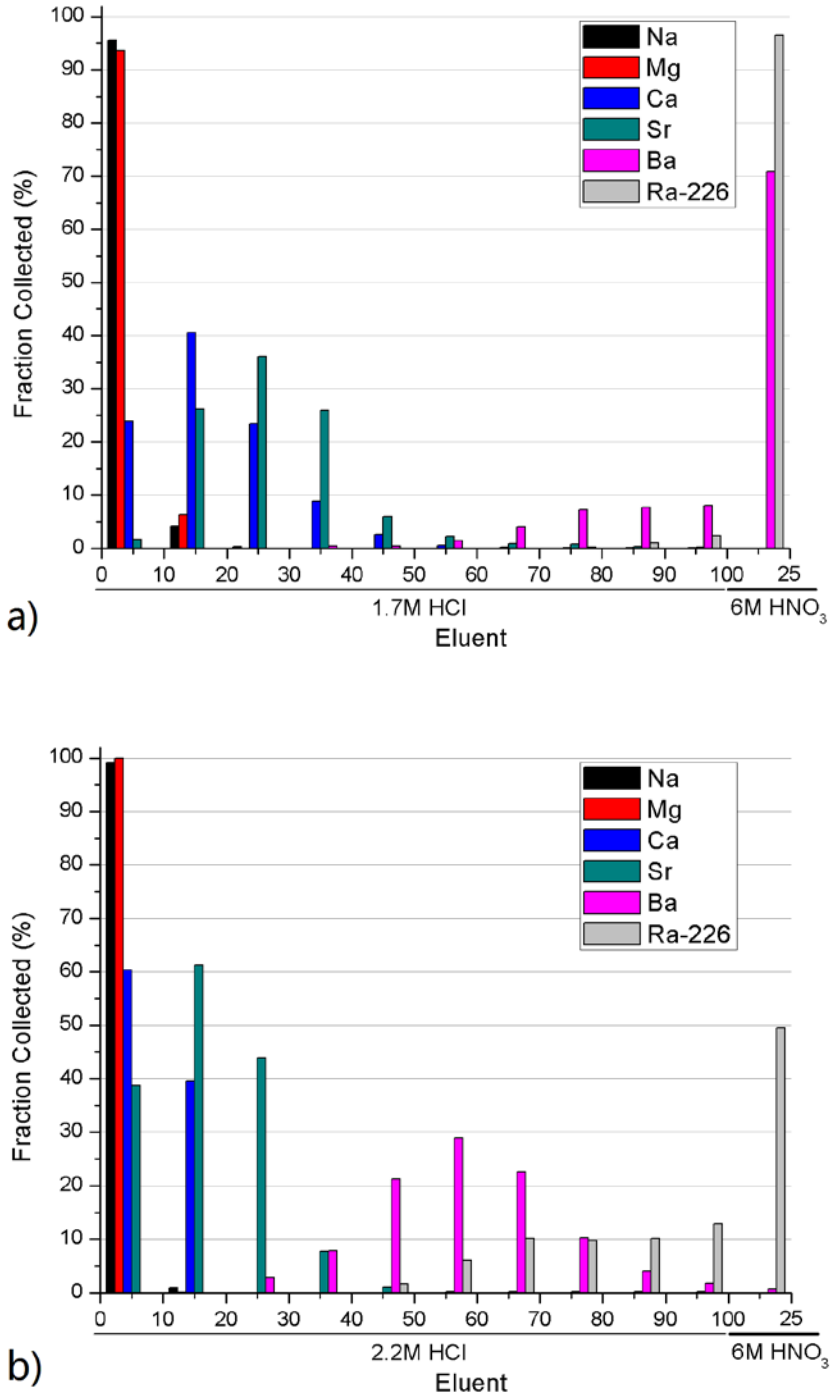

Figure 3.1 Elution profiles for major cations and Ra-226 in synthetic Marcellus Shale wastewater with (a). 1.7 M and (b) 2.2 M HCl from 4 mL of preconditioned 50W-X8 resin

3.3.3.3 Separation of Ra-226 from Ba and Sr

Previous work has shown that the uptake of alkali metal ions by a strong-acid exchange resin can be altered by the addition of crown ether functional groups.[17,35] The selectivity coefficient for radium on a Sr*Spec resin that contains 1M of 4.4'(5)-bis(t-butyl-cyclohexano)-18-crown-6 (crown ether) is more than 10 times lower than the selectivity coefficient for barium and strontium.[36,37] Previous studies have successfully separated radium from residual barium and strontium in groundwater and seawater using the Sr*Spec resin.[21,25] Even though barium and strontium concentrations in those samples are more than 10 times lower than in MSW samples, the same resin (i.e., Eichrom Sr*Spec resin) was used in this study to separate radium from remaining barium and strontium prior to ICP-MS analysis.

Two mL of synthetic solution containing 20mM of barium, 1mM of strontium and 50,000 pCi/L of Ra-226, which is representative of the eluent that is collected from the separation step with 50W-X8 resin, was evaporated to dryness, dissolved in 0.5 mL of 1M HNO_3 and passed through 1 mL of Sr*Spec resin. After that, 6 mL of 3M HNO_3 was used to selectively elute Ra-226 from the resin. Concentrations of Ra-226, barium and strontium were measured stepwise and are shown in Figure 3.2. These results indicate that 4.5 mL of 3M HNO_3 effectively elutes all Ra-226 from the Sr*Spec resin. However, the separation between radium and barium is not complete because 5% of barium was eluted with Ra-226, resulting in close to 60 mg/L of barium in the combined eluent. Previous study showed that the presence of barium and strontium interferes with Ra-226 measurement during ICP-MS analysis and that even 5 mg/L of barium and 5 mg/L of strontium could amplify the Ra-226 signal by as much as 50%.[18] The breakthrough of barium occurred because the Sr*Spec resin has a maximum capacity of

approximately 0.24 meq/mL and the working capacity should be between 10-20% of the maximum capacity to guarantee best performance.[36] Barium concentration in the Marcellus Shale wastewater is often very high[2] so that it could exceed the working capacity of Sr*Spec resin, thereby leading to poor separation between barium and radium.

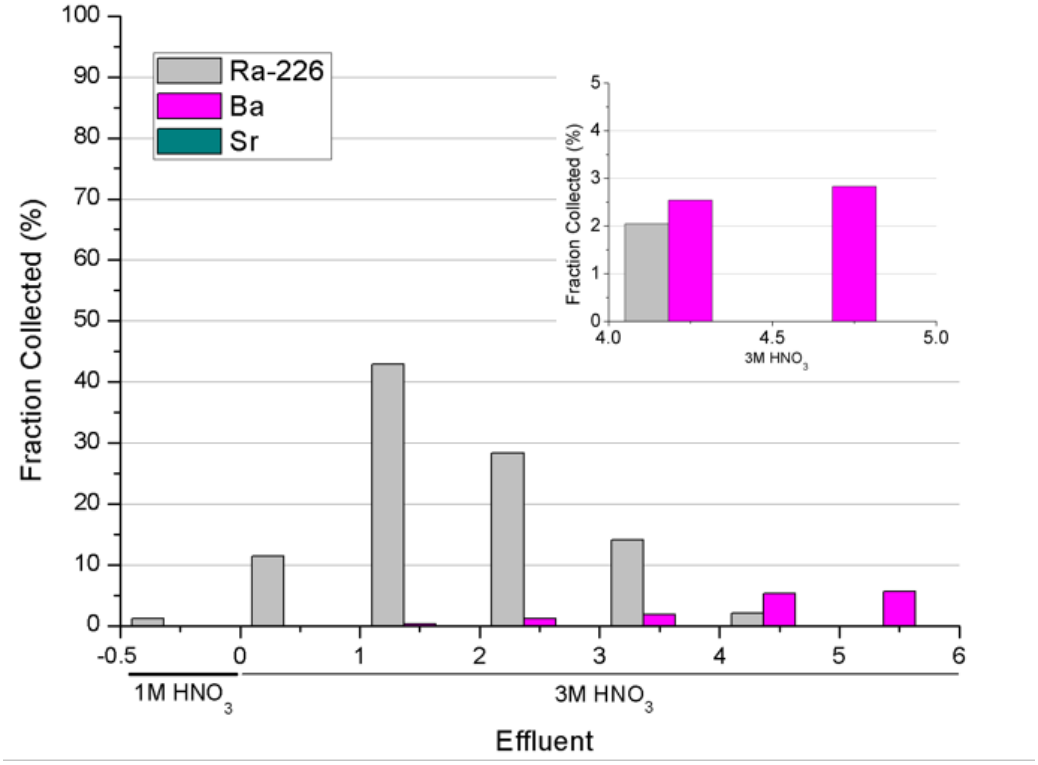

Figure 3.2 Elution profile for Ba, Sr and Ra-226 from Sr*Spec resin with 0.5 mL of 1M HNO_3 followed by 6 mL of 3M HNO_3

The impact of barium and strontium concentration on the performance of Sr*Spec resin was evaluated using synthetic MSW samples containing barium concentrations up to 80mM (11,000 mg/L) to represent the highest barium concentration reported in the Marcellus Shale wastewater[2] and Ra-226 concentration of 50,000 pCi/L. The results in Table 3.3 show that

barium breakthrough during elution with 3M HNO_3 can be substantial. If the initial Ba concentration in the sample is greater than 10 mM, barium concentrations in the final sample that would be injected in the ICP-MS will likely exceed 5 mg/L, which would cause strong interference during ICP-MS measurement. It is important to note that the radium recovery in 4.5 mL of 3M HNO_3 was consistently close to 100%.

Table 3.3 Impact of Ba and Sr concentration in the sample on the residual concentrations in the sample for Ra-226 analysis by ICP-MS

Element	Initial Concentration	Percent in Eluent		Expected Concentration in Purified Sample* (mg/L)
		0-0.5 mL 1M HNO_3	0-4.5 mL 3M HNO_3	
Ba	10 mM	0.0	0.4	4.8
Sr	1mM	0.0	0.0	0
Ba	20 mM	0.0	5.4	148
Sr	1 mM	0.0	0.0	0
Ba	40 mM	0.0	16.2	891
Sr	1mM	0.0	0.0	0
Ba	80 mM	0.0	24.2	2663
Sr	1mM	0.0	0.0	0

* Concentration in 2 mL of 2% HNO_3

Barium concentration in the eluent was reduced via a second separation step with Sr*Spec resin. After this second extraction step, the HNO_3 eluent was evaporated to dryness and re-dissolved in 2 mL of 2% nitric acid before analysis on ICP-MS. A schematic diagram of the optimized extraction procedure for the separation of radium from matrix elements in Marcellus Shale wastewater using a combination of 50W-X8 and Sr*Spec resin is shown in Figure 3.3.

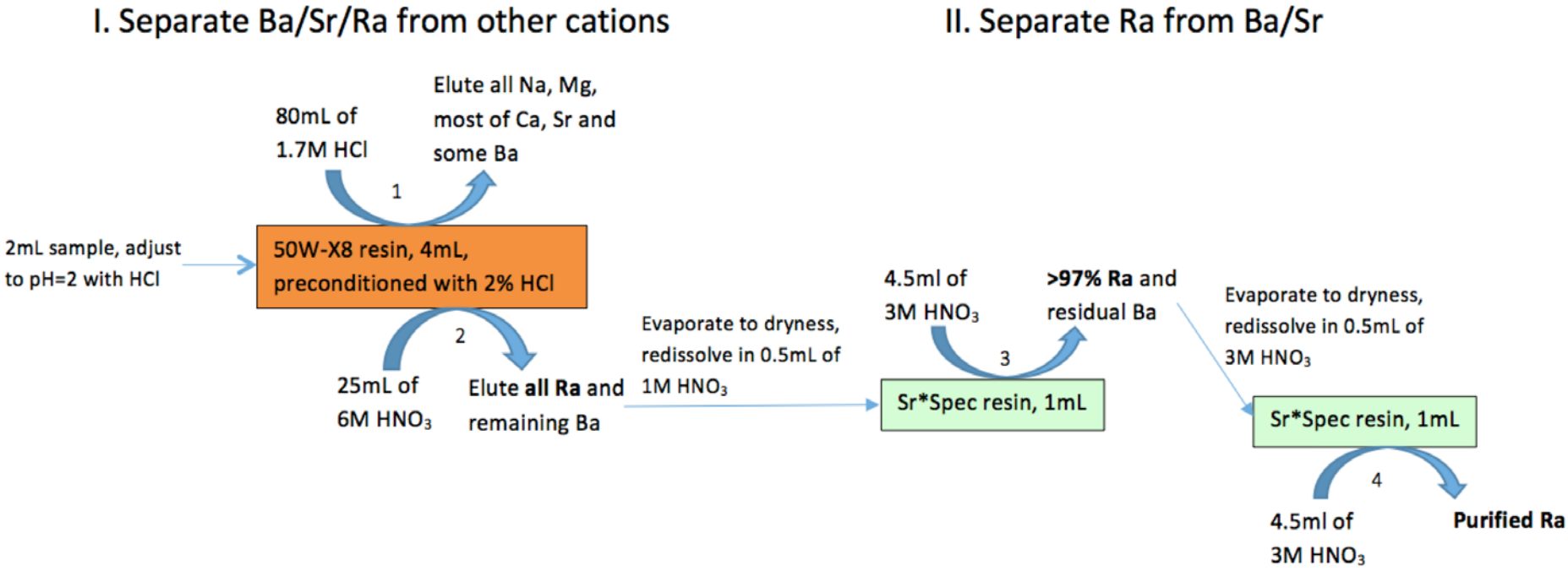

Figure 3.3 Schematic diagram of the separation protocol for Ra-226 analysis by ICP-MS in Marcellus Shale produced water

3.3.4 Radium-226 analysis in high salinity Marcellus Shale wastewater

In order to verify the analytical protocol developed in this study, four synthetic Marcellus Shale wastewater samples (Samples S1-S4) with varying salinities and concentrations of barium, strontium and calcium were analyzed for Ra-226 using the sample purification procedure depicted in Figure 3.3. Composition of synthetic MSW was selected based on typical characteristics of Marcellus Shale wastewater.[2] Samples S5-S7 reflect the use of regenerated Sr*Spec resin in the final step of Ra/Ba separation (2^{nd} purification step with Sr*Spec resin in Figure 3.3) to evaluate the possibility of reusing this relatively expensive resin. All samples were analyzed using ICP-MS in both standard and collision mode and the results are compared with reference values for Ra-226 measured using gamma spectrometry in Table 3.4.

Ra-226 recovery for these 4 synthetic wastewater samples using the procedure depicted in Figure 3.3 varied from 95-107% for analysis in the standard mode and between 90-104% in the collision mode. These results indicate excellent agreement between the analytical procedure developed in this study and widely accepted protocol using gamma spectrometry. Furthermore, they suggest that it may be possible to reuse Sr*Spec resin at least once to reduce the cost of this analytical procedure. The residual matrix elements in purified samples generally did not affect apparent Ra-226 recovery. The only exception was Sample S7 that had unusually high Ra-226 recovery, which is most likely due to high residual barium in the purified sample ([Ba] = 18 mg/L) caused by insufficient capacity of regenerated Sr*Spec resin to retain barium.

Table 3.4 Comparison of Ra-226 analysis in synthetic MSW samples by ICP-MS and gamma spectrometry

Sample	**MSW composition (mg/L)**					**Reference Ra-226 (pCi/L)**	**ICP-MS results**			
							Standard mode		Collision mode	
	Na	Ca	Ba	Sr	TDS		Ra-226 recovery	RSD	Ra-226 recovery	RSD
S1	11,500	3,440	1,060	808	28,500	5,000	101%	4%	90%	6%
S2	23,000	6,880	2,120	1,620	57,000	5,000	99%	5%	94%	2%
S3	46,000	13,760	4,230	3,230	114,000	5,000	104%	7%	91%	5%
S4	69,000	20,640	6,360	4,850	171,000	5,000	107%	6%	104%	1%
S5	11,500	3,440	1,060	808	28,500	5,000	100%	8%	90%	7%
S6	46,000	13,760	4,240	3,230	114,000	5,000	95%	5%	91%	8%
S7	69,000	20,640	6,360	4,850	171,000	5,000	118%	2%	97%	6%

Samples S1-S4 were purified by the procedure depicted in Figure 3.3; Samples S5-S7 were purified by the same procedure using regenerated Sr*Spec resin.

Nine actual MSW samples collected at different locations or different stages of Marcellus Shale wastewater management cycle were analyzed to further validate the effectiveness of the proposed analytical procedure. Samples 1-3 were collected during the early stages of the flowback period and have relatively low salinity and low concentration of matrix elements. Samples 4-5 were collected from two MSW storage impoundments after several cycles of MSW reuse for hydraulic fracturing and samples 6-9 were collected from gas wells that have been in production for as long as 2.5 years. All samples were analyzed using ICP-MS and compared with Ra-226 measurement by gamma spectrometry in Figure 3.4. Excellent agreement between analytical results obtained using the two analytical methods suggest that the ICP-MS protocol developed in this study is accurate and robust for a variety of unconventional gas wastewaters that may be encountered in different shale plays. Ra-226 recovery by the ICP-MS protocol in these real MSW samples was significantly higher than that of synthetic samples and ranged from 94 - 144% for standard mode and 90 – 118% for collision mode (Table B.3). Such large variance in Ra-226 recovery is expected due to a large variance of gamma spectrometry measurement in this study (i.e., ±11-31%).

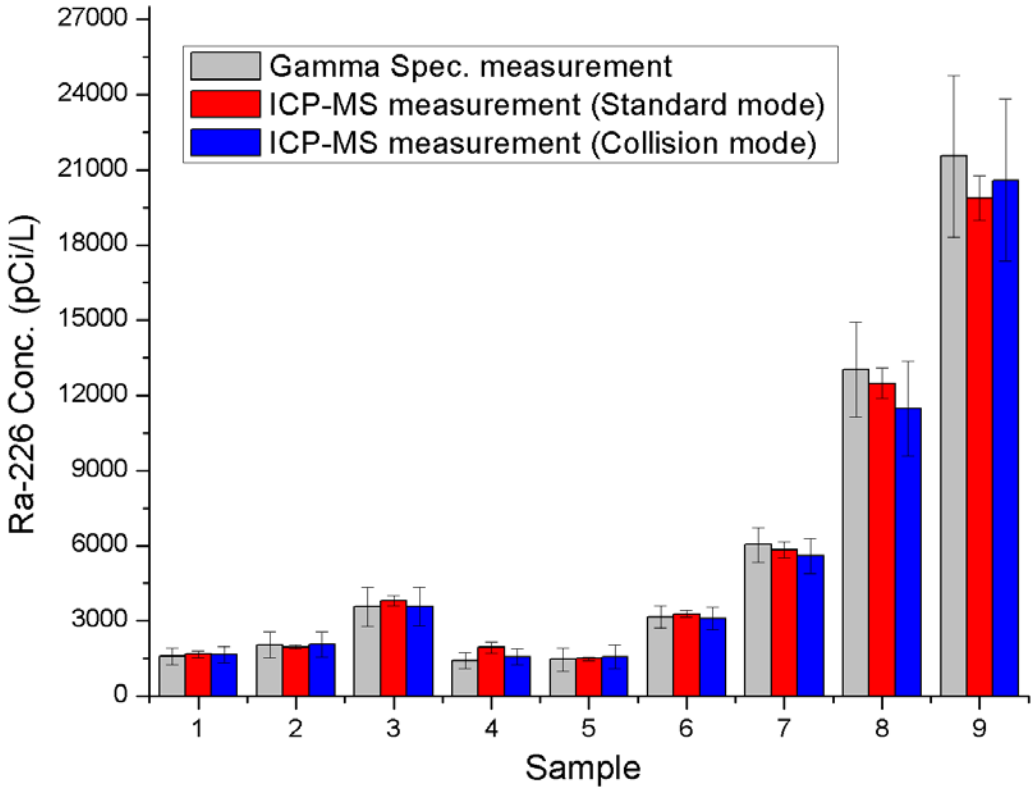

Figure 3.4 Comparison of Ra-226 analysis in field MSW samples by ICP-MS and gamma spectrometry

The combined use of 50W-X8 and Sr*Spec resins was very effective in separating sodium and strontium from both synthetic and field MSW samples regardless of salinity because their concentrations in the purified samples injected into the ICP-MS (residual concentrations) were consistently below 10 mg/L and 0.1 mg/L, respectively (Table B.3). The residual calcium and barium concentrations were slightly higher but most of the samples had residual calcium and barium concentrations below 30 mg/L and 10 mg/L, respectively. Based on the results shown in Table 3.1, such a low residual calcium and barium concentrations are not likely to cause significant matrix interference with ICP-MS detection. The only exception was the synthetic MSW Sample S7 that was prepared with reused Sr*Spec resin and had the highest initial (6,360

mg/L) and residual barium concentration (18 mg/L). If the purified sample does not meet the interference criteria for other ICP-MS models, it may be necessary to further purify the sample by increasing the volume of HCl eluent (Figure 3.3, step 1) to decrease residual sodium and calcium concentration or by adding another separation step with Sr*Spec resin to decrease residual barium concentration.

3.4 SUMMARY AND CONCLUSIONS

The primary objective of this study is to exploit the potential of ICP-MS for Ra-226 analysis. Traditional methods for Ra-226 determination require either a long sample holding time or a long detection time. Recent development in the ICP-MS or TIMS enables direct measurement of mass to charge ratio and could be used for rapid Ra-226 measurement. Marcellus Shale wastewater samples cannot be directly measured by ICP-MS due to its high TDS and matrix element concentrations.

This study shows that by careful control of radium recovery in each step to optimize the solid-phase extraction enabled the development of a reliable procedure to separate radium from the matrix elements with very high radium recovery and can be analyzed by ICP-MS. The method developed in this study enables rapid and accurate analysis of Ra-226 even for samples with TDS as high as 415,000 mg/L. Average radium recovery in synthetic samples of Marcellus Shale wastewater was 101% ± 6% when ICP-MS was operated in the standard mode and 97% ± 7% when it was operated in the collision mode (Table 3.4). Although the initial results suggest that it may be possible to reuse Sr*Spec resin at least once, additional evaluation is needed because of potential polyatomic interferences with Ra-226 analysis by ICP-MS in standard

mode. However, it is possible to effectively remove this interference if ICP-MS is configured in the collision mode. The results obtained in this study indicate that it is critical to maintain residual barium and calcium concentrations in the purified sample injected in the ICP-MS below 30 and 10 mg/L, respectively to achieve accuracy and reproducibility of Ra-226 measurements.

4.0 FATE OF RADIUM IN CENTRALIZED TREATMENT PLANT (CWT)

This work has been published as:

Zhang, T., Gregory, K., Hammack, R. W., & Vidic, R. D. (2014). Co-precipitation of Radium with Barium and Strontium Sulfate and Its Impact on the Fate of Radium during Treatment of Produced Water from Unconventional Gas Extraction. Environmental Science & Technology, 48(8), pp. 4596-4603.

Flowback and produced waters generated from hydraulic fracturing for unconventional gas extraction containing high concentrations of Ra, Ba, Sr and elevated salinity. This wastewater was often sending to centralized treatment facilities to remove the heavy metals prior to disposal or reuse and sulfate precipitation is the most common methods for heavy metal. This study investigates the fate of Radium during the sulfate precipitation in centralized treatment plant. Radium is often removed from this wastewater by co-precipitation with barium or other alkaline earth metals. Distribution equation for Ra in the precipitate is derived from the equilibrium of the lattice replacement reaction (inclusion) between Ra^{2+} ion and the carrier ions (e.g., Ba^{2+}, Sr^{2+}) in aqueous and solid phases and is often applied to describe the fate of radium in these systems. This study evaluates the equilibria and kinetics of co-precipitation reactions in Ra-Ba-SO_4 and Ra-Sr-SO_4 binary systems and in Ra-Ba-Sr-SO_4 ternary system under varying ionic strength (IS)

conditions that are representative of brines generated during unconventional gas extraction. Results show that radium removal generally follows theoretical distribution law in binary systems and is enhanced in Ra-Ba-SO_4 system and restrained in Ra-Sr-SO_4 system by high ionic strength. However, experimental distribution coefficient (K_d') varies over a wide range and cannot be described by the distribution equation that does not account for radium removal by adsorption. Radium removal in ternary system is controlled by the co-precipitation of Ra-Ba-SO_4, which is attributed to rapid $BaSO_4$ nucleation rate and closer ionic radii of Ra^{2+} with Ba^{2+} than with Sr^{2+}. Overall, sulfate precipitation is effective to remove >90% of Ra from produced water as long as all Ba has been removed. And the co-precipitation of Ba-Ra-SO_4 is the dominant mechanism to account for the Ra removal. Calculations based on experimental results show that Ra levels in the precipitate generated in centralized waste treatment facilities far exceed regulatory limits for disposal in municipal sanitary landfills and require careful monitoring of allowed source term loading (ASTL) for technically enhanced naturally occurring materials (TENORM) in these landfills.

4.1 INTRODUCTION

Radium-226/228 is formed by natural decay of uranium-238 and thorium-232 and it occurs in natural gas brines brought to the surface following hydraulic fracturing.[1] Because radium is relatively soluble over a wide range of pH and redox conditions, it is the dominant naturally occurring radioactive material (NORM) and an important proxy for radioactivity of waste streams produced during unconventional gas extraction.[2,3] Radium is a member of alkaline-earth

group metals and has properties similar to calcium, strontium and barium. Oral radium uptake can lead to substitution of calcium in bones and ultimately long-term health risks. Radium-226 activity in Marcellus Shale produced water ranges from hundreds to thousands pCi/L with a median of 5,350 pCi/L.[1] The total Radium limit for drinking water and industrial effluents is 5 and 60 pCi/L, respectively.[4]

Radium activity in flowback water from the Marcellus Shale play shows positive correlation with total dissolved solids (TDS) and barium content despite the differences in reservoir lithologies.[1,5] This finding is consistent with the fact that the radium-to-barium ratio is often constant in unconfined aquifers in natural systems, implying that the radium co-precipitation into barite controls the activity of radium.[6] The high TDS (680 mg/L to 345,000 mg/L)[7] in produced water from Marcellus Shale gas wells is one of the main considerations when choosing a proper radium treatment technology. While there are several treatment options for radium removal, none is as cost-effective in high TDS brines as sulfate precipitation.[8] Despite a very low solubility product for $RaSO_4$ ($K_{sp,RaSO4} = 10^{-10.38}$), [9] it is not likely to observe pure $RaSO_4$ precipitate because of very low radium concentrations in the produced water. However, radium may co-precipitate with other carrier metals.

Distribution equation has been intensively used to describe the co-precipitation of a soluble tracer with a carrier ion. Sulfate-based co-precipitation of radium in a binary system with barium has been examined previously[6, 9-12] and is described by the following distribution equation:

$$\frac{RaSO_4}{MSO_4} = K_d \frac{Ra^{2+}}{M^{2+}}$$

where, K_d is concentration-based effective distribution coefficient, MSO_4 and $RaSO_4$ are relative fractions (or "concentrations") of carrier and radium in solid precipitate and M^{2+} and

Ra^{2+} are equilibrium concentrations in solution. Derivation of theoretical distribution coefficient with associated thermodynamic parameters is summarized in Appendix C. Theoretical distribution coefficients of Ra in $BaSO_4$ and $SrSO_4$ in dilute solution are 1.54 and 237, respectively. Increase in the ionic strength of solution would lead to a decrease in the activity coefficients for Ra^{2+}, Ba^{2+} and Sr^{2+} as shown on Figure C.1. Changes in the activity coefficient ratio of tracer and carrier ion, which is critical when calculating distribution coefficient in binary systems (Equation C.9), are much more pronounced in the case of Sr^{2+} than Ba^{2+} (Figure C.1). Consequently, the theoretical distribution coefficient for Ra-Sr-SO_4 exhibits more than 50% decline when the ionic strength increased to 3M while the decrease in the case of Ra-Ba-SO_4 was less than 10% (Figure 4.1). Based on this analysis, it can be expected that an increase in the ionic strength of solution would have a much greater impact on the removal of Ra^{2+} by co-precipitation with $SrSO_4$ than with $BaSO_4$.

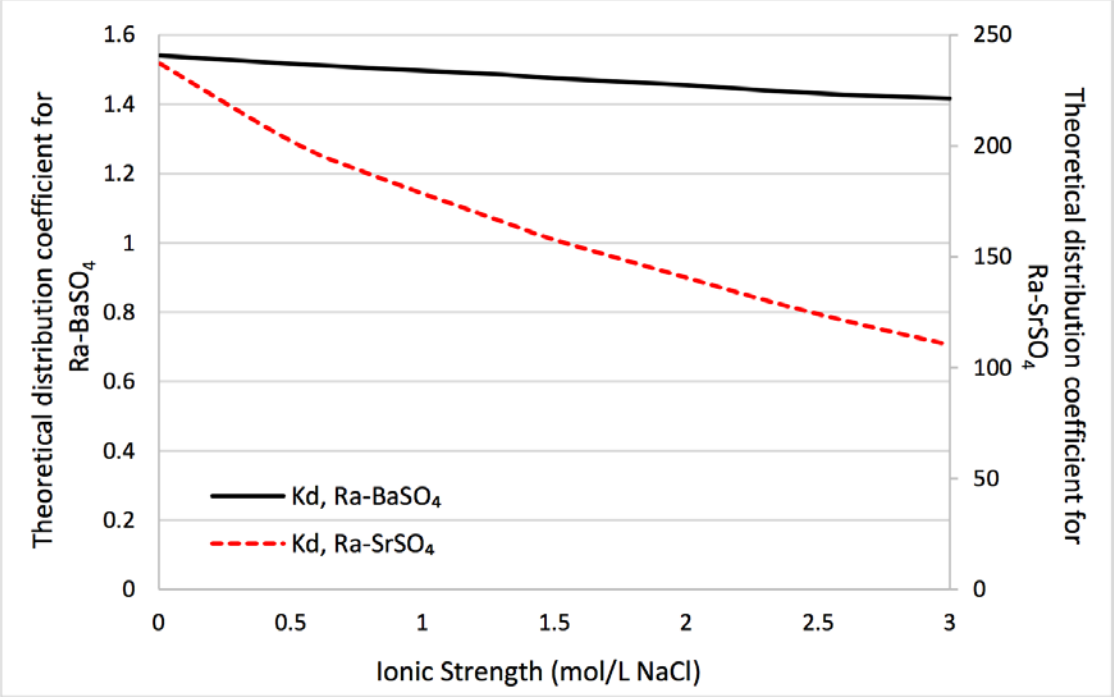

Figure 4.1 Theoretical distribution coefficient ($K_{d,Ra\text{-}MSO4}$) for Radium in $BaSO_4$ and $SrSO_4$ as a function of ionic strength

Even though the distribution equation has been used extensively to explain the co-precipitation reactions, it has several limitations. First, the presence of electrolytes in solution changes the surface properties (i.e., particle size/morphology, etch pits, etc.) of the carrier[13] and affects radium removal. Second, the distribution equation assumes that the ions in solution are in equilibrium with the ions throughout the entire solid phase.[14] However, the degree of Ra incorporated into the crystal would be uneven throughout the co-precipitation process if the crystal growth rate is faster than the rate of lattice replacement because the lattice replacement has not reached equilibrium during nucleation and crystal growth. Previous study showed that reduction in barite precipitation rate significantly increased Ra removal by co-precipitation.[15]

In addition, co-precipitation is a broad term to illustrate the phenomenon where a soluble substance is included into a carrier precipitate, which actually involves three distinct mechanisms: inclusion, occlusion, and adsorption (Figure 4.2).[16] Inclusion, or lattice replacement reaction, occurs when a tracer (i.e., Ra^{2+}) occupies a lattice site in the carrier mineral (e.g., barite, celestite) resulting in a crystallographic defect with the tracer in place of the main cation. Occlusion refers to the phenomenon where a tracer is physically trapped inside the crystal during crystal growth, which can be explained by the entrapment of solution or by adsorption of tracer during the crystal growth.[15-18] However, occlusion is not likely to play a major role in Ra removal during barite precipitation because of the low moisture content of barite crystal (< 3.5%)[17] and because Ra is present in solution at very low levels. Adsorption occurs when the tracer is weakly bound at the surface of the precipitate.[16] As described in the Supporting Information, distribution equation reflects only the inclusion (lattice replacement) mechanism while neglecting contributions to tracer uptake by adsorption and occlusion. Even though

occlusion is a minor mechanism for Ra removal, neglecting adsorption and occlusion during tracer uptake and kinetic effects would inevitably lead to uncertainty in theoretical predictions.[6]

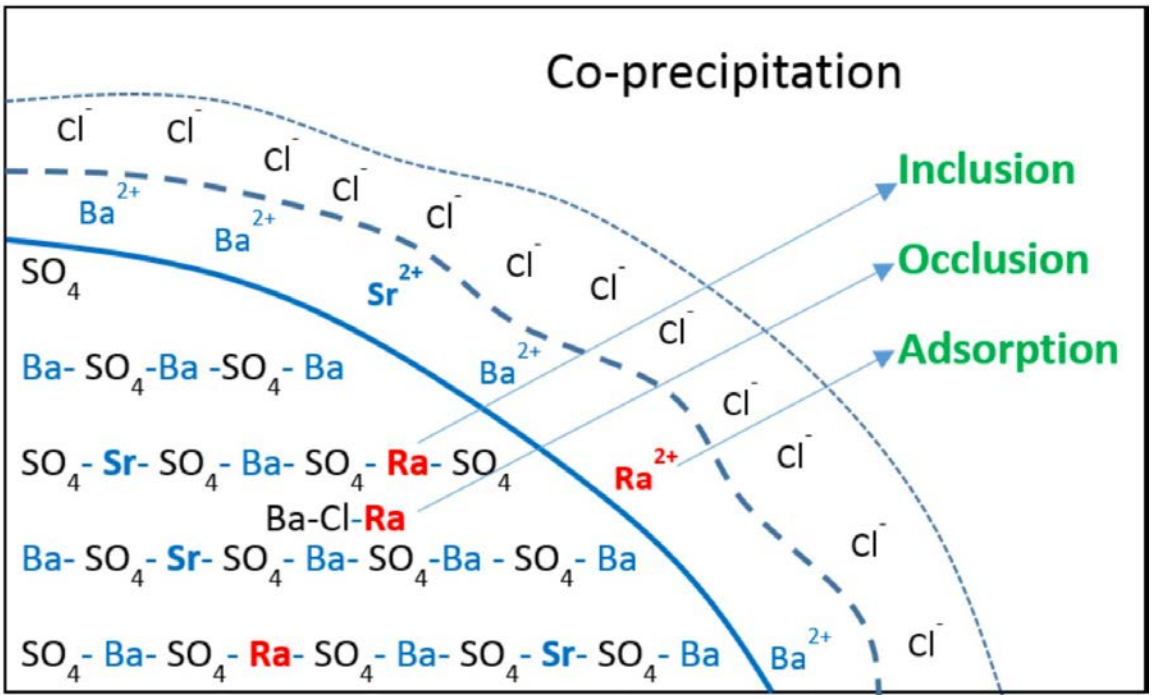

Figure 4.2 Three mechanism (inclusion, occlusion and adsorption) of Radium co-precipitation in binary solution with Ba-SO_4

This study focuses on understanding the fundamental mechanisms of Ra co-precipitation in Ba/Sr-SO_4 binary and ternary systems at high saturation levels and at different ionic strengths. The mechanisms of inclusion and adsorption for Ra incorporation in the precipitate were distinguished by carefully controlling test conditions so that experimentally determined distribution of key species in both Ra-Ba-SO_4 and Ra-Sr-SO_4 co-precipitation experiments can be compared with theoretical predictions and Ra leaching from solids generated during co-precipitation and post-precipitation studies. Impact of precipitation kinetics, activity coefficient ratios and volumetric mismatch between substituting end-members were analyzed as key factors influencing the fate of radium during co-precipitation with barite and celestite. Additionally,

uptake of radium by barite and celestite post-precipitation was compared with co-precipitation process to understand the relative impact of inclusion, occlusion and adsorption on the overall radium removal in sulfate precipitation. This study further elucidates fundamental mechanisms influencing the fate of radium during chemical precipitation of divalent cations from produced water (i.e., sulfate precipitation) and associated implications for its reuse for hydraulic fracturing following treatment.

4.2 MATERIALS AND METHODS

Radium-226 source was obtained from Penn State University and analyzed using Gamma-spectrometer[23] with high-purity germanium detector (Canberra BE 202). Barium Chloride Dihydrate (99.0% min, Mallinckrodt Chemicals), Strontium Chloride Hexahydrate (99.0%, Acros Organics), Sodium Chloride (99.8%, Fisher Scientific), anhydrous sodium sulfate (100%, granular powder, J.T. Baker), trace metal grade nitric acid, (65-70%, Fisher), trace metal grade hydrochloric acid (37.3%, Fisher) were ACS grade. Commercial standards (Ricca Chemicals and Fisher) were used to calibrate atomic absorption spectrophotometer and Ultima Gold™ High flash-point LSC-cocktail (PerkinElmer) was used for liquid scintillation counter. All reagents were tested and found to be free of Radium.

The concentration of dissolved Ba and Sr was measured by atomic absorption spectrometry (Perkin-Elmer model 1000 AAS) with a nitrous oxide-acetylene flame. The filtrate was diluted in a 2% nitric acid and 0.15% KCl solution prior to analysis to limit interferences during metal analysis. Dilution ratios were chosen based on the linear range of this instrument.

Radium-226 activity was analyzed using Packard 2100 LSC through the direct measurement of radium-226.[19] 4 mL of the liquid sample was mixed with 14 mL of Ultima Gold™ universal LSC-cocktail and counted by LSC for 60 min in the specific energy range (170 KeV to 230 KeV) to reject any contribution that is not produced by radium-226. The sample with high ionic strength was corrected by quench factor, and the ingrowth of radioactivity was compensated by the ingrowth factor.[19,20] Samples were occasionally calibrated by Gamma spectrometer[21] to insure accuracy of radium-226 detection, especially at different salinities. Results showed that LSC analysis deviated from gamma spectrometry by less than 7.4%. Activity in both liquid and solid was measured for selected samples to validate mass balance for radium-226.

Co-precipitation experiments were performed in 50 mL HDPE tubes. Ionic strength was adjusted to 1, 2 or 3 mol/L with concentrated NaCl solution. Radium-226 stock solution was diluted to a target level of 10,000 pCi/L and the initial Ba^{2+} and Sr^{2+} concentrations were always 5 mmol/L. Different doses of sodium sulfate were added to adjust barium and strontium removal and pH was not controlled in these experiments. HDPE tubes were placed on a horizontal shaker to promote mixing. Aqueous samples were taken after 24 hours of reaction and filtered through 0.45 µm mixed cellulose esters membranes (MF-Millipore, HAWP) prior to analysis for radium-226, barium and strontium. Due to the relatively slow kinetics of $SrSO_4$ formation[13], Ra-Sr-SO_4 solutions were sampled after 5, 24 and 48 hours. Ionic strength was adjusted by adding NaCl into solution.

Radium removal by barite/celestite post-precipitation was studied by adding a specific amount of pre-formed solids (barite and/or celestite) into 10,000 pCi/L radium-226 solution. Barite and celestite were prepared from the solution composition that is identical to that used in

co-precipitation experiments to ensure identical particle morphology and size. After 24 hours of moderate shaking, aqueous samples were removed and filtered through a 0.45 μm membrane prior to radium-226 analysis.

Experiments were performed to examine the equilibrium and kinetics of Ra-Ba-SO_4 and Ra-Sr-SO_4 formation alone and in combination using the initial conditions listed in Table 4.1. The binary and ternary systems were studied at high ionic strength to simulate radium removal from brines generated by unconventional gas extraction. The distribution coefficient was calculated for each system and was compared with theoretical values. Both kinetics and equilibrium studies were conducted to provide fundamental understanding of the fate of radium during chemical precipitation employed to remove divalent cations from natural gas brines (i.e., sulfate precipitation) and facilitate its reuse for hydraulic fracturing.

4.3 RESULTS AND DISCUSSION

4.3.1 Impact of ionic strength on Ra removal by co-precipitation in binary systems

Radium removal and experimental distribution coefficient (K_d') for Ra-Ba-SO_4 co-precipitation at different ionic strengths (IS) is shown in Figure 4.3a. Radium co-precipitation in dilute solutions (i.e., IS of about 0.02 was due to addition of $BaCl_2$ and Na_2SO_4 only) was proportional to barium removal, which can be described by the distribution law. Decrease of Kd' with increase in Ba removal is expected because the inclusion of Ra into $BaSO_4$ during the initial stages of $BaSO_4$ precipitation decreases Ra concentration in solution, resulting in much lower Ra concentration to co-precipitate with subsequent $BaSO_4$. Experimental distribution coefficient

(K_d'=1.07 - 1.54) was always below the theoretical value (K_d=1.54) in dilute solutions, which can be attributed to the fast barite crystal growth at high supersaturation levels used in these experiments (Saturation Index (SI) = 3.7 - 4.6). Under these conditions, barite precipitation was completed within just 10 minutes, which adversely impacts radium removal because inclusion and occlusion processes only occur during nucleation and crystal growth of barite. Rosenberg et al.[22] reported that experimental K_d' can be as high as 3 when precipitation kinetics is controlled by continuously adjusting the concentration of reactants in the solution.

Dependence of distribution coefficient on ionic strength (Figure 4.1) suggests only a slight decrease in K_d for Ra-Ba-SO_4 with an increase in ionic strength. However, experimental results show that radium co-precipitation was enhanced in the presence of electrolytes with experimental K_d' increasing to 3.17 at I = 1.02 M and 7.49 at I = 3.03 M for barium removal of 10% (Figure 4.3b). Such high values of the distribution coefficient cannot be explained by thermodynamics of lattice replacement reactions. It has been reported that the solubility of $BaSO_4$ increases with ionic strength,[23,24] which would lead to a decrease in the equilibrium constant as shown by Equation 6 in Supporting Information. However, the solubility of $RaSO_4$ would also increase with ionic strength, which would offset the increase in $BaSO_4$ solubility. Hence, change in thermodynamic driving force at high salinity is an unlikely reason for enhanced radium removal.

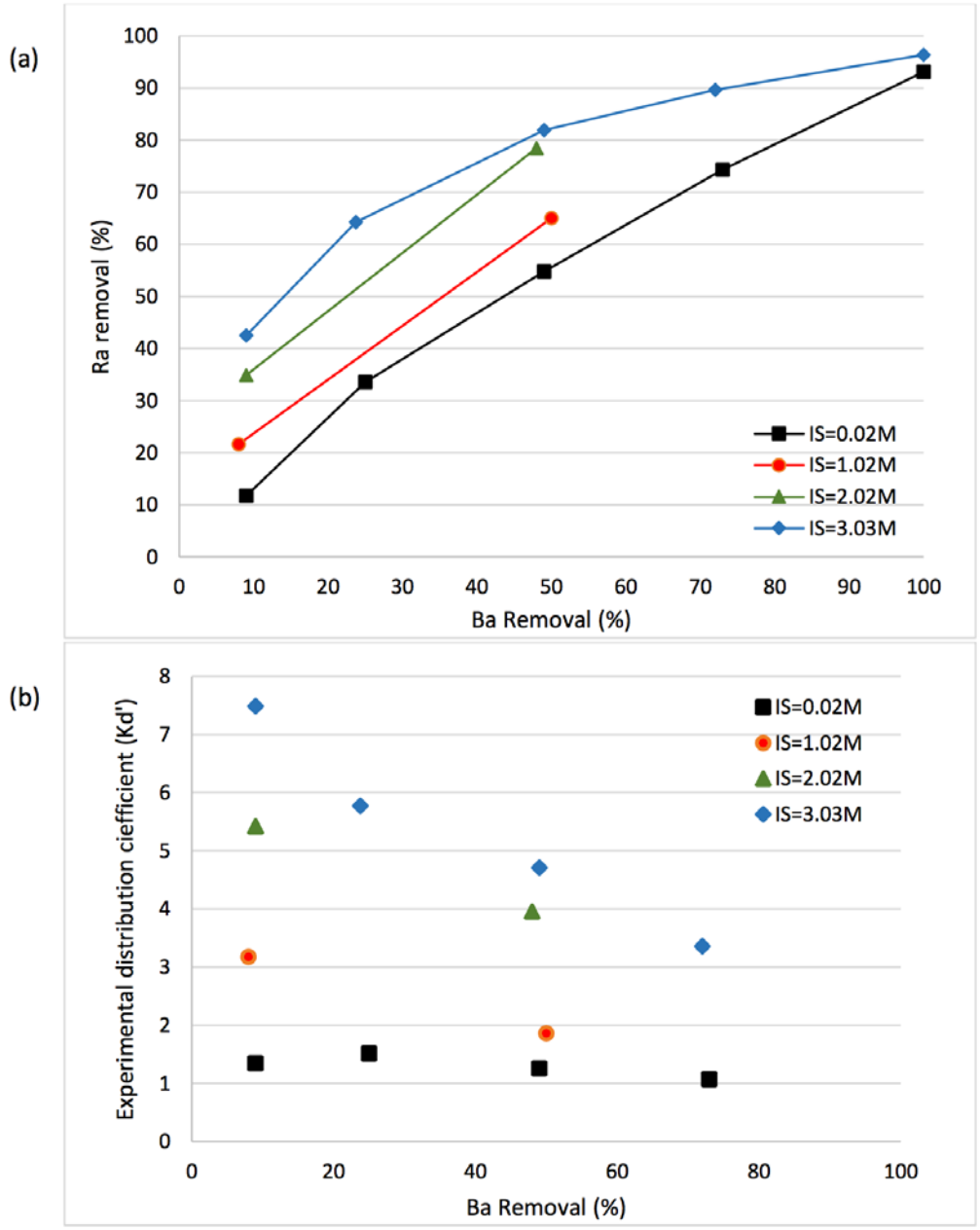

Figure 4.3 Radium co-precipitation with $BaSO_4$ as a function of barium removal at different ionic strengths adjusted with NaCl. (a) Radium removal and (b) experimental distribution coefficient. pH=7; $Ba^{2+}_{initial}$=5mM; Ba removal was adjusted with sulfate addition

There are several explanations for the increase in radium removal with an increase in ionic strength. First, the activities of electrolytes decrease with an increase in ionic strength (Table 4.1), which reduces supersaturation. Because nucleation of $BaSO_4$ follows the

homogeneous nucleation theory with diffusion controlled crystal growth,[25-27] a decrease in supersaturation leads to a sharp decrease in the nucleation rate[28] and a decrease in the crystal growth rate.[26] This reduction in the rate precipitation would enhance incorporation of Radium into the $BaSO_4$ as it would allow more time for lattice replacement reactions during the crystal growth. In addition, the increase in ionic strength would decrease the crystal-solution interfacial tension,[28] increase etch density,[29] and compress the electric double layer,[30] which increases the probability of Ra^{2+} reaction with $BaSO_4$ lattice.

Table 4.1 Experimental conditions for Ra removal in binary and ternary systems

System	Initial concentrations					Ion Activity			Saturation Index	
	NaCl (mol/L)	Ba (mmol/L)	Sr (mmol/L)	SO_4 (mmol/L)	IS (mol)	Ba (mmol/L)	Sr (mmol/L)	SO_4 (mmol/L)	SI_{BaSO4}	SI_{SrSO4}
Ba-Ra-SO_4 binary	0	5	0	0.5	0.0165	3.155	-	0.173	3.71	-
		5	0	1.25	0.01875	2.943	-	0.483	4.09	-
		5	0	5	0.03	2.146	-	1.9	4.58	-
	3	5	0	0.5	3.0165	1.276	-	0.02	2.22	-
		5	0	1.25	3.01875	1.277	-	0.349	2.62	-
		5	0	5	3.03	1.285	-	0.139	3.22	-
Sr-Ra-SO_4 binary	0	0	5	1.25	0.01875	-	3.01	0.537	-	0.85
		0	5	5	0.03	-	2.323	2.143	-	1.33
		0	5	10	0.045	-	1.773	4.164	-	1.51
	3	0	5	5	3.03	-	2.246	0.137	-	0.13
		0	5	10	3.045	-	2.234	0.273	-	0.42
		0	5	20	3.075	-	2.21	0.542	-	0.72
		0	5	50	3.165	-	2.142	1.324	-	1.09
Ba-Sr-Ra-SO_4 ternary	0	5	5	1.25	0.03375	2.674	2.767	0.339	3.92	0.6
		5	5	5	0.045	2.166	2.417	1.453	4.47	1.18
		5	5	10	0.06	1.702	2.016	3.064	4.69	1.43
	3	5	5	1.25	3.03375	1.279	2.255	0.035	2.62	-0.47
		5	5	5	3.045	1.286	2.246	1.382	3.22	0.13
		5	5	10	3.06	1.296	2.233	0.275	3.52	0.43

*SI=log(IAP/K_{SP}), where IAP=ion activity product; K_{SP}=solubility product; ionic strength was adjusted with NaCl; Activity coefficients were calculated using Pitzer equation.

High distribution coefficient for Ra-$SrSO_4$ co-precipitation (Figure 4.1) is attributed to large differences in solubility products of $RaSO_4$ ($K_{Sp,RaSO_4} = 10^{-10.38}$) and $SrSO_4$ ($K_{Sp,SrSO_4} = 10^{-6.63}$). However, the possibility of inclusion reaction decreases when the volumetric mismatch between the two end members (i.e., $RaSO_4$ and $SrSO_4$) is large,[31] which would significantly depress radium incorporation into $SrSO_4$ precipitate. The mismatch phenomenon can be quantified by the Margules parameter (W) as described in Table C.2. The Margules-corrected distribution coefficient for Ra-$SrSO_4$ (K_d =237) is very large compared with that for Ra-$BaSO_4$ (K_d =1.54), which implies that $SrSO_4$ should have stronger affinity for radium. Experimental results (Figure 4.4a) show that radium removal in dilute solutions is always around 80% regardless of Sr removal. Consequently, experimental distribution coefficient for Ra-$SrSO_4$ varies from 43 to below 1 (Figure 4.4b) and is much lower than the theoretical value.

Significant decrease in activity coefficient ratios of ($\frac{\gamma_{Ra^{2+}}}{\gamma_{M^{2+}}}$) at elevated ionic strength (Figure C.1) would reduce theoretical distribution coefficient. Theoretical distribution coefficient for Ra-$SrSO_4$ at IS = 3M of 110 is still very large compared with Ra-$BaSO_4$ (Figure 4.1). Experimental results show that radium removal is greater than 75% as long as Sr removal is greater than 8% (Figure 4.4a). The discrepancy of K_d and K_d' is attributed to the kinetic limit for Ra inclusion into $SrSO_4$ and underestimation of incompatibility (volumetric mismatch) of Ra-SO_4 in Sr-SO_4 lattice, which limits Ra removal at relatively short reaction times (<48 hours) and exacerbates the competition of Ra with other cations for lattice replacement reaction.

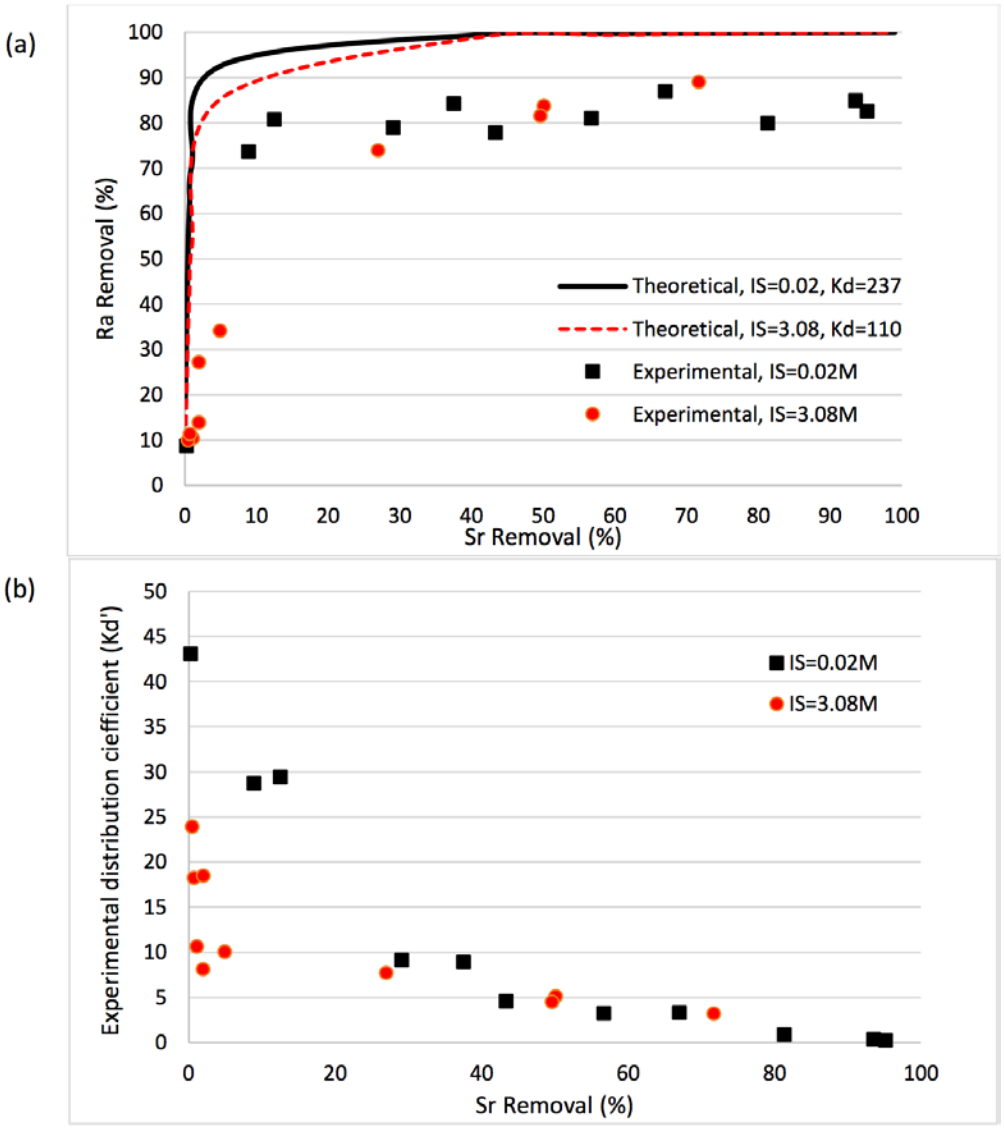

Figure 4.4 Radium co-precipitation with $SrSO_4$ as a function of strontium removal at different ionic strengths adjusted with NaCl: (a) Radium removal and (b) experimental distribution coefficient. pH=7; Sr removal is adjusted with sulfate addition (1.25-10mM for dilute system and 5-50mM for IS≈3)

4.3.2 Ra removal by co-precipitation in a ternary system

In actual flowback and produced water from unconventional gas extraction, both barium and strontium are present at concentrations that are of the same order of magnitude.[7] Synthetic

solutions used for the study of ternary system contained 10,000 pCi/L of radium and 5mM each of barium and strontium and the ionic strength was adjusted using sodium chloride. Sulfate dosage between 1.25 – 10 mM was added to control Ra-Ba-Sr-SO_4 precipitation and radium removal was compared to barium removal as a function of ionic strength (Table 4.1).

Since both $BaSO_4$ and $SrSO_4$ are good radium carriers, overall radium removal in the ternary system was expected to be enhanced by the synergy of the two co-precipitation processes. However, kinetics of $BaSO_4$ precipitation was much faster than that of $SrSO_4$ under the experimental condition used in this study because the saturation index for $BaSO_4$ (SI= 2.6 - 4.7) was much higher than that for $SrSO_4$ (SI= -0.47 - 1.43). Previous study[32] showed that the kinetic of $BaSO_4$ precipitation under similar conditions was much faster than $SrSO_4$ (i.e., $BaSO_4$ precipitation was completed within 30 minutes while it took several days for $SrSO_4$ to reach equilibrium). It is expected that faster $BaSO_4$ precipitation is likely to control radium removal by inclusion in the precipitate.

As shown in Figure 4.5, the dependence of radium removal on barium removal in Ra-Ba-Sr-SO_4 ternary system follows that for Ra-Ba-SO_4 binary system. Slight decrease in Ra removal observed in the ternary system can be attributed to the presence of Sr that competes with radium for co-precipitation with $BaSO_4$.[33]

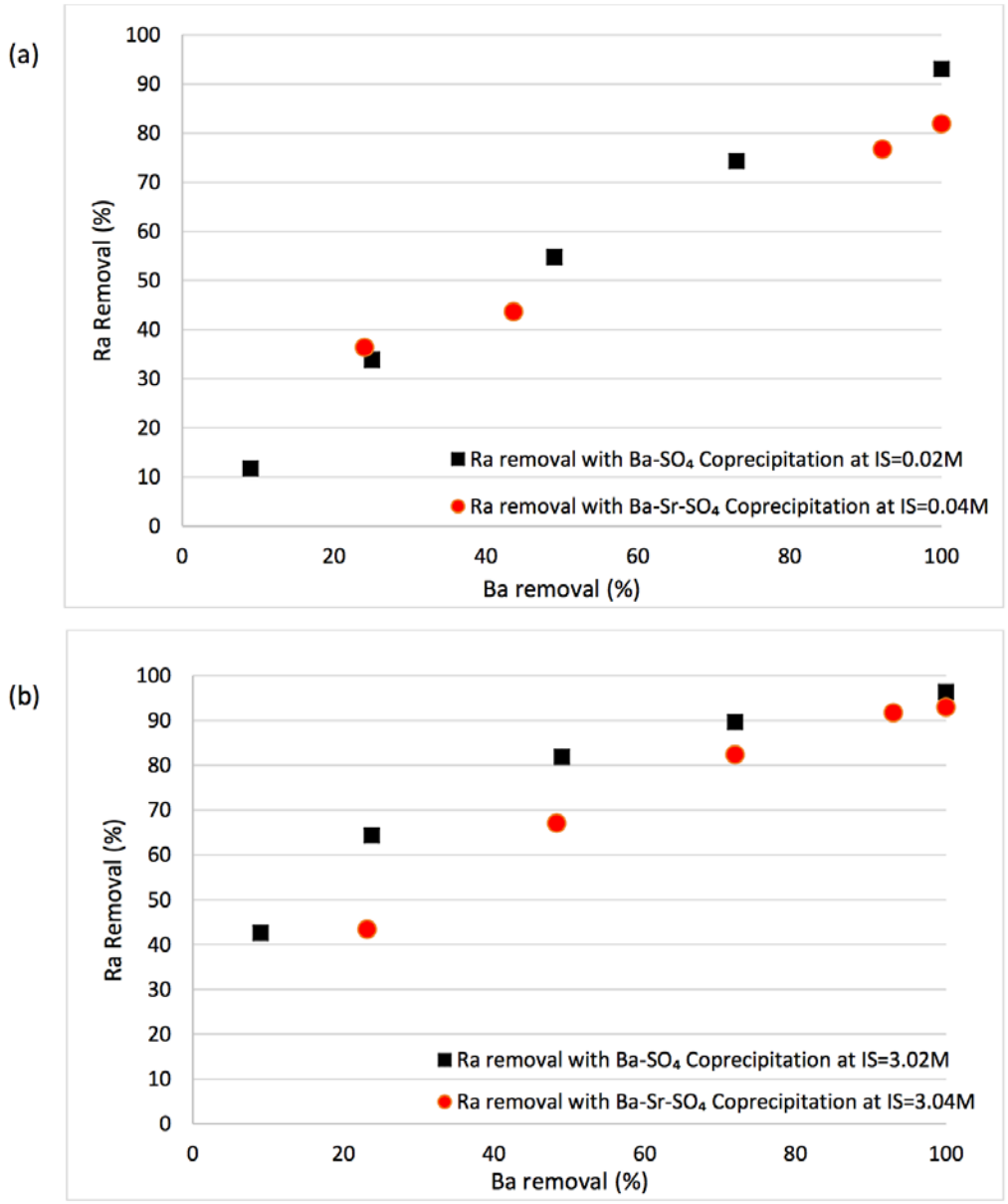

Figure 4.5 Radium co-precipitation with $BaSO_4$ and Ba-Sr-SO_4 systems; (a) Impact of Sr addition to Ra-Ba-SO_4 in dilute solution; (b) Impact of Sr addition to Ra-Ba-SO_4 in solution with elevated ionic strength. Initial Ba and Sr concentrations were 5mM; Ba removal was controlled by sulfate addition (sulfate addition up to 10mM was needed to precipitate $SrSO_4$ in ternary system at high ionic strength)

To verify that $BaSO_4$ is the main Ra carrier in Ba-Sr-SO_4 system, precipitates created in binary and ternary systems were collected on 0.45µm filter membrane and added into 50 mL of 5mM barium and strontium solution to suppress re-adsorption of radium on the remaining solids.

Hydrochloric acid was then added to adjust pH to 0.5 and dissolve $SrSO_4$. After that, aqua regia was added to dissolve any remaining solids and radium mass balance closure above 80% was required to accept the results from these tests. Dissolution of Ra, Ba and Sr from the solid phase at pH=0.5 is summarized in Table 4.2.

Table 4.2 Radium, barium and strontium dissolution from solids generated in binary and ternary co-precipitation systems after 24 h at pH=0.5

Sample	Initial Concentration [mmol/L]			Solids Concentration [mg/L]	Fraction Dissolved [%]		
	Ba	Sr	SO4		Ba	Sr	Ra
Ba-Ra-SO_4 binary	5	-	5	1167	3.0	-	5.4
Sr-Ra-SO_4 binary	-	5	5	918	-	47.0	73.3
Ba-Sr-Ra-SO_4 ternary	5	5	10	2085	3.0	51.0	6.7

*Initial Ra concentration in all tests was 10^4 pCi/L

The results for Sample A obtained using the solids precipitated in Ra-Ba-SO_4 binary system show that very little radium was released into solution (5.4%) at pH 0.5 when $BaSO_4$ was the only radium carrier. This is expected because there was minimal (3.0%) $BaSO_4$ dissolution at pH 0.5. Test with Sample B that was obtained using the solids precipitated in Ra-Sr-SO_4 binary system showed that strontium dissolution was significant at pH=0.5 (47.0%) and that a large fraction of radium was released into the solution (73.3%) under these conditions. Higher percentage of radium released to solution compared to strontium indicates that radium is not tightly bound in $SrSO_4$ lattice, which can be explained by the large molecular volume mismatch between the two (Table C.2). In the Sample C collected from the Ra-Ba-Sr-SO_4 ternary system, only 6.7% of radium was released to the solution after 24h at pH=0.5 while the fractions of

strontium (51.0%) and barium (3.0%) released to the solution were similar to those observed in the case of binary systems. Very low radium release from solids collected in both Ra-Ba-SO_4 and Ra-Ba-Sr-SO_4 system confirmed that radium is mainly bound to $BaSO_4$ solids during Ra-Ba-Sr-SO_4 co-precipitation.

4.3.3 Co-precipitation versus post-precipitation for radium removal

Co-precipitation is defined as simultaneous removal of both tracer and carrier from an aqueous solution and is due to inclusion (lattice replacement), occlusion and adsorption reactions (Figure 4.2). The term post-precipitation refers to tracer removal by previously formed carrier precipitate when only lattice replacement and adsorption are feasible removal mechanisms. Removal of Ra by preformed barite and celestite may be an important mechanism for Ra sequestration in a treatment process that uses solids recycling to enhance the precipitation kinetics in the reactor and was evaluated in this study using the experimental conditions outlined in Table 4.3.

Table 4.3 Radium post-precipitation removal by preformed barite and celestite

Adsorbent	Solid concentration (g/L)	Solution Composition	Ra Removal after 24 hours	Ra desorption ratio	Ra desorption (pCi/L)b
Barite	0.2	Deionized Water (D.I.)	84.3%	36.2%	3052
	0.5	D.I.	84.0%	19.3%	1621
	1	D.I.	87.2%	11.6%	1012
	1	5mM Ba	32.0%	24.8%	794
	1	5mM Ba; 5mM Sr	29.5%	26.4%	779
	1	3M NaCl	94.8%	4.1%	389
	5	5mM Ba	66.2%	15.6%	1033
	10	5mM Ba	81.9%	14.1%	1155
Celestite	1	D.I.	85.9%	-	-
	1	5mM Sr	52.7%	-	-
	1	5mM Ba	69.8%	-	-

*All samples were equilibrated for 24 hours; Initial Ra concentration in all test was 10^4 pCi/L;

[a] Ra desorption percentage denotes the desorbed amount as a percentage of total Ra present in the carrier

[b] Ra desorption denotes the total activity of Ra desorbed from the carrier.

The first set of experiments revealed that radium post-precipitation removal by barite did not change much even as barite concentration varied from 0.2 to 1 g/L. In addition, when radium enriched barite was returned into a fresh radium solution (10,000 pCi/L in D.I water), radium removal was the same as for a freshly prepared barite (Table 4.4). Such behavior can be explained by the fact that the impurities (i.e., radium) in the $BaSO_4$ lattice are always negligible ($<2.6\times10^{-8}$ g Ra/g Barite) even after 5 cycles of barite reuse, which makes fresh and reused barite identical in terms of their ability to remove radium.

Table 4.4 Post-precipitation of Radium in recycled barite in deionized water

Adsorbent	Solid Amount	Initial Ra Conc. in Barite (pCi Ra/g Barite)	Solution Composition	Ra Removal
Barite	1g/L	0	10,000 pCi/L Ra	84.30%
	1g/L	8430		87.47%
	1g/L	17177		84.87%
	1g/L	25664		85.07%

*All samples were measured after 24 hours.

In order to identify the extent of radium adsorption on preformed solids in comparison with inclusion, desorption studies were performed at pH 0.5 for 24 hours. Desorption ratio is defined as the fraction of total radium in the solids that is released into the solution. Table 4.3 show that most of the radium was strongly bound to barite lattice under experimental conditions evaluated in this study. Desorption ratio decreased with increasing barite dose, suggesting that adsorption is less significant radium removal mechanism during post-precipitation compared to inclusion.

Ra post-precipitation removal by preformed barite is strongly suppressed in the presence of Ba in solution (Table 4.3) because of the competition for inclusion into the barite matrix. The adverse impact of Sr in solution is not as substantial due to significant volumetric mismatch between $BaSO_4$ and $SrSO_4$. Ionic strength has similar impact on radium incorporation into barite in the case of post-precipitation (Table 4.3) as it did in the case of co-precipitation (Figure 4.3) as demonstrated by an increase in radium removal with an increase in ionic strength.

Radium removal by the preformed celestite was strongly depressed in the presence of competition ions (i.e., strontium or barium). This phenomenon was expected because the effective solid-solution interface area for inclusion reactions is limited in the absence of the crystal growth phase during post-precipitation uptake of radium. However, the decreases in

radium removal in the presence of competing ions is less pronounced compared with $BaSO_4$ post-precipitation, which is expected due to very high theoretical distribution coefficient for Ra-$SrSO_4$ and much lower solubility of $SrSO_4$.[34] Desorption of Ra-$SrSO_4$ was not evaluated since celestite is largely dissolved at pH=0.5.

4.3.4 Implications for flowback/produced water treatment by sulfate precipitation

Flowback/produced water generated from Marcellus Shale gas extraction was initially treated in municipal wastewater treatment facilities that are generally not capable of removing TDS and high conductivities were reported in Monongahela River basin[35] as a result of this practice. The PA Department of Environmental Protection then issued a request in mid-2011 to exclude municipal treatment facilities from this practice and industry complied.[36] Centralized waste treatment (CWT) facilities play a major role in treatment of Marcellus Shale wastewater prior to disposal or reuse in subsequent hydrofracturing operations.[36,37] The volume of unconventional gas wastewater treated in these facilities increased from 644.4 million liters in 2008 to 1752.8 million liters in 2010.[37] Sulfate precipitation is a common practice CWT facilities for barium, strontium and radium removal.

Based on the behavior of Ra-Ba-Sr-SO_4 ternary system at high ionic strength documented in this study it can be concluded that Ra inclusion in $BaSO_4$ is likely the primary mechanism for its removal in CWT facilities that employ sulfate precipitation. Experimental distribution coefficient for Ra in $BaSO_4$ ranges from 1.07 to 1.54 for dilute solution and 1.86 to 7.49 at IS≈3M, suggesting that Ra removal in CWT facilities will be higher than Ba removal. This study also suggests that it would be beneficial to recycle barite solids in the treatment process to enhance Ra removal because recycled barite (i.e., Ra-enriched barite) showed very similar Ra

removal compared with freshly prepared barite (Table 4.4). Once radium is incorporated into the barite lattice, it is unlikely to desorb even at very low pH (e.g., pH = 0.5).

Recent study on the impact of shale gas wastewater disposal on water quality in western PA revealed elevated levels of radium in sediments at the point of discharge from a CWT facility.[38] Because the CWT evaluated in that study employed sulfate precipitation to achieve over 90% Ba removal, it is expected that Ra concentration in the effluent would be about three orders of magnitude lower than in the raw wastewater. Continuous low level flux of Ra into the receiving stream would lead to increase in Ra content of the sediments downstream of the discharge point.[36] It is also possible that some of the Ra discharge into the receiving stream would be in the form of barite solids containing co-precipitated Ra that were not captured in the CWT. High density of barite (4.5 g/cm^3) would lead to a fairly limited transport of insoluble barite downstream of the CWT and contribute to TENORM buildup in the river sediments.

Assuming an average initial Ra and Ba concentration in flowback water treated at a CWT facility of 3,000 pCi/L[38] and 5 mmol/L[7], respectively, the estimated level of Ra activity in precipitates would range from 2571 to 18087 pCi per gram of $BaSO_4$, depending on Ba removal and distribution coefficient (Figure 4.6). Compared with TENORM limits for municipal waste landfills, which range from 5 to 50 pCi/g depending on state regulations (Ra levels in the solids produced in these CWT facilities far exceed these limits. Municipal waste landfills are the main disposal alternative for this solid waste as long as they do not exceed Allowed Source Term Loading (ASTL) for TENORM on an annual basis.[39] However, a back-of-envelope calculation for the total generation and landfill capacity for Ra in Pennsylvania shows the landfill itself is not capable to accepting all the Ra generated from the Marcellus Shale gas extraction (Appendix D). Therefore, sustainable management of solid radioactive waste produced in these treatment

facilities may require alternative management strategies. One potential approach to avoid the creation of Ra-enriched solid waste is to use carbonate precipitation for Ra removal because, unlike barite, carbonate solids generated by the treatment plant could be dissolved in mildly acidic solution and disposed by deep well injection.[40] Another alternative is to reuse the Ra-enriched Barite generated at CWTs used as weighting agent in drilling mud that is typically added to maintain the integrity of well bore.[41] In addition, a comprehensive analysis of the fate of Ra disposed in municipal solid waste landfills is needed to properly assess radiation exposure risks.[42] These risks will be associated with the emission of volatile progenies (i.e., Rn) because the results of this study suggest that Ra will not leach out in a relatively mildly acidic environment of municipal solid waste landfills[43] once it is sequestered in barite solids.

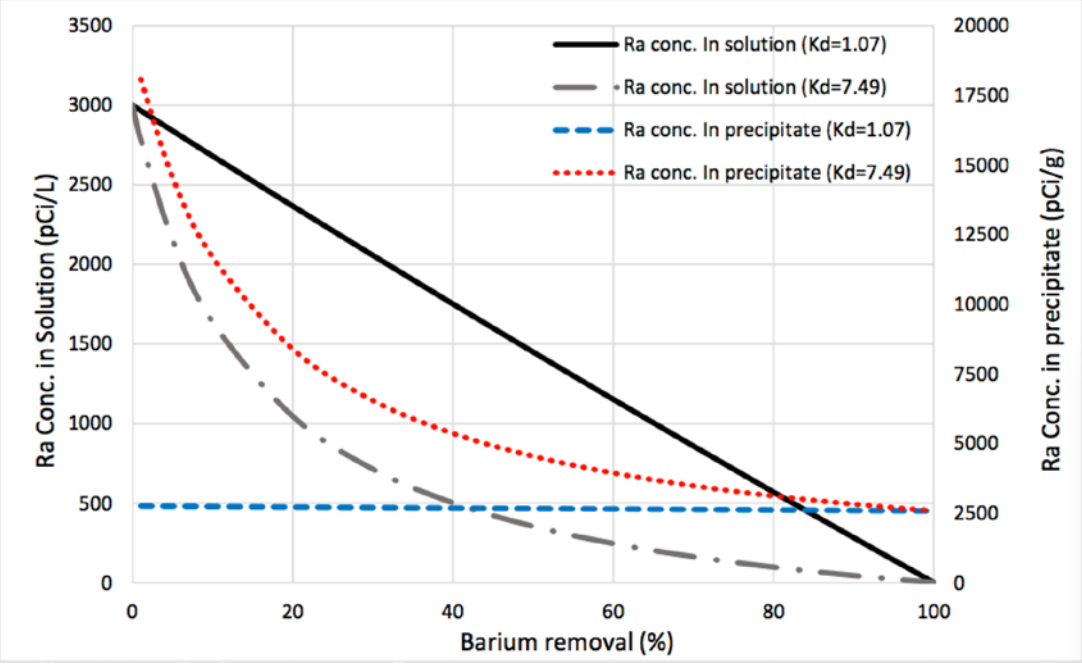

Figure 4.6 Theoretical Radium concentrations in solution and precipitated solids resulting from sulfate addition to flowback water. Distribution coefficients for these calculations (K_d=1.07 and K_d=7.49) were those measured for Ra-Ba-SO_4 binary co-precipitation system as shown in Figure 4.4; initial Ra concentration=3,000 pCi/L and initial Ba concentration=5mM

4.4 SUMMARY AND CONCLUSIONS

The objective of this task is to investigate the fate of Radium during sulfate precipitation, which is commonly used for flowback water treatment in centralized treatment plants. During the sulfate precipitation, it is less likely to observe pure $RaSO_4$ precipitates because Ra^{2+} concentrations are too low to reach saturation limit ($K_{sp,RaSO4} = 10^{-10.38}$). However, it is common for Ra^{2+} to co-precipitate with carrier metals. This work evaluates radium removal in barium–strontium sulfate co-precipitation system at different ionic strengths and identifies the main carrier for radium during sulfate precipitation. Experimental results show that radium removal generally follows theoretical distribution law in binary systems and is enhanced in Ra-Ba-SO_4 system and restrained in Ra-Sr-SO_4 system by high ionic strength. However, experimental distribution coefficient (K_d') varies over a wide range and cannot be described by the distribution equation alone. Radium removal in ternary system is controlled by the co-precipitation of Ra-Ba-SO_4, which is attributed to rapid $BaSO_4$ nucleation rate and closer ionic radii of Ra^{2+} with Ba^{2+} than with Sr^{2+}. Overall, sulfate precipitation is effective to remove >90% of Ra from produced water as long as all Ba has been removed. And the co-precipitation of Ba-Ra-SO_4 is the dominant mechanism to account for the Ra removal.

Calculations based on experimental results show that Ra levels in the precipitate generated in centralized waste treatment facilities far exceed regulatory limits for disposal in municipal sanitary landfills and require careful monitoring of allowed source term loading (ASTL) for technically enhanced naturally occurring materials (TENORM) in these landfills.

5.0 FATE OF RADIUM IN FLOWBACK WATER STORAGE FACILITIES

This chapter, written by Tieyuan Zhang and coauthored by Richard W. Hammack, and Radisav D. Vidic, are combined with parts from Chapter 6 and submitted for publication.

Natural gas extraction from Marcellus Shale generates large quantities of flowback water that contain high levels of salinity, heavy metals, and naturally occurring radioactive material (NORM). This water is typically stored in centralized storage impoundments or tanks prior to reuse, treatment or disposal. The fate of Ra-226, which is the dominant NORM component in flowback water, in three centralized storage impoundments in southwestern Pennsylvania was investigated during a 2.5-year period. Field sampling revealed that Ra-226 concentration in these storage facilities depends on the management strategy but is generally increasing during the reuse of flowback water for hydraulic fracturing. In addition, Ra-226 is enriched in the bottom solids (e.g., impoundment sludge) where it increased from less than 10 pCi/g for sample collected in 2010 to several hundred pCi/g for sample collected in 2013. A combination of sequential extraction procedure (SEP) and chemical composition analysis of impoundment sludge revealed that barite is the main carrier of Ra-226 in the sludge. Toxicity characteristic leaching procedure (TCLP) (EPA Method 1311) was used to assess the leaching behavior of Ra-

226 in impoundment sludge and its implications for waste management strategies for this low-level radioactive solid waste. This study expands our understanding of the fate of radium during wastewater storage and could influence strategies for management of flowback water impoundments.

5.1 INTRODUCTION

Marcellus Shale is the lowest unit of the Devonian age Hamilton Group and is mainly composed of black shale, which typically contains much higher uranium and thorium concentrations than other common sedimentary rocks.[1] Ra-226 and Ra-228 are formed by natural decay of U-238 and Th-232, respectively. Unlike uranium and thorium, radium is relatively water soluble and may be released into the adjacent pore water and into the flowback and produced water following hydraulic fracturing.[1,2] Uranium and thorium concentrations in Marcellus flowback water are generally below 10 pCi/L, while the Ra-226 concentration ranges from several hundreds to more than ten thousand pCi/L with an median value of 5,350 pCi/L.[1] Ra-228 concentration is generally lower than Ra-226 because of the low Th-232:U-238 ratio of the reservoir lithologies. The Ra-228:Ra-226 ratio in the flowback water generally ranges from 0.05 - 0.30 with a median of 0.16.[1] Thus, Ra-226 is the dominant radionuclide and an important proxy for the radioactivity of Marcellus flowback water.

Disposal of wastewater by underground injection is the dominant management approach that accounts for more than 95% of oil and natural gas associated wastewater in the U.S.[3,4] However, there are only 8 Class II underground injection control wells in Pennsylvania, which limits opportunities for flowback water disposal.[4] Prior to 2010, more than 80% of the flowback

water was sent to municipal or industrial treatment plants for limited treatment (e.g., precipitation of metals, flocculation and sedimentation of suspended solids) prior to discharge.[3] These plants could not remove dissolved ions from the wastewater and the TDS load on surface waters in Pennsylvania increased dramatically during this period.[5-7] The Pennsylvania Department of Environmental Protection (PA DEP) effectively banned discharge of this wastewater in 2011 and the reuse of flowback water for subsequent hydraulic fracturing operations became the main management option.[8] The flowback water is typically stored in centralized impoundments or storage tanks prior to reuse to increase management flexibility and meet the drilling and hydraulic fracturing schedule.

In this study, we investigated the fate of Ra-226 in three centralized water storage impoundments located in southwestern Pennsylvania by tracking its content in both wastewater and sludge contained in these impoundments during a 2.5-year period. The sequential extraction procedure (SEP)[9] and elemental analysis of sludge was performed to interpret partitioning of Ra-226 in different fractions of sludge and identify the main radium carrier. Toxicity characteristic leaching procedure (TCLP)[10] was utilized to predict radium leaching behavior in RCRA-D landfill. The fate of Technologically-Enhanced Naturally Occurring Radioactive Materials (TENORM) in storage impoundment is discussed in relation to current sludge management strategies.

5.2 MATERIALS AND METHODS

5.2.1 Sampling

Wastewater samples were collected from three centralized flowback water impoundments in southwest Pennsylvania (Impoundments A, B, and C) in October 2010. The source water for hydraulic fracturing gas wells in this region is typically a mix of fresh water (80 - 90%) and recycled flowback water (10 - 20%). Each impoundment was about 4 m deep and contained around 5 million gallons of wastewater. Impoundments A and B contained untreated wastewater, while Impoundment C initially contained the flowback water that was treated using sulfate addition for heavy metal precipitation, settling and granular media filtration to remove solids. Wastewater in Impoundments B and C was also sampled in May 2013 while Impoundment A had already been drained prior to the second round of sampling. Liquid samples were collected in 1L polypropylene bottles from the center of each impoundment at different depths, filtered through 0.45 μm membrane to separate suspended solids, and stored at 4 $^{\circ}$C. The sludge samples were collected in 1L polypropylene bottles from the bottom of the impoundments and stored at 4 $^{\circ}$C for further analysis.

5.2.2 Analytical Methods

Major cations were analyzed by atomic absorption spectrometry (PerkinElmer model 1000 AAS). The filtrate was diluted with 2% nitric acid and 0.15% KCl solution prior to analysis to limit interferences during metal analysis.[15] Dilution ratios were chosen based on the linear range

of the instrument. Anions were measured by ion chromatography (Dionex ICs-1100) and TDS was measured according to EPA gravimetric method (EPA Method 160.1).

Ra-226 activity was analyzed using Canberra gamma spectrometer with a broad energy germanium (BeGe) detector (BE2020). The solids in sludge samples were separated by filtration through 0.45 μm pore size membrane, washed with deionized (DI) water, dried at 105 ^{o}C to constant weight, crushed and transferred to a petri dish. The liquid samples were filtered through 0.45 μm pore size membrane and filtrate was transferred into Teflon bottle and evaporated to dryness. The residual solids were transferred to a petri dish. All solid samples were spread as a 1 mm thick layer in 46 mm diameter petri dish to minimize the impact of sample geometry on the accuracy of gamma spectrometry. All petri dishes were sealed with vinyl tape and stored for over 22 days prior to analysis to ensure equilibrium between Ra-226 and its progenies, Pb-214 and Bi-214.[11,12] Ra-226 activity was determined based on the analysis of Pb-214.

The chemical composition of solids was analyzed using Energy Dispersive X-ray Spectroscopy (EDS, EDAX Inc., Mahwah, NJ).

5.2.3 Leachibility test

Sequential Extraction Procedure (SEP)[9] was adopted in this study to determine the form on Ra in bottom solids collected from surface impoundments. One gram of dried sludge was homogenized by grinding in a mortar. Appropriate leaching solutions were used to extract trace metals that partition in the following five fractions: exchangeable, bound to carbonate, bound to Fe-Mn oxides, bound to organic matter, and residual. Each leaching solution was contacted with solid samples for 18 hours in a rotary shaker and liquid samples collected from each extraction step were filtered through 0.45 μm membrane and evaporated to dryness to measure Ra-226 activity

by gamma spectrometry. Ra-226 activity in the residual was also measured by gamma spectrometry to verify the mass balance.

The toxicity characteristic leaching procedure (TCLP) is designed to simulate the leaching of organic compounds and metals from liquid, solid, and multiphase wastes (EPA method 1311).[9] This study specifically investigates the leaching behavior of Ra-226 and Ba from the impoundment sludge. Extraction Fluid #2 (Acetic acid at pH=2.8) was selected for TCLP test based on the alkalinity of the solid waste. The extraction fluid was mixed with one gram of ground dry sample at 20:1 weight ratio in a polypropylene bottle and equilibrated on a rotary shaker for 20 hours. The extraction fluid was then separated from the solid phase by filtration through 0.45 μm membrane and analyzed for Ra-226 and Ba as described above.

5.3 RESULTS AND DISCUSSION

5.3.1 Chemical characterization of impoundment wastewater

Chemical characteristics of wastewater collected from different depths at three impoundments are shown in Table 1. Concentrations of major elements in these impoundments are similar to those reported in previous studies of flowback and impoundment wastewater.[8,13,14] TDS of impoundment wastewater was between 48,100 to 117,500 mg/L, which is in agreement with TDS values reported for flowback water.[15] Barium concentrations in Impoundments A and B ranged from less than 100 to several hundred mg/L and were notably lower than the average Ba concentration in Marcellus Shale produced waters in Pennsylvania (Ba_{avg}=2,224 mg/L) but within the range of Ba concentrations reported in the flowback water.[15] Relatively low Ba

concentration is expected since the flowback water collected in southwest PA has lower Ba concentration compared with that from northeast PA. In addition, impoundment wastewater is a mixture of flowback water and produced water and surface or municipal water that is typically used as makeup water in hydraulic fracturing operations.[14] The wastewater in Impoundment C was pretreated by sulfate precipitation prior to storage in the impoundment so that Ba and Ra-226 concentrations were undetectable in 2010.[15,16]

Table 5.1 Aqueous chemical composition of flowback water at different depth of the impoundment

Site	Date	Depth	TDS (mg/L)	Na (mg/L)	Ba (mg/L)	Cl (mg/L)	Ra-226 (pCi/L)	Ra-226/Ba (pCi/mg)
A	Oct. 2010	Surface	85,700	20,700	43	57,600	295	6.9
		6ft*	95,600	21,900	126	61,400	1,150	9.1
		3ft*	108,600	22,300	135	65,900	1,115	8.3
		Bottom	102,200	22,500	144	66,000	1,260	8.8
B	Oct. 2010	Surface	70,000	18,800	198	37,700	742	3.8
		9ft*	77,800	19,700	269	56,600	1,206	4.5
		3ft*	96,400	19,900	278	57,900	1,330	4.8
		Bottom	90,500	20,900	297	57,500	1,410	4.7
	May 2013	Bottom	117,500	28,400	188	66,200	2,510	13.4
C	Oct. 2010	Surface	48,100	16,600	1	25,900	0	0
		10ft*	65,000	17,500	2	33,000	0	0
		5ft*	61,100	17,700	1	33,200	0	0
		Bottom	65,500	18,100	3	40,700	0	0
	May 2013	4ft*	76,400	21,500	108	42,000	813	7.5
		Bottom	88,900	23,600	156	59,000	1,470	9.4

*Distance from bottom.

As can be seen in Table 5.1, concentrations of cations, including Ra-226, and anions increased with depth, suggesting density separation.[14] However, the ratio of heavy metals, such as Ra-226/Ba, did not show strong correlation with depth**.**

TDS and Ra-226 concentration in the impoundments were elevated after several cycles of reuse for hydraulic fracturing. Ra-226 concentration at the bottom of Impoundment B increased from 1,410 to 2,510 pCi/L and from 0 to 1,470 pCi/L at the bottom of Impoundment C. Wastewater stored in Impoundment C was no longer pretreated after reuse for hydrofracturing and elevated Ba and Ra-226 concentrations were observed in the samples collected from this impoundment in 2013. The increase in Ra-226, Ba, and TDS was not very dramatic because of constant dilution with relatively clean makeup water to maintain the TDS in the range that is acceptable for fracturing fluid formulation. It is important to note that Ra-226/Ba ratio for site B increased from 4.7 pCi/mg in 2010 to 13.4 pCi/mg in 2013, suggesting potential enrichment in Ra-226 in the storage impoundment during recycling of wastewater. It is possible that some of the increase in Ra-226/Ba ratio is due to the fact that leaching of Ra-226 from shale is less sensitive to salinity than Ba.[17] As the salinity of the fracturing fluid increases during the flowback water reuse, more Ra-226 will be extracted from Marcellus Shale than Ba and will lead to an increase in Ra-226/Ba ratio in the centralized storage facilities.

5.3.2 Evolution of Radium in impoundment sludge

As can be seen from Figure 5.1, Ra-226 concentration in the bottom sludge collected in Impoundment B increased from 8.8 pCi/g in 2010 to 872 pCi/g in 2013. There was no sludge in the Impoundment C in 2010 because the flowback water was treated prior to storage in this impoundment. After the wastewater in Impoundment C was recycled several times (it is not known how many cycles of reuse were implemented from October 2010 to May 2013), Ra content in the sludge collected in Impoundment C increased to 121 pCi/g. It is not possible to

accurately compare the total activity of Ra-226 in liquid and solid phase because the total mass of solids in these impoundments is not known.

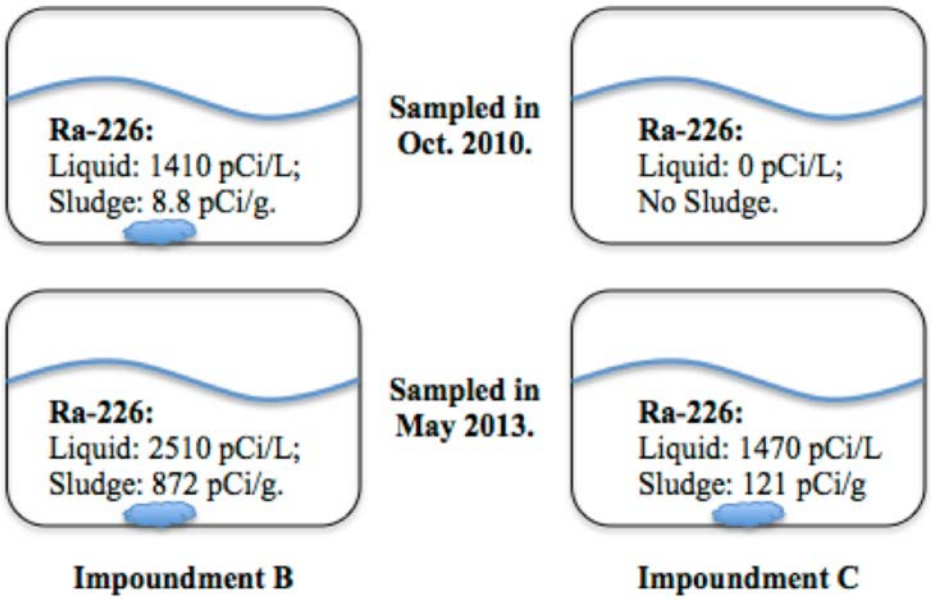

Figure 5.1 Ra-226 in liquid phase and bottom sludge in Impoundment B and C collected in 2010 and 2013

Sequential Extraction Procedure (SEP) and sludge composition analysis were performed to investigate the mechanisms that account for the increase in Ra-226 in aged sludge (collected in 2013) and identify its major carrier. SEP is used to identify the partitioning of target component (e.g., Ra-226) in different portions of impoundment sludge by stepwise extraction of Ra-226.[9] Results depicted in Figure 5.2 show that about half (55.6%) of Ra-226 was present in the residual phase in the Impoundment B collected in 2010. Ra-226 content in the sludge in Impoundment B increased 100-fold during 2.5 years of wastewater recycling. The exchangeable Ra-226 and the amount of Ra-226 bound to carbonate and organic matter in sludge collected in 2013 did not change notably. The amount of Ra-226 bound to Fe-Mn oxides increased from below detection limit to 3.2 pCi/g (less than 0.5% of total Ra-226 was bound to Fe-Mn oxides),

indicating that the adsorption of Ra-226 by iron and manganese oxides[18] is limited under the prevailing impoundment conditions. Adsorption of Ra-226 on hydrous metal oxides, such as Fe, Mn, Zr, is highly dependent on solution pH and increases with an increase in pH.[18] However, the pH of samples collected in both 2010 and 2013 was close to 6.

The majority of the increase in Ra-226 content is bound to the residual phase comprised of primary and secondary minerals and is not likely to be released into liquid phase under the conditions normally encountered in nature.[9] Nevertheless, the elevated NORM content in sludge collected in 2013 requires careful management and the current management approach is discussed in the next section.

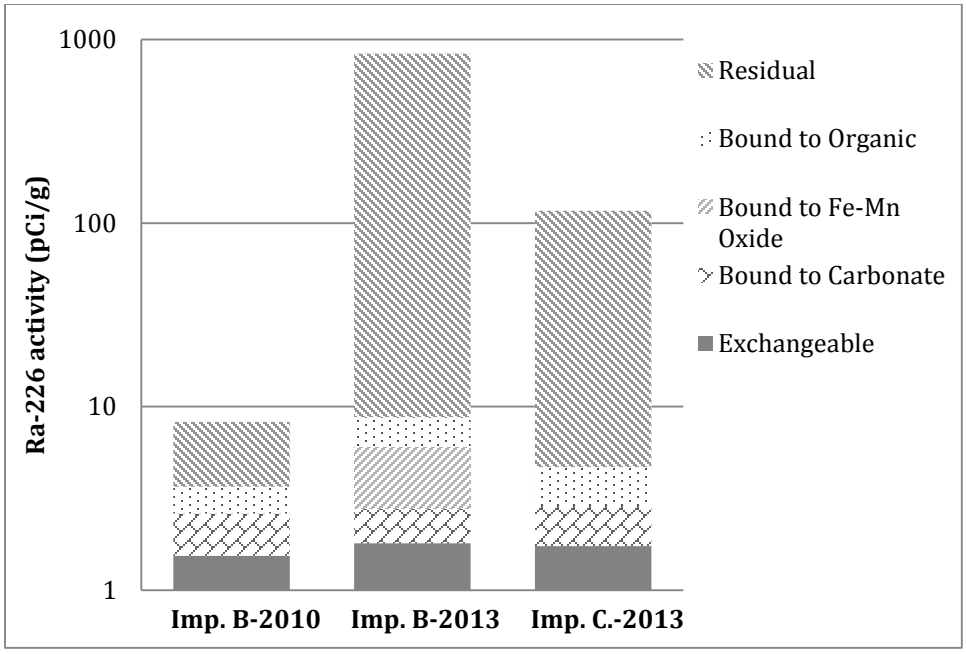

Figure 5.2 Distribution of Ra-226 in different fractions of sludge samples

The increase in Ra-226 concentration during sludge accumulation in the impoundment can be explained by the changes in elemental composition of the sludge. Chemical composition of the sludge shown in Figure 5.3 indicates that it is mainly comprised of C, O, Si, Fe and

alkaline earth metals (Pd presence is due to the coating protocol used in sample preparation for EDS measurement). C and O are suspected associated with clays and metabolites of microbial activity in the impoundment.[14] Si likely originates from the proppant (i.e., silica sand)[8] that is recovered with the flowback water, while Fe is contributed by the iron oxide complexes formed during impoundment aeration. The primary difference in chemical composition between the fresh sludge collected in 2010 and aged sludge collected in 2013 is a significant increase in Ba and S content, while the content of Ca and other major elements is reduced. The Ba/S molar ratio in the sludge from Impoundment B increased from 0.23 in 2010 to 1.20 in 2013, indicating that $BaSO_4$ precipitation contributed to sludge generation in this impoundment. The Ba/S molar ratio in the sludge collected from Impoundment C of 0.68 is within the range found in Impoundment B. During the flowback period, some sulfate will return to the surface but its concentration decreases with time due to barium sulfate precipitation.[13] Ra-226 might co-precipitate with $BaSO_4$[18] leading to an increase in NORM concentration in the sludge that accumulates in flowback storage facilities.

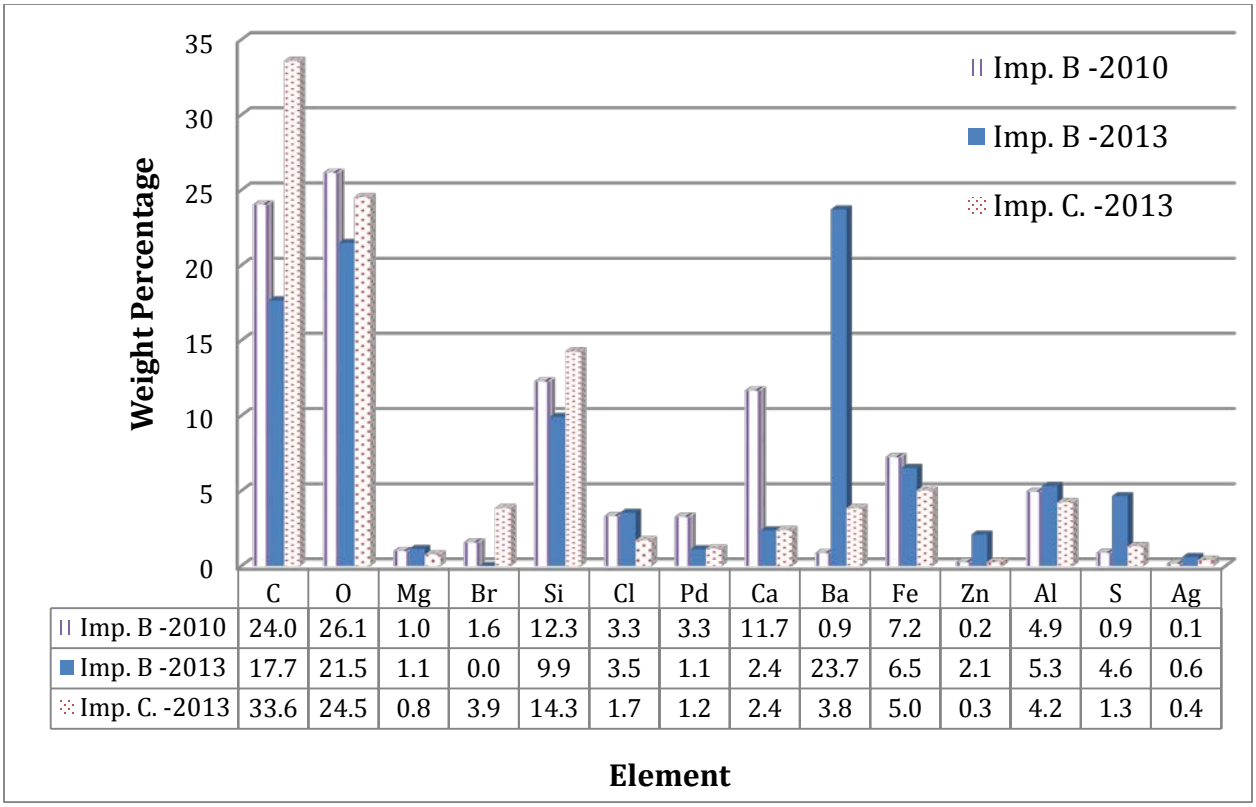

	C	O	Mg	Br	Si	Cl	Pd	Ca	Ba	Fe	Zn	Al	S	Ag
Imp. B -2010	24.0	26.1	1.0	1.6	12.3	3.3	3.3	11.7	0.9	7.2	0.2	4.9	0.9	0.1
Imp. B -2013	17.7	21.5	1.1	0.0	9.9	3.5	1.1	2.4	23.7	6.5	2.1	5.3	4.6	0.6
Imp. C. -2013	33.6	24.5	0.8	3.9	14.3	1.7	1.2	2.4	3.8	5.0	0.3	4.2	1.3	0.4

Figure 5.3 Chemical compositions of impoundment sludges

5.3.3 Leaching behavior of impoundment sludge in landfill

According to federal regulations (40 CFR §261)[19], a waste cannot be disposed in RCRA-D landfill if the Toxicity Characteristic Leaching Procedure (TCLP) test exceeds the limit for specified hazardous constituents. Therefore, the leaching behavior of Ba and Ra-226 from impoundment sludges was evaluated in this study. As shown in Table 3, Ba concentrations in the leachate never exceeded 3 mg/L, which is significantly below the EPA limit of 100 mg/L. On the other hand, leaching of Ra-226 was highly dependent on the sludge age. A large fraction (86±57%) of the total Ra-226 was found to be released from the fresh sludge, while less than 1% would leach from the aged sludge. Extensive leaching of Ra-226 from fresh sludge is expected

because the TCLP Extraction Fluid #2 (Acetic acid at pH=2.8) could dissolve Ra-226 bound to carbonate, Fe-Mn oxide, and organic phase and most of the Ra-226 in the exchangeable fraction.[9] Despite a large variance in Ra-226 measurements, it can be concluded that the fraction of Ra-226 that was not released during a TCLP test corresponds to the Ra-226 that is bound in the residual sludge phase, which is mainly comprised of primary and secondary minerals. Because Ra-226 in the aged sludge is mostly incorporated in barite, it is unlikely to be released in a landfill because barite is not soluble under the conditions that may occur in a landfill even in the presence of microbial activity.[20] Although Ra-226 concentrations in the landfill leachate is not regulated, the concentrations in the leachate observed in this study ranged from 98 to 378 pCi/L (Table 3) and are far above the limit for total Ra in drinking water (5pCi/L) and industrial effluents (60 pCi/L).[21] This finding suggest that management of landfill leachate may be impacted by the addition of sludges from flowback and produced water storage impoundments.

Table 5.2 Leaching behavior of Ra-226 from impoundment sludges in TCLP tests

Sample	Ra-226 in sludge (pCi/g)	Ra-226 Leached (pCi/g)	Ra-226 Leaching %	Ra-226 conc. In leachate (pCi/L)	Ba leaching %	Ba conc. In leachate (mg/L)
Imp. B- 2010	8.8±3.4	7.6±5.1	86±57%	378±250	N.D.	N.D.
Imp. B- 2013	872±157	5.4±2.8	0.62±0.07%	268±30	1.0%	2.4
Imp. C- 2013	121±24	2.0±0.9	0.13±0.10%	98±43	4.5%	1.7

Common practices for leachate treatment, such as aerobic and anaerobic biological treatment, physiochemical treatment, and advanced techniques (e.g., reverse osmosis), are designed for the removal of both organic and inorganic contaminants.[22] Without specific evaluation of the fate of Ra in leachate during biological treatment process, the physiochemical

treatment, such as sulfate precipitation, and advanced techniques such as reverse osmosis are recommended to control the Ra-226 concentration in leachate.[15,23]

5.3.4 Disposal of radioactive solid waste generated from Marcellus Shale gas extraction in landfill – An overview of Pennsylvania

Due to the limit number of disposal wells in Pennsylvania, disposal of Marcellus Shale produced water into disposal wells are not feasible. Most Ra isotopes in the Marcellus Shale produced water will be eventually enriched in the solid waste generated from centralized treatment facility[15] and impoundments. There are three options for radioactive solid waste disposal: municipal & industrial solid waste landfill (i.e., RCRA-D landfill), hazardous waste landfill (i.e., RCRA-C landfill), and low-level radioactive waste (LLRW) landfill.[24,25] Limit for Ra-226 for disposal as nonhazardous solid in RCRA-D landfill is 25 pCi/g in Pennsylvania.[25] Waste containing higher Ra-226 activity but lower than Low Level Radioactive Waste limit (i.e., Ra-226 < 2,000 pCi/g) is to be evaluated on a case-by-case basis and can generally be accepted by RCRA-C landfill. Waste contain more than 2,000 pCi/g of Ra-226 shall be disposed in LLRW facilities that are licensed by NRC.[27]

However, there is no federal requirement to test radionuclide concentrations in solid residuals prior to disposal. In addition, in order to provide increased flexibility to manage low-level radioactive mixed waste, EPA allows the disposal of waste with higher radium concentrations in RCRA-D landfills as long as environmental assessment and pathways analysis demonstrate that the annual dose to any recipient will not exceed the limit approved by the Bureau of Radiation Protection (40 CFR §266).[26] This strategy is highly depend on the total Ra generation and the landfill capacity.

5.3.4.1 Total Ra production from Marcellus Shale produced water in PA

Recent study shows there are 7,500 active Marcellus Shale wells in PA (http://stateimpact.npr.org/pennsylvania/drilling/). Each well produces 10 bbl/day of produced water containing 5,000 pCi/L of Ra-226

Annual Ra production from produced is:

$$Ra-226_{produced} = 5000\frac{pCi}{L} \times \frac{10bbl}{day * well} \times \frac{159L}{bbl} \times 365d \times 7500wells = 2.18 \times 10^{13} pCi$$

$$= 21.8Ci$$

5.2.4.2 Municipal waste landfill capacity in PA

The municipal waste landfills in the Pennsylvania have a total capacity of 4,436,405 tons/year. The locations of the landfills and resource recovery facilities are shown in Figure D.1.

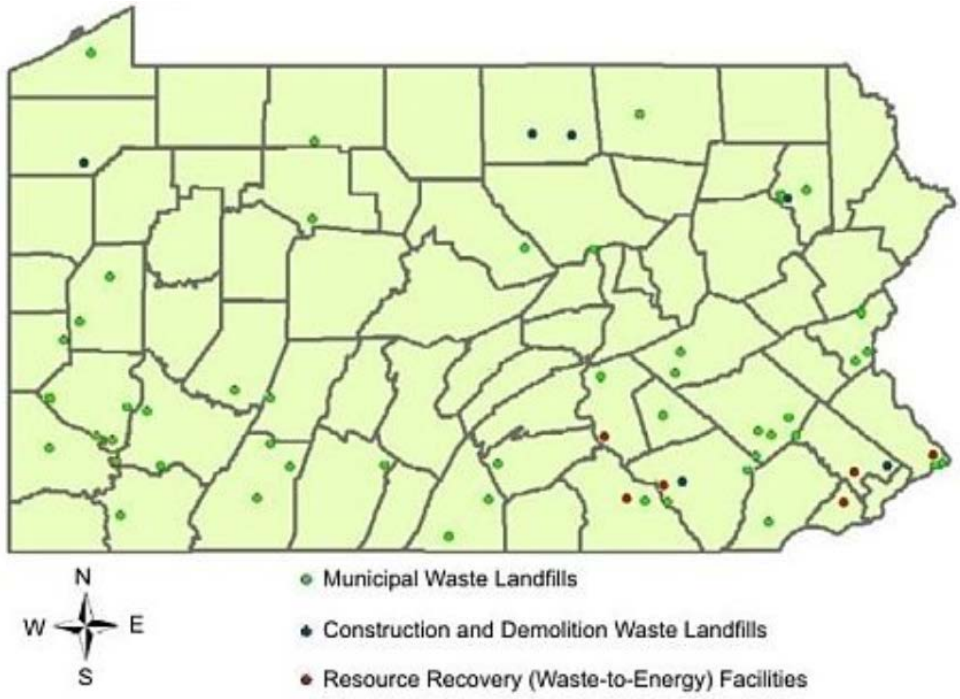

Figure 5.4 Landfill and resource recovery facilities in PA

Assume the total Landfill capacity is 5,000,000 tons. If all the residual Ra-226 was ultimately disposed in the landfill, the average Ra-226 concentration is:

$$Ra-226=\frac{2.18\times10^{13}}{5\times10^{6}ton\times\frac{10^{6}g}{ton}}=4.36pCi/g$$

If all the Ra-226 generated from the Marcellus Shale produced water was enriched in the solid waste, such as co-precipitated with $BaSO_4$, and all the solid waste that containing elevated Ra-226 content was disposed into the landfill, then the average Ra-226 concentration in the landfill would be increased by 4.36pCi/g. Such a Ra-226 concentration is higher than the Ra-226 –surface soil cleanup standard (5 pCi/g) but lower than the landfill limit in Pennsylvania (25 pCi/g). Thus, radium produced from Marcellus shale produced water would be a major radioactive material contributor for landfills.

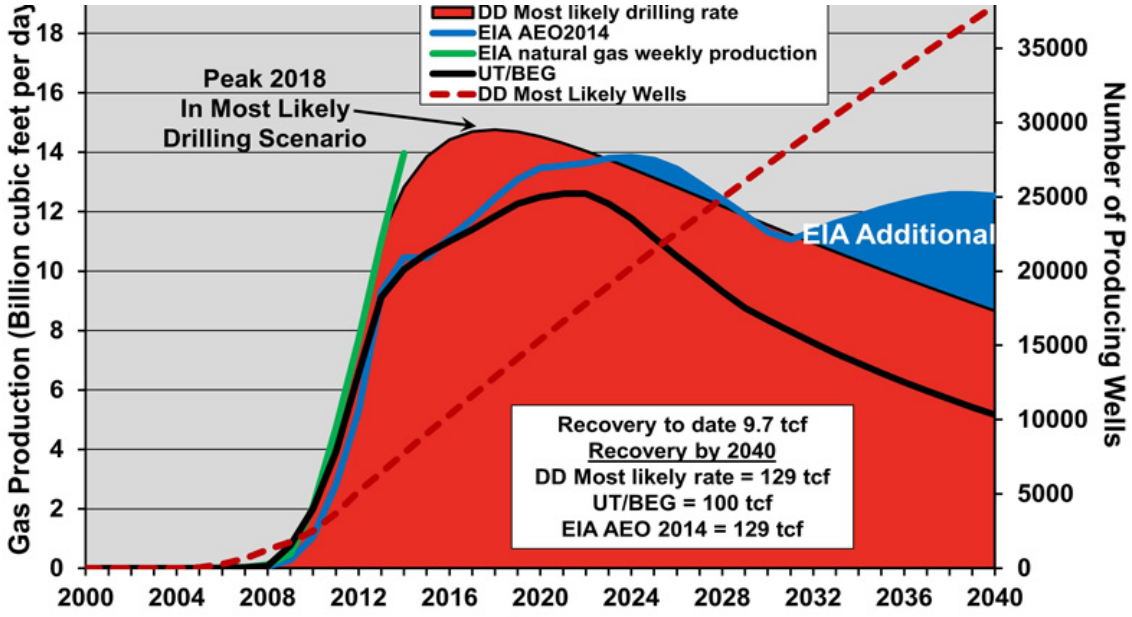

Figure 5.5 Shale gas production projections for the Marcellus Play through 2040

(http://www.postcarbon.org/fracking-fracas/)

In addition, the drilling Deeper report (DD) predicts the number of active Marcellus Shale producing wells in PA will increase from 7,500 in 2014 to 37,000 in 2040. The Ra generation solely from Marcellus Shale gas paly will exceed the landfill capacity in Pennsylvania when the number of active wells is 43,000, which is expected on the mid 2040s. Thus, development of other disposal options other than landfill is crucial to alleviate the pressure on dumping radioactive solid waste into the landfill.

5.4 SUMMARY AND CONCLUSIONS

This study investigated the fate of Ra-226 in impoundment flowback water and bottom sludge over a 2.5 years period. Results suggest that Ra-226 concentration generally increases during the recycling of flowback water for hydraulic fracturing. In addition, Ra-226 keeps accumulating in the bottom sludge and generates highly radioactive solid waste. Ra-226 is enriched in the bottom solids (e.g., impoundment sludge) where it increased from less than 10 pCi/g for sludge collected in 2010 to several hundred pCi/g for sludge collected in 2013. A combination of sequential extraction procedure (SEP) and chemical composition analysis of impoundment sludge revealed that barite is the main carrier of Ra-226 in the sludge.

Current disposal practice for radioactive solid waste in municipal solid waste landfills may result in Ra-226 concentration in landfill leachate in the range from 98-378 pCi/L, which is much higher than the limit for total Ra in drinking water (5 pCi/L) and industrial effluents (60 pCi/L). Management of landfill leachate may be impacted by the addition of sludges from flowback and produced water storage impoundments. Disposal of radioactive solid waste in RCRA-D landfills may be feasible as long as landfill operators abide by the PA DEP guidance to

monitor and track the radioactivity of incoming solid waste. However, the total Ra production from Marcellus Shale gas extraction will keep increasing and will exceed the landfill capacity for Ra isotopes by mid 2040s. The development of other disposal/management options is crucial to alleviate the NORM pressure on municipal solid waste landfills.

6.0 HEALTH RISKS ASSOCIATED WITH NORM GENERATED FROM MARCELLUS SHALE GAS EXTRACTION

Part of this chapter, written by Tieyuan Zhang and coauthored by Richard W. Hammack, and Radisav D. Vidic, were combined with Chapter 5 and submitted for publication.

There are two aspects of the risks associated with NORMs generated during the Marcellus Shale gas extraction. The risks associated with radionuclide concentration are discussed first. For example, Ra concentration in the liquid phase is limited to 5 pCi/L for drinking water and 60 pCi/L for industrial effluents. Previous study showed that sulfate precipitation in a centralized wastewater treatment plant could effectively remove Ra from Marcellus Shale flowback and produced water as long as all Ba is removed. Elevated Ra concentration in the intermediate step of flowback water management, such as storage in impoundments, is not regulated since this water is not intended for final disposal.

The other aspect of the risk associated with NORMs is its biological effect, which is expressed as Total Effective Dose Equivalent (TEDE). The average Total Effective Dose Equivalent (TEDE) from all natural sources of radiation in the U.S. is around 300 mrem/yr.[1] Added radiation dose equivalent (DE) contributed by other sources for those that are classified as

radiation workers should be As Low As Reasonably Achievable (ALARA) and not to exceed the annual dose of 5 rem/yr. Added DE limit for workers in other industries, such as oil and gas production, should comply with the limit for general public, which is 100 mrem/yr.[2]

Recent study by the Pennsylvania DEP assessed the potential worker and public radiation exposure at well sites, wastewater treatment plants, landfills, gas distribution and end use, and oil & brine treated roads that are affected by oil and gas operations in Pennsylvania.[3] DE calculated in that study based on on-site gamma radiation and radon measurements revealed that there is little potential (< 100 rem/yr) for radiation and radon exposure in those scenarios, except for fluids spills and in certain areas in wastewater treatment facilities.[3] This study used another approach (RESRAD model) to estimate direct exposure to external radiation, internal dose from inhalation of airborne radionuclides (e.g., radon), and internal dose from ingestion of contaminated materials. The outcome of this task would provide realistic information on the radiation health risks to potential receptors (i.e., on-site workers) in different scenarios that are related to Marcellus Shale operation. Radionuclide exposure in each steps of waste handling, including drilling pads, storage impoundments, centralized treatment plants, and landfills, was evaluated for both external radiation, inhalation and ingestion pathways. Results show that the TEDE for baseline conditions at drilling pads, storage impoundments, treatment facilities, and landfills are 4.6, 5.1, 1030 and 52.8 mrem/yr. The TEDE at drilling pads, storage impoundments and landfills are well below the NRC limit for general public (100 mrem/yr) and should be considered safe for on-site workers. Workers in the treatment facilities might receive excessive DE and appropriate measures recommended by NRC should be applied.

6.1 INTRODUCTION

Any living tissue can be damaged by ionizing radiation in a unique manner that may have stochastic (the probability of developing a disease, such as cancer) and non-stochastic health effect (sickness caused by acute exposure, such as nausea, skin burns, etc.). The most common forms of ionizing radiation are alpha particles, beta particles, and gamma rays, which all have different ability to damage different types of tissues. Alpha particles can travel only a few inches in air and lose their energy almost as soon as they collide with any barrier. Beta particles can travel a few feet in the air and can pass through a sheet of paper but can be stopped by a sheet of aluminum foil or glass. Even though alpha particles and most beta particles can be stopped by skin, they would be hazardous if the radionuclides were swallowed or inhaled. Gamma rays are waves of pure energy and travel at the speed of light through air or open spaces. They can penetrate most solid barriers and only concrete, lead, or steel can block gamma rays. If alpha-emitting radionuclides enter the body by inhalation or ingestion, they are the most destructive form of ionizing radiation. It is estimated that chromosome damage from alpha particles is anywhere from 15 to 20 times greater than that caused by an equivalent amount of gamma or beta radiation.[4]

In order to quantify the health risks associated with potential radiation exposure from NORM that is correlated with radionuclide activity, three different measures to assess the impact of radiation can be used. A short summary of these measures and their meanings are shown in Table 6.1.

Table 6.1 Measures relative to the biological effect of radiation exposure

Measure	Definition	Unit		Note
Exposure	The strength of a radiation field at some point in air	Roentgen (R)	1 R will deposit 2.58×10^{-4} coulombs of charge in 1kg of dry air	Can be directly measure with a meter, but only valid for deposition in air
Dose/ Absorbed Dose	Amount of radiation energy that is absorbed by an object	Gray (Gy) or Radiation Absorbed Dose (rad); 1 rad= 0.01 Gy	1 Gy equals to a dose of one joule of energy absorbed by 1 kg of mass	Measures the amount of energy imparted to a given mass of matter
Dose Equivalent (DE)	The biological effect of the absorbed dose	Sievert (SV) or Roentgen Equivalent Man (rem); 1 rem=0.01 SV	1 rem= 1 rad × Q. where Q is the quality factor that depends on the type of radiation.	1 rem exposure carries a 0.055% chance of eventually developing cancer

TEDE is the sum of DE from all individual pathways.

Radiation exposure, with a unit of Roentgen, can be directly measured with a meter and is regulated by EPA for specific scenarios. For example, PA DEP issued a guidance document on radioactivity monitoring at solid waste processing and disposal facilities that requires the exposure level for the solid waste not to be more than 10 μR/h above background.[5] Solid waste containing higher exposure level would trigger the action to notify DEP and isolate the load unless a license was already issued.

On the other hand, TEDE cannot be directly measured since it is not simply controlled by the types and concentrations of radionuclides, but is also affected by other parameters. In order to calculate TEDE, the radionuclide type, concentration, geometry of contaminated zone, exposure time and the receiving pathways should be considered (Figure 6.1). Major exposure pathways that contribute to TEDE for a recipient are illustrated in Figure 6.2. Since the industrial workers did not consume water or food obtained on the site, only four major pathways were

selected in this study, namely external radiation, inhalation of dust, radon inhalation, and ingestion of soil. The external radiation represents radiation received by recipient, which is mainly contributed by gamma radiation, from radionuclides outside of the body. The inhalation pathway includes suspended dust in air and airborne radionuclides (e.g., radon). Their concentrations were calculated based on the processes of transportation and dilution from contaminated zone to human exposure location. The ingestion of soil represents the direct ingestion of soil while working in contaminated areas. Details of different pathway factors can be found in "User's Manual for RESRAD".[6]

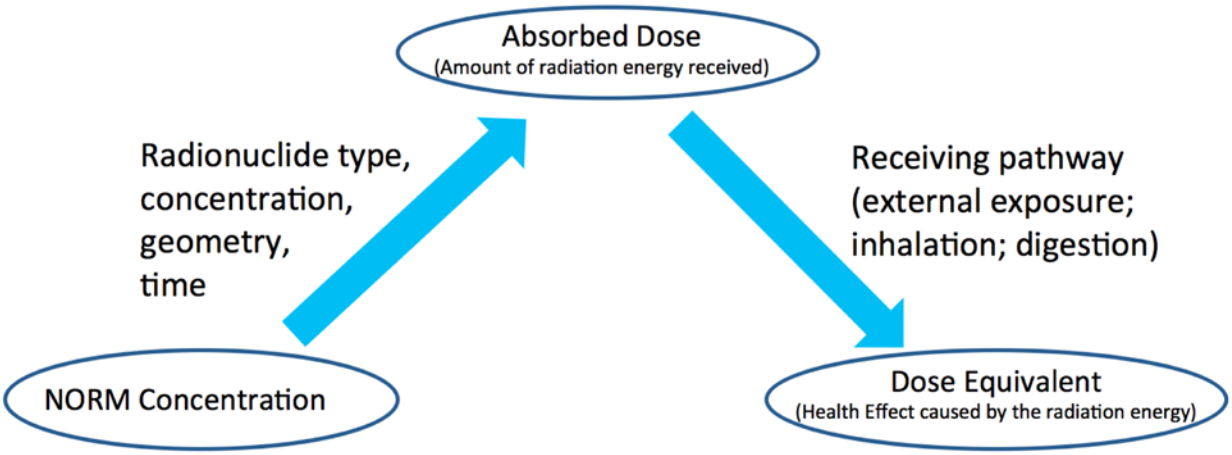

Figure 6.1 Correlation between NORM concentrations and dose equivalent

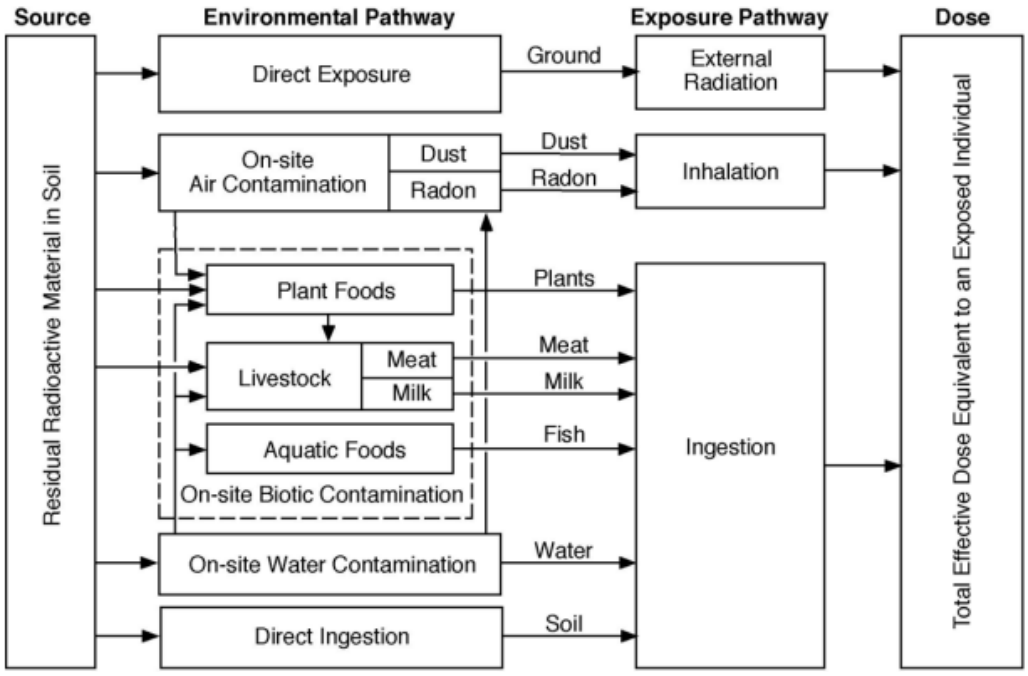

Figure 6.2 Schematic representation of radiation exposure pathways[6]

EPA and Nuclear Regulatory Commission (NRC) have prescribed the annual dose equivalent limit for public.[7] A site will be considered acceptable for unrestricted use if the residual radioactivity results in a total effective dose equivalent (TEDE) to an average person that does not exceed 25 mrem/year. In addition, the annual total effective dose equivalent for general public should not exceed 100 mrem (0.1 rem).[8] In specific cases, if NRC issues a license, the annual dose limit for an individual member of the public may be increased to 500 mrem (0.5 rem). This study estimated TEDE for on-site workers in several scenarios that are relevant for Marcellus Shale gas extraction and compared it with regulatory limits that may be relevant for each scenario.

6.2 METHODS

Estimation of TEDE was performed by a commercial software RESRAD (Version 7), which is developed by Argonne National Laboratory to estimate the radiation dose equivalents and risks from RESidual RADioactive materials.[6] This model incorporates both ionizing radiation absorbed by tissue and a relative ability of that radiation to produce particular biological change. It has adaptability to specify exposure conditions and is widely used by the U.S. Department of Energy (DOE) and its contractors, the U.S. Nuclear Regulatory Commission (NRC), and the U.S. Environmental Protection Agency (EPA).

The derivation of TEDE in a given scenario should consider all possible pathway segments where a member of critical population can be exposed to radiation. Those pathways include direct exposure to external radiation, internal dose from inhalation of airborne radionuclides (e.g., radon), and internal dose from ingestion of contaminated material that intruded into food chain. Details of the calculation of radiation exposure can be found in RESRAD manual. Key assumptions used in this study to estimate Total Effective Dose Equivalent (TEDE) are summarized in Table 6.2.

Table 6.2 Key assumptions applied to estimate Total Effective Dose Equivalents (TEDE)

Input Parameter	Storage Impoundment	Drilling Pad (trailer contains drilling cutting)	Flowback Water Treatment Facilities	Landfill
Pathways	External Gamma; Inhalation; Soil Ingestion; Radon			
Contaminated Zone	50-100m(L) ×50m(W)×2-4m(H) Impoundment	6m(L)×4m(W)×2m(H) Trailer	2m(L)×2m(W)×0.83m(H) (Solid waste in tank)*	100m(L)×100m(W)×1m(H)
Radionuclide Concentration	Ra^{226}=1,000-18,000 pCi/L; Ra^{228}=100 – 1,800 pCi/L; U^{238}=10 pCi/L; Th^{232}=1pCi/L	U^{238}=U^{234}=Th^{230}=Ra^{226}=5-25 pCi/g; Th^{232}=Th^{228}=Ra^{228}=1 pCi/g	Ra^{226}=500-10,000 pCi/g**; Ra^{228}=50 – 1000 pCi/g**	Ra^{226}=5 pCi/g; Ra^{228}=0.5 pCi/g
Density	1 g/mL	2.55 g/cm^3	4 g/cm^3	1.5 g/cm^3
Amount of contaminated material	2.6-10.6 million gallons of flowback water (i.e., 5.1 – 369.5 mCi of Ra^{226})	122 tons of shale cuttings (i.e., 1.7 – 8.4 mCi of Ra^{226})	13.2 tons of solid (i.e., 6.6 – 132.8 mCi of Ra^{226})	15,000 tons (i.e., 75 mCi of Ra^{226})
Radon emanation ratio	1.0	0.22		
Shortest Distance**	0 m			
Exposure Time	Outdoor: 3 hr/day; Indoor: 0 hr/day.			Outdoor: 4hr/day; Indoor: 3hr/day.
Inhalation rate	11,400 m^3/yr***			
Soil ingestion	36.5 g/yr***			

*: solid waste generated from sulfate precipitation during 30 days of operation for a 100,000 gallon/day treatment facility; **: Based on the Ba and Ra-226/228 concentrations Marcellus Shale flowback and produced water. Assuming complete co-precipitation of Ra-$BaSO_4$; ***: Default value in RESRAD manual; ****: Shortest distance between recipient and contaminated zone.

6.3 RESULTS AND DISCUSSION

6.3.1 TEDE for on-site workers in centralized flowback storage facilities

The impoundment is assumed to contain 2.6 - 10.6 million gallons of flowback water (depending on the size and depth of impoundment) with Ra-226 activities ranging from 1,000 to 18,000 pCi/L.[9] Activity of Ra-228 is assumed equal to 10% of Ra-226.[28] The impoundment is equipped with a liner system as required by RCRA hazardous waste permitting program so that the leaching is neglected (http://www.epa.gov/epawaste/hazard/tsd/permit/). The operational-phase receptors (i.e., workers who dispose and/or withdraw the flowback water into or from the impoundment) are assumed to be located next to the impoundment with a shortest distance of 0 m. Radon emanation coefficient, which is the fraction of radon generated from radium decay that is released into the air, is assumed to be 1.[14]

Modeling results show total effective dose equivalent (TEDE) for on-site workers at the impoundment are ranging from 2 – 35 mrem/yr (Table 6.3), which are well below the NRC limit for general public of 100 mrem/yr. This value is equivalent to the DE for several coast-to-coast round trip flights in a commercial airplane (3 mrem/each) or chest (posteroanterior and lateral view) X-ray (6 mrem/each).[1] Among the exposure pathways, external gamma radiation is dominant as it contributes 98.8% of TEDE. TEDE contributed by inhalation of radon, dust and other airborne radionuclides and soil ingestion is negligible. Among the radionuclides that are typically found in Marcellus Shale flowback water, Ra-226 is the dominant source that

contributes more than 94% of TEDE. Thus, estimation of TEDE for any impoundment can be simplified by considering only the external gamma radiation from Ra-226.

The risk assessment was conducted by converting the radiation dose to carcinogenic risk by using risk factors recommended by the International Commission on Radiological Protection (ICRP).[10] Risks are expressed as the increased probability of fatal cancer over a lifetime. Results in Table 6.3 indicate that the total carcinogenic risk for on-site workers involved in the impoundment management ranging from 5E-5 to 9E-4. EPA generally uses carcinogenic risk of 1E-4 as cleanup level for Comprehensive Environmental Response, Compensation, and Liability Act (CERCLA) remediation sites.[11] However, a specific risk of around 1E-4 is considered "acceptable"[11] for impoundments since it would not impact the public.

Table 6.3 Total Effective Dose Equivalent contributions for individual Radionuclides and Pathways in storage impoundment

Radionuclide Contributor	Pathways				Total (mrem/yr)	Risks
	External Gamma (mrem/yr)	Radon inhalation (mrem/yr)	Inhalation (mrem/yr)	Soil (mrem/yr)		
Ra-226	1.91 – 34.44	< 0.01 - 0.07	<0.01 – 0.04	<0.01 – 0.03	1.9 – 34.8	4.90E-5 – 8.83E-4
Ra-228	0.12 – 2.02	<0.01 – 0.02	<0.01	<0.01 – 0.05	0.12 – 2.11	2.42E-6 – 4.35E-5
Th-232	< 0.01	<0.01	<0.01	<0.01	<0.01	< 1E-6
U-238	<0.01	<0.01	<0.01	<0.01	<0.01	< 1E-6
Total	2.02 – 36.41	<0.01 – 0.10	<0.01 – 0.05	0.02 - 0.03	**2.05 – 36.86**	5.15E-5 – 9.26E-4

Range of DE depending on the size of impoundment and radionuclides concentration as shown in Table 6.2.

Sensitivity analysis was conducted for several key input parameters. These parameters include the radionuclide concentration, location of the recipient, geometry of the impoundment, radon emanation ratio and indoor and outdoor exposure time. Results show that all parameters

had some impact on the estimated TEDE but the indoor exposure and the location of the recipient had by far the greatest impact. In the worst case scenario (Ra-226= 18,000 pCi/L, Geometry of impoundment is 100m(L)×50m(W)×4m(H)), addition of 4 hours of indoor exposure would increase the DE contributed by radon inhalation to from 0.10 to 456 mrem/yr, which comprised of 90% of TEDE in that case (Figure 6.3a.). This result is in agreement with previous studies which showed that the inhalation of radon gas is an important and often the primary source for TEDE to human.[1, 12] For example, the average DE by inhalation of natural radon sources in the U.S. is about 200 mrem/yr, which makes up 67% of TEDE from all natural sources of radiation.[1] DE contributed by radon inhalation is mainly due to indoor accumulation of radon gas from drinking water off-gasing and migration from Ra-bearing materials. However, since RESRAD calculates the indoor DE by assuming the building is located directly on the contaminated zone, which is unrealistic for the impoundment scenario, such high DE is not expected to occur in reality. The airborne radon gas that is released from the impoundment would be dispersed with outdoor air and the inhalation of radon would be minimal for on-site workers. However, this result indicates it is important to consider the DE contributed by radon inhalation while the construction is built upon the contaminated areas.

External gamma radiation DE is highly sensitive to the location of the recipient and decreases significantly with the increasing distance between receptor and contaminated zone. TEDE would decrease from 2 - 36 mrem/yr for baseline conditions to < 0.1 – 1.9 mrem/yr when the distance between the recipient and the impoundment is 10 m (Figure 6.3b.). The highest and lowest TEDE were calculated using the range of impoundment sizes and radionuclide concentrations as shown in Table 6.2. Although TEDE for on-site workers are well below the EPA limit, a safety distance is recommended to minimize TEDE.

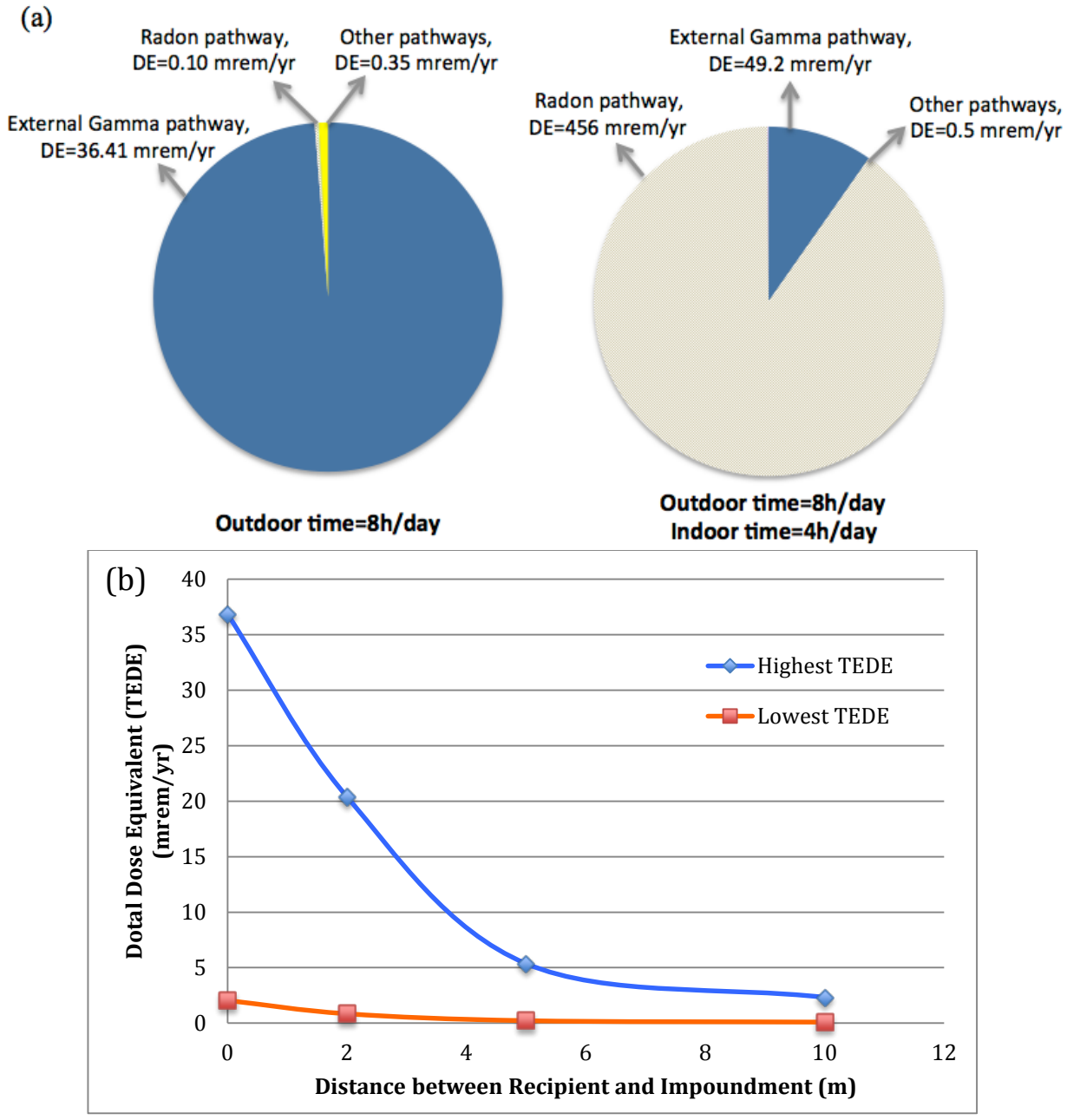

Figure 6.3 Sensitivity analysis for impoundment scenario: (a) Impact of outdoor and indoor time on TEDE for individual pathways and (b) Impact of distance between recipient and impoundment on TEDE. TEDE depends on the size of impoundment and radionuclide concentrations as shown in Table 6.2.

6.3.2 TEDE for on-site workers at a drilling pad

Drilling of a horizontal well generates large quantities of shale core, which is generally stored in an on-site trailer. Considering the average length of the horizontal portion of Marcellus Shale well is around 10,000 ft, and a typical diameter of a drilling bit of 5.5 inch, each horizontal well would generate around 48 m^3 of shale cuttings. The shale cuttings are assumed to be stored in a 6m(L)×4m(W)×2m(H) trailer. The average density of Marcellus Shale is 2.55 g/cm^3 and the radionuclide content in the shale core is ranging 5- 25 pCi/g for radionuclides in U-238 series and 1 pCi/g for Th-232 series (Table 2.2). The operational-phase receptors (i.e., on-site drilling pad workers) are assumed to be located next to the shale core storage trailer with a shortest distance of 0 m. Since the Radium is embedded inside the shale core, a radon emanation coefficient of 0.22 was selected for modeling studies.[14,15]

Model calculations for baseline conditions resulted in TEDE for an on-site worker at a drilling pad of 2.6 – 10.6 mrem/yr, depending on the radionuclide concentrations (Table 6.4). This value is far below the NRC limit for general public and with the TEDE range for impoundment scenario. Among the exposure pathways, external gamma radiation is the dominant one as it contributed to 98% of TEDE. Ra-226 is the dominant radiation source that contributes more than 76% of TEDE while DE contributed by Ra-228 and Th-228 is also notable. Risk assessment shows the risks associated with drilling pad scenario of 5.95E-5 – 2.47E-4, which is within the range of "acceptable" levels (i.e., 10^{-6} – 10^{-4}).[11]

Sensitivity analysis was conducted for several key input parameters. Results suggest that parameters controlling the TEDE at a drilling pad were very similar to those that have the greatest impact for impoundment scenario, which is expected since the external gamma radiation is the dominant pathway for TEDE in both scenarios. For example, TEDE would decrease from

10.6 mrem/yr for baseline condition to 0.6 mrem/yr when the distance between the recipient and the impoundment is 5m.

Table 6.4 Total Effective Dose Equivalent Contributions for Individual Radionuclides and Pathways in drilling pad

Radionuclide Contributor	Pathways				Total (mrem/yr)	Risks
	External Gamma (mrem/yr)	Radon inhalation (mrem/yr)	Inhalation (mrem/yr)	Soil (mrem/yr)		
Pb-210	<0.01	0	<0.01 – 0.01	<0.01 – 0.02	<0.01 – 0.03	< 10E-6
Ra-226	1.94 – 9.71	<0.01	<0.01 – 0.01	<0.01	1.94 – 9.72	4.58E-5 – 2.29E-4
Ra-228	0.23	<0.01	<0.01	<0.01	0.23	4.48E-6
Th-228	0.28	<0.01	<0.01	<0.01	0.29	8.18E-6
Th-230	<0.01	<0.01	0.02 – 0.13	<0.01	0.02 – 0.13	< 10E-6
Th-232	0.01	<0.01	<0.01	<0.01	0.02	< 10E-6
U-234	<0.01	<0.01	<0.01	<0.01	<0.01 – 0.01	< 10E-6
U-238	<0.01 – 0.15	<0.01	<0.01	<0.01	0.03 – 0.16	< 10E-6 – 2.48E-6
Total	2.50 – 10.39	<0.01	<0.01 – 0.02	<0.01 – 0.03	**2.55 – 10.60**	5.95E-5 – 2.47E-4

6.3.3 TEDE for on-site workers in a Centralized Waste Treatment plant (CWT)

A typical centralized waste treatment facility with a capacity of 100,000 gallon/day is assumed in this study. During the sulfate precipitation in centralized treatment plant, most of Ra will co-precipitate with $BaSO_4$ and become concentrated in the solid phase[16], the DE for the treated wastewater is not evaluated. However, a total of 13.2 tons of radioactive solid waste (i.e., Ra-Ba-SO_4) would be generated during 30 days of operation and it is assumed that this solid waste is stored in 2m(L)× 2m(W) ×0.83m(H) tank. Ra-226 and Ra-228 concentration in the solid waste

was depend on the Ba and Ra isotopes concentration in the flowback water. In this study, we assume the Ra-226 concentration ranging from 500 to 10,000 pCi/g, which are representative for the characteristics of Marcellus Shale flowback waters.[9] Activity of Ra-228 is assumed equal to 10% of Ra-226.[13] Radon emanation coefficient is assumed to be 0.22, which is common for Ra that is bound in mineral phase.[15] DE for on-site workers in the treatment facility is calculated by assuming the recipient is located next to the tank for 3h/day.

RESRAD results show that the TEDE for on-site workers in a centralized treatment facility ranging from 120 – 2,390 mrem/yr (Table 6.5), which is far above the NRC limit. Among the exposure pathways, external gamma radiation is the dominant one as it contributes 99.8% of TEDE. TEDE contributed by inhalation of radon, dust and soil ingestion are below 3 mrem/yr. The carcinogenic risk in these cases ranges from 2.71E-3 – 5.43E-2 and is "unacceptable" for general public.[11]

Sensitivity analysis was conducted for several key input parameters. These parameters include the radionuclide concentration, location of the recipient, geometry of the storage tank, radon emanation factor, and exposure time. Results also showed that all parameters had some impact on the estimated TEDE but the location of the recipient had by far the greatest impact. For example, the highest TEDE, which is calculated based on the highest Ra isotopes concentrations in solid waste, would decrease from 2,390 mrem/yr for baseline conditions to 288, 38.5 and 11.1 mrem/yr when the distance between the recipient and the solids storage tank is 2, 5 and 10m (Figure 6.4). Thus, a safe distance of 5 m was recommended for on-site workers.

Table 6.5 Total Effective Dose Equivalent Contributions for Individual Radionuclides and Pathways in CWT

Radionuclide Contributor	Pathways				Total (mrem/yr)	Risks
	External Gamma (mrem/yr)	Radon inhalation (mrem/yr)	Inhalation (mrem/yr)	Soil (mrem/yr)		
Ra-226	113 – 2,250	<0.01	0.19 – 3.77	0.01 – 0.02	113 – 2256	2.63E-3 – 5.23E-2
Ra-228	6.7 – 133	<0.01	0.04 – 0.85	<0.01 – 0.04	6.71 – 134.20	9.77E-3 – 1.95E-3
Total	119 - 2390	<0.01	0.23 – 4.62	0.01 – 0.01	**119 – 2,390**	2.71E-3 – 5.43E-2

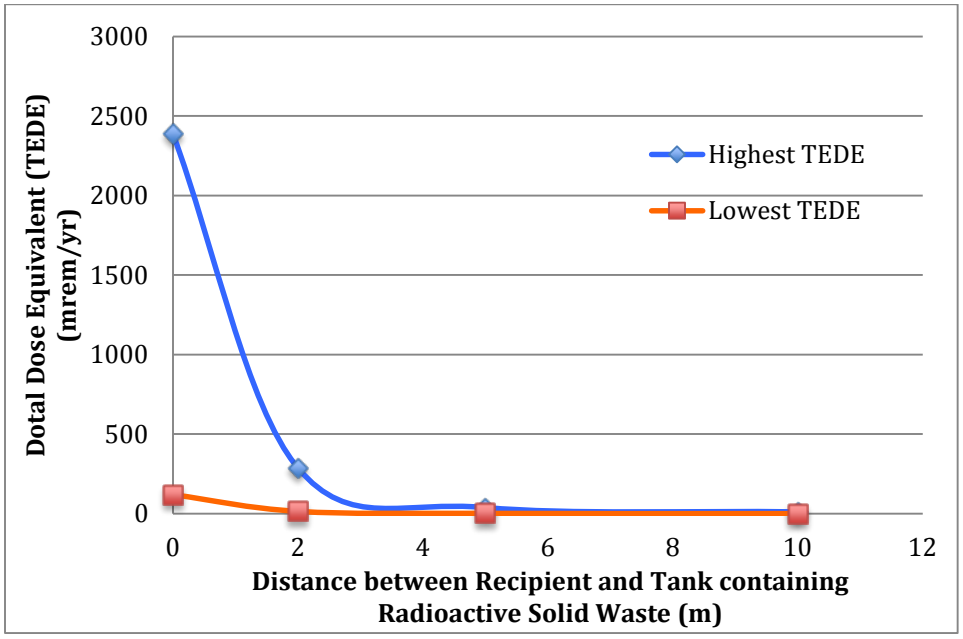

Figure 6.4 Sensitivity analysis for CWT scenario: Impact of distance between recipient and contaminated zone (i.e., tank containing radioactive solid waste) on TEDE. TEDE depends on the size of radionuclide concentrations as shown in Table 6.2.

6.3.4 TEDE for on-site workers in a landfill

TEDE for landfill scenario is calculated assuming that Ra-226 and Ra-228 concentrations in the solid waste are 5 and 0.5 pCi/g, respectively. Inhalation of indoor radon gas is considered in this

scenario since a building might be built on the closed landfill. Exposure time for on-site workers in landfill are assumed to be 4h/day at indoor conditions and 3h/day at outdoor conditions.

RESRAD results show that the TEDE for on-site workers under baseline conditions in the landfill scenario is 52.8 mrem/yr (Table 6.6), which is lower than the NRC limit and should be considered safe. TEDE contributed by both external gamma radiation and inhalation of radon is significant. In order to further identify the major contributor to TEDE, a specific analysis for TEDE contributed by outdoor and indoor exposure is conducted. Result show that the TEDE contributed by gamma radiation under indoor and outdoor exposure conditions are comparable while TEDE contributed by inhalation of radon is mainly due to indoor exposure (Table 6.7). Elevated TEDE contributed by indoor radon inhalation is expected because of possible indoor accumulation of radon gas.

Table 6.6 TEDE contributions by individual radionuclides and pathways in a landfill scenario

Radionuclide Contributor	Pathways				Total (mrem/yr)	Risks
	External Gamma (mrem/yr)	Radon inhalation (mrem/yr)	Inhalation (mrem/yr)	Soil (mrem/yr)		
Ra-226	12.0	40.2	6.67E-03	6.18E-02	52.2	2.03E-3
Ra-228	0.703	1.40E-02	1.50E-03	1.35E-02	0.732	1.11E-5
Total	12.6	40.2	8.17E-03	6.53E-02	**52.8**	2.04E-3

Table 6.7 TEDE contributed by outdoor and indoor exposure conditions for individual pathways in a landfill scenario

Radionuclide Contributor	Pathways				Total (mrem/yr)
	External Gamma (mrem/yr)	Radon inhalation (mrem/yr)	Inhalation (mrem/yr)	Soil (mrem/yr)	
Outdoor	6.49	5.28E-03	5.29E-03	3.19E-02	6.53
Indoor	6.17	40.2	2.88E-03	4.34E-02	46.4
Total	12.6	40.2	8.17E-03	6.53E-02	**52.8**

Sensitivity analysis was also performed for several key input parameters in a landfill scenario. Since the external gamma radiation is not a major pathway contributing to TEDE, the impact of the distance between recipients to contaminated zone has little impact on the result. On the other hand, factors controlling the radon inhalation pathway would have great impact on TEDE. Among all the parameters affecting TEDE contributed by radon inhalation, the depth of cover layer had by far the greatest impact. Placement of 1, 3, and 5m of cover layer would decrease TEDE to 39.7, 4.7 and 0.6 mrem/yr, respectively (Figure 6.5).

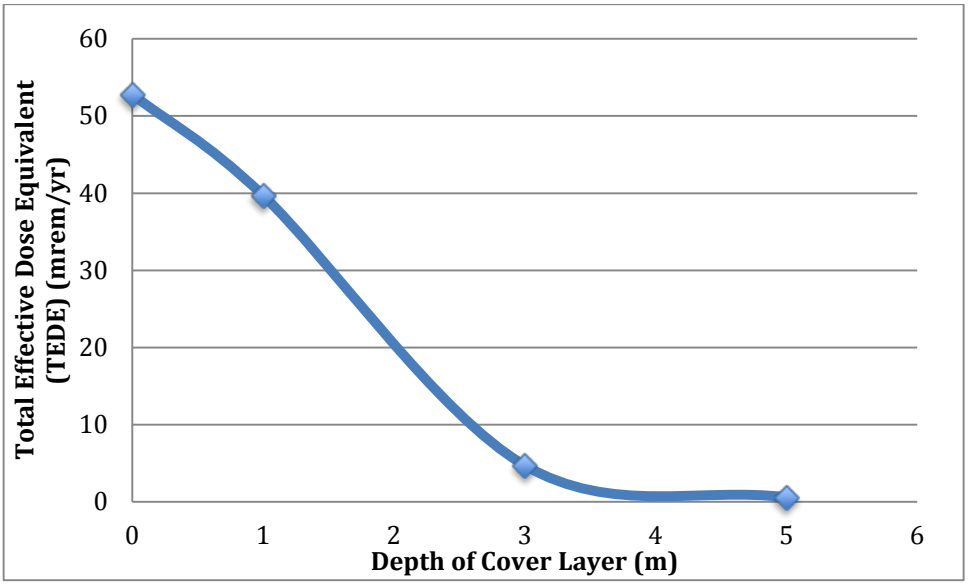

Figure 6.5 Impact of depth of cover layer on TEDE for landfill

6.4 SUMMARY AND CONCLUSIONS

The primary objective of this study was to estimate the health risks from TEDE in several representative scenarios related to Marcellus Shale operations and waste handling. Those scenarios include the drilling pad, flowback/produced water storage impoundment, centralized

treatment facility and the landfill that accepts radioactive waste. RESRAD results show that range of TEDE for baseline conditions at drilling pads, storage impoundments, treatment facilities, and landfills are 2 – 37, 3 – 11, 119 – 2,390 and 53 mrem/yr, respectively. TEDE for on-site workers at drilling pads, storage impoundments and landfills are well below the NRC limit for general public (100 mrem/yr) and should be considered safe for on-site workers. Workers in the treatment facilities might receive excessive DE and appropriate measures recommended by NRC (http://www.nrc.gov/about-nrc/radiation/protects-you/protection-principles.html) should be applied. However, a safe distance of 5 m is recommended to reduce TEDE to acceptable level (2 - 39 mrem/yr).

External gamma radiation is the dominant pathway that contributes to TEDE for the first three scenarios while radon inhalation is the dominant pathway for the landfill scenario. Sensitivity analysis showed that increasing the distance between recipients and contaminated zone had the greatest impact on reducing TEDE contributed by gamma radiation pathway. A safe distance of 5 m is recommended to reduce more than 85% of TEDE contributed by external gamma radiation for the scenarios investigated in this study. Placement of a cover layer could effectively reduce TEDE contributed by radon inhalation in a landfill scenario.

7.0 SUMMARY, CONCLUSIONS AND FUTURE WORK

7.1 SUMMARY AND CONCLUSIONS

These studies were designed to investigate the key environmental and public health issues associated with Naturally Occurring Radioactive Material (NORM) generated by Marcellus Shale gas extraction. The specific objectives of this study were to: 1) understand the origin of key components (including Ra-226) in Marcellus Shale flowback and produced water; 2) develop a rapid method for Ra-226 measurement by ICP-MS; 3) investigate the fate of Ra-226 in centralized waste treatment facilities; 4) investigate the fate of Ra-226 in centralized water storage facilities; and 5) evaluate the health risks associated with NORM generated by Marcellus Shale gas extraction. The main findings of this study are summarized in the following sections with respect to the five objectives described above.

7.1.1 Origin of key components and radioactivity in flowback and produced water

The major dissolved solids (i.e., Cl, Na) and divalent ions (e.g., Ca, Mg) in Marcellus Shale flowback and produced water originate from the mixing of the fracking fluid with ancient connate water. Br concentration in connate water is around 2,000 ppm (50 meq/L), which suggests that seawater was concentrated almost 1,300 times. If the volume of connate water or

the stimulated shale volume is known, the plateau of Cl and MCl_2 concentrations in produced water can be predicted based on the mixing ratio of frac fluid to connate water.

A novel isotopic tracing based on Ra-228:Ra-226 and Th-228:Ra-228 ratios was developed to estimate the residence time of NORM in the liquid phase. The isotopic fingerprint of Marcellus Shale produced water shows the mean residence time of radium in liquid phase is between 0.4-6 years. The relatively short residence time suggests that Ra originated from rapid shale core leaching during frac fluid injection and implies that the concentration of Ra may keep increasing during the lifetime of a gas well.

7.1.2 Development of a rapid method for Ra-226 measurement by ICP-MS

Traditional methods for Ra-226 determination require either a long sample holding time or a long detection time. Recent developments in the ICP-MS and TIMS enable direct measurement of mass to charge ratio and could be used for rapid Ra-226 analysis. Produced water sample cannot be directly measured by ICP-MS due to its high TDS. In order to separate radium isotopes from the matrix elements in produced water, a combination of strong-acid resin and a strontium-specific resin was used. The separation method developed in this study would effectively reduce the residual Ca^{2+}, Ba^{2+}, Na^{+} and Sr^{2+} in the purified sample to below 20, 10, 2 and 0.1 ppm, respectively, which is suitable for ICP-MS analysis. The method optimization achieved high radium recovery (101±6% for standard mode and 97±7% for collision mode) with relative standard deviation (RSD) below 15% for samples with total dissolved solids as high as 230,000 mg/L.

7.1.3 Fate of Ra-226 in centralized waste treatment facilities

Sulfate precipitation is commonly used for flowback water treatment in centralized waste treatment facilities. During sulfate precipitation, it is unlikely to observe pure $RaSO_4$ precipitates because Ra^{2+} concentration is usually too low to reach saturation limit ($K_{sp,RaSO4} = 10^{-10.38}$). However, it is common for Ra^{2+} to co-precipitate with carrier metals. This study evaluated radium removal in barium–strontium sulfate co-precipitation system at different ionic strengths and identified the main carrier for radium during sulfate precipitation. Experimental results show that radium removal generally follows theoretical distribution law in binary systems and is enhanced in Ra-Ba-SO_4 system and restrained in Ra-Sr-SO_4 system by high ionic strength. However, experimental distribution coefficient (K_d') varies over a wide range and cannot be described by the distribution equation alone. Radium removal in ternary system is controlled by the co-precipitation of Ra-Ba-SO_4, which is attributed to rapid $BaSO_4$ nucleation rate and closer ionic radius of Ra^{2+} with Ba^{2+} than with Sr^{2+}. Overall, sulfate precipitation is effective in removing more than 90% of Ra from produced water as long as all Ba is removed. Co-precipitation of Ba-Ra-SO_4 is the dominant mechanism for Ra removal.

Calculations based on experimental results show that Ra levels in the precipitate generated in centralized waste treatment facilities far exceed regulatory limits for disposal in municipal sanitary landfills and require careful monitoring of allowed source term loading (ASTL) for technically enhanced naturally occurring materials (TENORM) in these landfills.

7.1.4 Fate of Ra-226 in centralized storage facilities

A field study over a 2.5-year period indicates that Ra-226 concentrations in centralized produced water storage facilities generally increase during the recycling of flowback water for hydraulic fracturing. In addition, Ra-226 keeps accumulating in the bottom sludge that can be classified as low-level radioactive solid waste as it exceeds the limit for RCRA-D landfill disposal. Accumulation of Ra-226 in the aged sludge was attributed to co-precipitation of Ba-Ra-SO_4 during the flowback water reuse for hydraulic fracturing. In addition, the legitimacy of the current disposal option for radioactive solid waste was discussed. Analysis showed that the disposal of radioactive solid waste in RCRA-D solid waste landfills is feasible as long as the landfill operators abide by the PA DEP guidance to monitor and track the radioactivity of incoming solid waste.

7.1.5 Health risks associated with NORM generated by Marcellus Shale gas extraction

The health risks associated with NORM, which is expressed as Total Effective Dose Equivalent (TEDE), was evaluated for several typical scenarios associated with Marcellus Shale gas extraction. Modeling results showed the range of TEDE for baseline conditions at drilling pads, storage impoundments, treatment facilities, and landfills are 2 – 37, 3 – 11, 119 – 2,390 and 53 mrem/yr, respectively. TEDE at drilling pads, storage impoundments and landfills are well below the NRC limit for general public (100 mrem/yr) and should be safe for on-site workers. Workers in the treatment facilities might receive excessive DE and appropriate measures recommended by NRC to minimize TEDE (http://www.nrc.gov/about-nrc/radiation/protects-

you/protection-principles.html) should be applied. For example, a safe distance of 5 m is recommended to reduce TEDE to acceptable level (2 - 39 mrem/yr).

External gamma radiation is the dominant pathway that contributes to TEDE for the first three scenarios while radon inhalation is the dominant pathway for the landfill scenario. Sensitivity analysis showed that increasing the distance between recipients and contaminated zone had the greatest impact on reducing TEDE contributed by gamma radiation pathway. A safe distance of 5 m is recommended to reduce more than 85% of TEDE contributed by external gamma radiation for the scenarios investigated in this study. Placement of a cover layer could effectively reduce TEDE contributed by radon inhalation in a landfill scenario.

7.1.6 Overall findings

In summary, this study investigated the key issues associated with Naturally Occurring Radioactive Material (NORM) generated from Marcellus Shale gas extraction. Ra-226 in produced water originated from shale leaching and its mean residence time in the liquid phase is between 0.4 – 6 years. This finding suggests that radium concentration is likely to increase during the lifetime of a gas well. Ra-226 can be effectively removed in centralized waste treatment facilities by sulfate precipitation as long as all barium is removed. Ra-226 concentration in centralized impoundments used in flowback water reuse for hydraulic fracturing would increase with time and would also keep accumulating in the sludge formed at the bottom of these impoundment. The solid waste generated at centralized waste treatment facilities and in impoundments contains elevated Ra-226 content and should be properly managed. TEDE at drilling pads, storage impoundments and landfills are well below the NRC limit for general public (100 mrem/yr) and should be safe for on-site workers. Workers in the centralized waste

treatment facilities might receive excessive TEDE and appropriate measures recommended by NRC should be applied.

Overall, this study contributes to the understanding of the fate of NORMs associated with Marcellus Shale gas wastewater management and expands the ability to resolve the environmental concerns associate with NORMs. A novel rapid analytical for Ra-226 measurement by ICP-MS offers an alternative for researchers to quickly analyze environmental samples. The fate of Ra-226 in centralized treatment facilities and storage facilities is important for operators to choose proper management strategy for liquid and solid waste disposal/reuse. The health risk associated with NORM that is assessed in this study will help to resolve the public concern stemming from the high NORM extracted from Marcellus Shale play and provides several options to further reduced its risks.

7.2 KEY CONTRIBUTIONS

These studies investigated the life cycle of Naturally Occurring Radioactive Material generated during Marcellus Shale gas extraction. Ra-226 is identified as the dominant radionuclide in Marcellus Shale flowback and produced water. A rapid method for analysis of Ra-226 by ICP-MS was developed in this study. Fate of Ra-226 in different scenarios associated with the shale gas extraction, including underground shale gas reservoir, flowback water storage facilities, flowback water treatment facilities, and solid waste disposal facilities, was evaluated in this study. Analysis showed that radium originated from a combination of fracturing fluid mixing with connate water and shale leaching. High concentrations of Ra in the Marcellus Shale

wastewater can be controlled by proper treatment (e.g., sulfate precipitation). However, solid waste generated in treatment facilities and impoundments containing elevated Ra content far exceed the limits for disposal in RCRA-D landfills. Current regulatory practice allows landfills to accept that solid waste by controlling the Allowed Source Term Loading (ALST) on annual basis. However, if the landfill capacity is insufficient to accept all Ra generated from Marcellus Shale gas extraction, other disposal or beneficial use options for solid waste should be developed.

The health risk associated with NORM, which is expressed as total effective dose equivalent (TEDE), at drilling pads, storage impoundments and landfills are well below the NRC limit for general public (100 mrem/yr). Workers in centralized waste treatment facilities could receive excessive DE and appropriate measures to minimize TEDE recommended by NRC should be applied.

7.3 FUTURE DIRECTIONS

These studies point out several potential hazards associated with solid waste due to Ra-226 generated by Marcellus Shale gas extraction. Those hazards include the high content of Ra-226 in the solid waste generated in centralized waste treatment facilities and bottom sludge in produced water storage impoundments. These solid waste streams are currently disposed in municipal solid waste landfills but this is not a sustainable strategy since the Ra-226 concentration may ultimately increase to unacceptable levels. Thus, other disposal options might be needed to manage Ra-226 generated by Marcellus Shale gas extraction.

Underground deep well injection, which is managed by the underground injection control (UIC) program, might be an option for radioactive wastewater disposal since there is currently no limit for NORM levels. However, the number of UIC wells in Pennsylvania is limited and may not be adequate for disposal of large volume of flowback and produced water. However, if Ra-226 can be separated in a limited solid waste that can be dissolved to produce liquid with high Ra-226 concentration, it may be disposed in UIC well. Previous study showed the co-precipitation of Ra-$BaSO_4$ results in solid waste that is very inert and cannot be dissolved even at pH=0.5. Microbial reduction of sulfate from barite by sulfate-reducing bacteria is not practical to achieve $BaSO_4$ decomposition. However, barium sulfate can be reduced to barium sulfide by heating at 850-1100 °C and using carbon as the reducing agent. Therefore, reducing $BaSO_4$ into soluble BaS and disposal into UIC well might be a promising method for radioactive $BaSO_4$ disposal and should be studied in the future.

Another method to generate soluble solid waste for UIC well injection is to use carbonate instead of sulfate in treatment facilities for radium removal. Previous study showed that carbonate precipitation may be suitable for Ra removal and all carbonates can be dissolved to generate the concentrate for UIC disposal. A future study to quantify radium removal during carbonate precipitation in Marcellus Shale flowback water would be helpful to validate the effectiveness for Ra treatment.

Disposal of solid waste containing elevated radium content may be avoided by its beneficial reuse for other purposes. Barite, which is the major carrier for radium, may be reused as a weighting agent in drilling mud to help cool the drill bit and maintain integrity of the well bore. Barite used as weighting agent should fulfill the API (American Petroleum Institute) standards, which specify barite content, particle size and presence of impurities. Therefore, a

feasibility study for the production of API grade barite for beneficial reuse would be helpful to turn hazardous waste (Ra-Ba-SO_4) into profitable resource.

Marcellus Shale flowback and produced water has a unique fingerprint of isotopic ratios, such as Sr-87:Sr-86 and Ra-226:Ra-228. Previous study used the isotopic fingerprint in river sediments to identify the impact of shale gas wastewater disposal on water quality in western Pennsylvania. The isotopic signature of Ra-226:Ra-228 is also highly dependent on the residence time since the decay rate of Ra-228 is much faster than that of Ra-226. Therefore, a future work to investigate the Ra-228:Ra-226 ratios in river sediments to identify the environmental legacy of Marcellus Shale industry would be helpful to alleviate public concern and support regulatory developments.

APPENDIX A

SUPPORTING INFORMATION FOR CHAPTER 2

Table A. 1 Major element and Ra isotope Data for Marcellus Produced Water Samples

Well	Time (Days)	Ra226 (pCi/L)	Corrected Ra-228 (pCi/L)	TDS	Cl	Br	Ba	Sr	Ca	Mg	SO_4	Ra-228: Ra-226
A-1	1	633±195	-	17785	6852	90	207	46	349	39	-	-
	4	1470±327	-	44018	26686	281	504	381	2278	217	29	-
	5	1430±340	-	54915	29653	256	632	450	2880	254	8	-
	7	2044±512	-	64421	41025	361	1409	651	3938	381	6	-
	12	2925±605	264±61	84293	44036	385	2193	934	5603	518	4	0.090
	15	3325±595	-	94005	52640	470	2687	1127	6292	630	4	-
	29	3600±770	336±89	103250	57403	500	2987	1215	6236	671	1	0.093
	730	6040±685	616±146	145868	85246	947	4283	2298	12353	1233	1	0.102
A-2	1	417±42	-	22000	18551	176	333	214	1239	694	34	-
	5	1365±187	-	69255	41513	366	1058	738	2782	490	7	-
	7	2044±512	-	77330	47225	418	1490	900	4627	559	5	-
	11	3560±740	254±83	78000	55291	497	2306	1063	5749	211	5	0.071
	16	3883±915	-	96405	59747	526	2700	1380	6278	366	2	-
	730	7520±1428	855±132	173032	100045	995	4716	2666	14146	1398	1	0.114

Table A. 1 (continued)

B	1	250±27	-	135564	90504	891	151	1393	12278	1267	-	-
	3	540±100	-	155812	92899	915	194	1694	14028	1478	-	-
	5	716±353	386±92	158406	101641	1017	253	1832	15269	1632	-	0.539
	7	1027±272	360±70	167730	103506	1033	296	1872	15875	1671	-	0.351
	10	1250±293	511±75	173333	104985	1051	328	1888	16509	1820	-	0.401
	15	1557±372	-	175683	115128	1165	349	2045	17612	1896	-	-
	20	1585±377	678±92	182702	111511	1111	379	2151	18080	1933	-	0.428
	1240	3408±727	1458±163	230268	123897	1319	428	3034	24141	1991	-	0.428
C-1	<30	1185±465	-	43000	24256	261	255	398	3567	229	-	-
	<30	2570±962	-	69840	55606	410	515	609	4247	339	-	-
	<30	3550±910	-	85350	52601	520	818	838	5211	474	-	-
	475	10650±2070	1041±128	194020	112917	1169	3417	3157	16439	1477	-	0.098
C-2	<30	595±123	-	22390	8071	113	125	275	1300	102	-	-
	<30	1350±185	-	69000	24478	256	428	639	5234	398	-	-
	<30	3100±720	393±108	89925	36073	378	840	887	5894	531	-	0.127
	475	10400±2004	1485±205	182340	104609	1117	2984	2871	15792	1449	-	0.143
C-3	<30	-	-	44720	27805	277	298	447	2397	192	-	-
	<30	3730±1020	-	94420	57855	589	861	838	5400	468	-	-
	<30	-	-	99365	58391	593	1035	1165	6905	604	-	-
	475	13033±1893	1386±228	186472	102547	1086	3417	2912	15557	1327	-	0.106

-: not measured/ detected.

Table A. 2 Ra-226/228 activities in Marcellus Shale core samples collected in Washington County, PA

Name	Depth	Ra-226 (pCi/L)	Ra-228 (pCi/L)	Ra-228: Ra-226
Marcellus Middle 1	6381.5-6381.8’	5.91	1.27	0.21
Marcellus Middle 2	6388.6-6389.0’	8.38	0.89	0.11
Marcellus Middle 3	6398.1-6398.5’	24.50	0.50	0.02
Marcellus Lower 1	6407.5-6407.9’	16.45	0.52	0.03
Marcellus Lower 2	6419.3-6419.6’	1.60	0.66	0.41
Average		11.37	0.77	0.16

A.1 Activity to Mass Unit Conversion

Radioactivity and mass of radionuclide are two concepts and their conversion is subject to decay rate. The term "specific activity" is defined as the radioactivity (i.e. decay rate) of a radionuclide per unit mass of the radionuclide. For example, the specific activity of Ra-226 is 1, meaning that 1 g of Ra-226 contains 1 curie. It also means that there are 3.7×10^{10} Ra-226 atoms disintegrating every second in a gram of Ra-226. In general, the higher a radionuclide's specific activity, the shorter its half-life (decay rate), and the more "radioactive" it is when compared to one with a lower specific activity.

There are two common activity units: Becquerel (Bq) is a SI unit of radioactivity, and 1 Bq=1 decay per second; A Curie is a non-SI unit of radioactivity, named after Marie and Pierre Curie, and defined as: $1\mathrm{Ci} = 3.7 \times 10^{10}\mathrm{decays\ per\ second}$.

The specific activity of a radionuclide can be converted by decay model:

$$\lambda = \frac{ln2}{t_{1/2}} \quad \text{(A-1)}$$

Where λ denotes decay constant, and t1/2 is half-life of a radionuclide.

Activity (A) of a radionuclide equals to the number of atoms ($N_{(t)}$) times decay constant:

$$\mathrm{A} = -\left(\frac{dN_{(t)}}{dt}\right) = \lambda \times \mathrm{N(t)} \quad \text{(A-2)}$$

Since the Avogadro constant is 6.02×10^{23}, the molar mass is M.

Thus, the specific activity (SA), which is also called activity to mass factor, of a radionuclide is:

$$\text{SA (Bq/gram)} = \frac{6.02\times10^{23}\times\lambda}{1\text{gram}\times\text{M}} \quad \text{(A-3)}$$

Activity to mass conversion factor was summarized in Table A.3.

Table A. 3 Decay parameters for isotopes in U-238 and Th-232 series

Isotope	Half-life ($t_{1/2}$, years)	Decay constant (λ, y-1)	Activity to mass Factor (g/Ci)
U-238	4.5E+9	1.54E-10	2995841
U-234	2.4E+5	2.89E-06	157
Th-232	1.4E+10	4.95E-11	9085426
Th-228	1.9	3.65E-1	0.00121
Th-234	6.57E-2	1.05E+1	0.00004
Th-230	7.7E+4	9.00E-06	50
Ra-228	5.8	1.19E-1	0.00370
Ra-226	1.6E+3	4.33E-4	1

A.2 Decay model & Equilibrium

Since the activity stands for the decay rate of a radionuclide, the activity of a decay product is related to the activity of its parent. The secular equilibrium between Ac-228 to Ra-228 and transient equilibrium between Th-228 and Ra-228 was derived to calculate their activity ratios in equilibrium condition.

Secular equilibrium between Ac-228 and Ra-228

The time dependence of number of atoms versus activity follows the equation:

$$\text{A}_{\text{Ra228,t}} = \frac{\text{dN}_{\text{Ra228}}}{\text{dt}} = \lambda_{\text{Ra228}} \cdot \text{N}_{\text{Ra228}} = \text{A}_{\text{Ra228,0}} \cdot \text{e}^{-\lambda_{\text{Ra228}}\cdot\text{t}} \quad \text{(A-4)}$$

Where: A: activity of a radionuclide (pCi), 0 means start time 0.

The activity of progeny Ac-228 equals to the Ac-228 generation rate (based on Ra-228 decay) deduct decay rate.

$$\frac{dN_{Ac,228}}{dt} = \lambda_{Ra228} \cdot N_{Ra228} - \lambda_{Ac228} \cdot N_{Ac228} \quad \text{(A-5)}$$

Substitute equation A-4 to A-5,

$$\frac{dN_{Ac228}}{dt} + \lambda_{Ac228} \cdot N_{Ac228} = \lambda_{Ra228} \cdot N_{Ra228,0} \cdot e^{-\lambda_{Ra228} \cdot t} \quad \text{(A-6)}$$

Thus, the activity of direct progeny Ac-228 at time t is:

$$A_{Ac228,t} = \lambda_{Ac228} \left(\frac{A_{Ra228,0} \times e^{-\lambda_{Ra228} \cdot t}}{\lambda_{Ac228} - \lambda_{Ra228}} + \frac{A_{Ra228,0} \times e^{-\lambda_{Ac228} \cdot t}}{\lambda_{Ra228} - \lambda_{Ac228}} \right) \quad \text{(A-7)}$$

The activity ratio of Ac-228 to Ra-228 at time t is:

$$\frac{A_{Ac228,t}}{A_{Ra228,t}} = \left(\frac{\lambda_{Ac228}}{\lambda_{Ac228} - \lambda_{Ra228}} + \frac{e^{(-\lambda_{Ac228} + \lambda_{Ra228}) \cdot t}}{\lambda_{Ra228} - \lambda_{Ac228}} \right) \quad \text{(A-8)}$$

When the activity ratio of Ac-228 to Ra-228 reaches equilibrium,

$$\frac{A_{Ac228,t}}{A_{Ac228,t}} = \frac{\lambda_{Ac228}}{\lambda_{Ac228} - \lambda_{Ra228}} = 1 \quad \text{(A-9)}$$

Transient equilibrium between Th-228 and Ra-228

Th-228 is a direct daughter of Ac-228 and indirect daughter of Ra-228. The activity of Th-228 can be further calculated based on the following equation:

$$A_{Th228,t} = \lambda_{Th228} \left(\frac{A_{Ra228,0} \cdot \lambda_{Ac228} \cdot e^{-\lambda_{Ra228} \cdot t}}{(\lambda_{Ac228} - \lambda_{Ra228})(\lambda_{Th228} - \lambda_{Ra228})} + \frac{A_{Ra228,0} \cdot \lambda_{Ac228} \cdot e^{-\lambda_{Ac228} \cdot t}}{(\lambda_{Ra228} - \lambda_{Ac228})(\lambda_{Th228} - \lambda_{Ac228})} + \frac{A_{Ra228,0} \cdot \lambda_{Ac228} \cdot e^{-\lambda_{Th228} \cdot t}}{(\lambda_{Ra228} - \lambda_{Th228})(\lambda_{Ac228} - \lambda_{Th228})} \right) \quad \text{(A-10)}$$

The activity ratio of Th-228: Ra-228 at time t is:

$$\frac{A_{Th228,t}}{A_{Ra228,t}} = \lambda_{Th228} \left(\frac{\lambda_{Ac228}}{(\lambda_{Ac228} - \lambda_{Ra228})(\lambda_{Th228} - \lambda_{Ra228})} + \frac{\lambda_{Ac228} \cdot e^{(-\lambda_{Ac228} + \lambda_{Ra228}) \cdot t}}{(\lambda_{Ra228} - \lambda_{Ac228})(\lambda_{Th228} - \lambda_{Ac228})} + \frac{\lambda_{Ac228} \cdot e^{(-\lambda_{Th228} + \lambda_{Ra228}) \cdot t}}{(\lambda_{Ra228} - \lambda_{Th228})(\lambda_{Ac228} - \lambda_{Th228})} \right) \quad \text{(A-11)}$$

When the activity ratio of Th-228 to Ra-228 reaches equilibrium,

$$\frac{A_{Th228,t}}{A_{Ra228,t}} = \frac{\lambda_{Th228} \cdot \lambda_{Ac228}}{(\lambda_{Ac228} - \lambda_{Ra228})(\lambda_{Th228} - \lambda_{Ra228})} = 1.48 \quad \text{(A-12)}$$

APPENDIX B

SUPPORTING INFORMATION FOR CHAPTER 3

Table B.1. Parameters and operating conditions for ICP-MS

ICP-MS	Type/Value/Mode
Mode	Standard/ Kinetic mode
Spray chamber	SIS
RF power	1400 W
Vacuum Pressure	4.30e-7
RF Voltage	200 V
Sample uptake rate	270 µL/min
Coolant	1.092 gal/min
Auxiliary Gas Flow	1.2 L/min
Nebulizer Gas Flow	0.9 L/min
Plasma Gas Flow	17 L/min
Sample cone	Standard, Ni
Skimmer cone	Standard, Ni
Spray Chamber	Peltier-cooled baffled quartz cyclonic
Nebulizer	PFA ST
Replicates per Sample	3

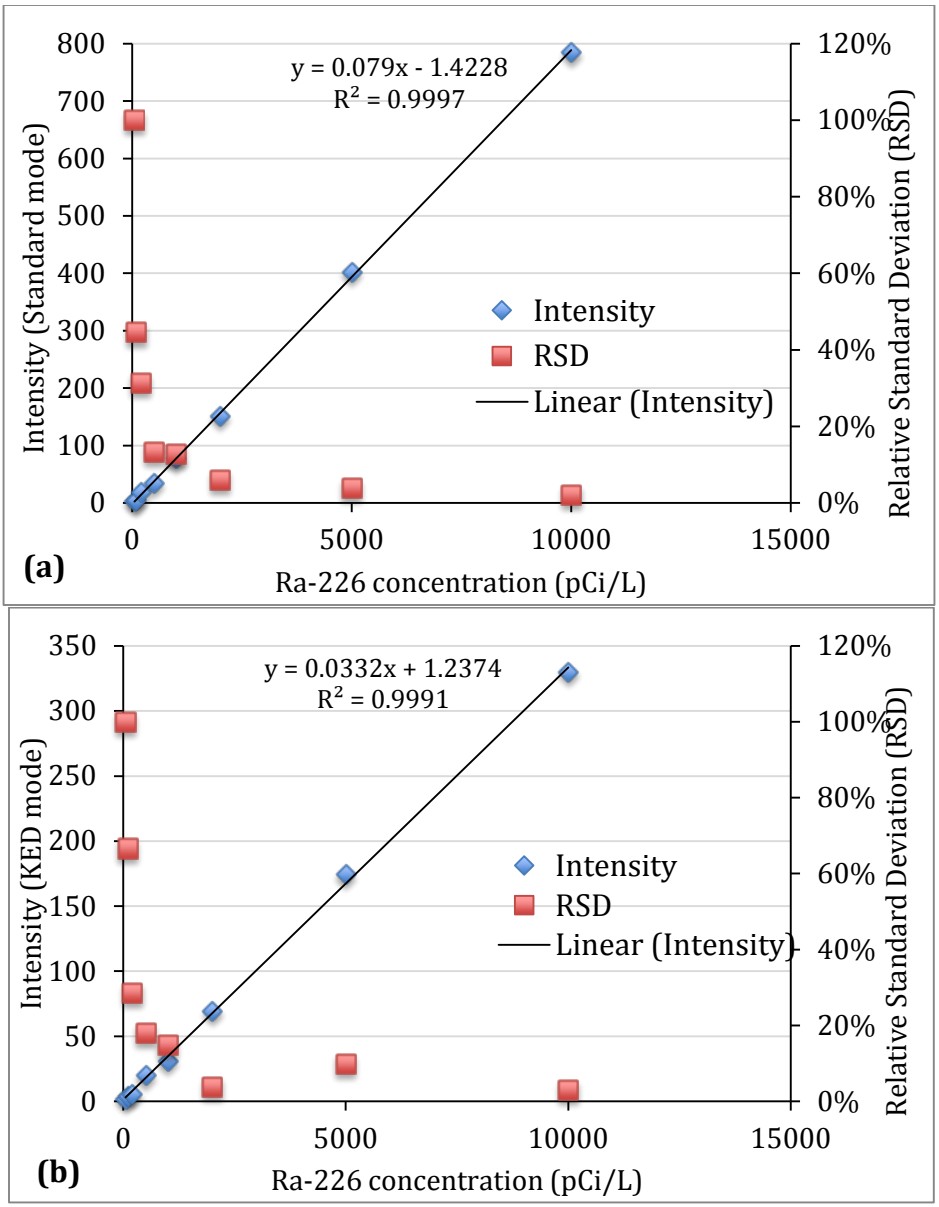

Figure B. 1 Ra-226 calibration curve for ICP-MS operated in: a) standard mode and b) collision mode

Table B.2. Comparison of Ra-226 measurement methods

Detection method	Sample preparing time per series of samples	Sample holding time	Detection time per sample
Liquid Scintillation Counter	3 h	22 days*	1-2 h
Gamma spectroscopy	0-2 h	22 days**	24-48 h
ICP-MS	12 h	No	6 min

*Some studies suggest the sample holding time can be omitted[1] but this needs to be carefully evaluated because of potential interferences from: 1) alpha and beta particle emissions by other radionuclides (e.g. Ra-228, Ba-233 etc.)[2] and 2) high Ba concentration in Marcellus Shale PW, which would result in insufficient Ra recovery during sample preparation.[3]

** The sample holding time can be omitted as long as the interference from U-235 on Ra-226 signal at 186 KeV is negligible.[3, 4]

Even though the sample preparation for the method developed in this study is relatively long (up to 12 hours), ICP-MS analysis is more efficient compared with other methods since it does not require the sample holding time (~ 22 days). In addition, the detection time for ICP-MS is only 6 min/sample, which is significantly shorter than that for LSC (1-2 h/sample) and gamma spectrometry (24-48 h/sample).

Table B.3. Chemical composition of actual Marcellus Shale wastewater samples used in this study and comparison of Ra-226 analysis by ICP-MS and gamma spectrometry

Sample	Type	MSW composition (mg/L)					Residual ion concentrations in purified samples (mg/L)				Reference Ra-226 (pCi/L)[1]	ICP-MS results			
												Standard mode		Collision mode	
		Na	Ca	Ba	Sr	TDS	Na	Ca	Ba	Sr		Ra-226 recovery[2]	RSD	Ra-226 recovery[2]	RSD
1	Low salinity MSW	11,800	2,280	740	381	44,000	5	31	1	<0.1	1,580±327 (1,580±21%)	111±23%	8%	110±22%	22%
2		18,300	3,940	1,400	651	64,400	3	24	2	<0.1	2,044±512 (2,044±25%)	102±26%	4%	108±27%	17%
3		26,300	6,240	2,990	1,220	103,000	3	14	8	<0.1	3,560±770 (3,560±22%)	112±24%	5%	105±23%	9%
4	MSW istorage	20,900	9,610	297	3,330	90,500	4	15	2	<0.1	1,410±320 (1,410±23%)	144±33%	10%	116±26%	28%
5		23,600	7,960	155	3,160	88,900	4	26	3	<0.1	1,470±463 (1,470±31%)	112±35%	5%	118±37%	9%
6	High salinity MSW	39,800	12,400	3,920	2,230	146,000	1	11	1	<0.1	3,156±446 (3,156±14%)	106±15%	4%	99±14%	6%
7		42,700	15,600	3,420	2,910	186,000	1	9	2	<0.1	6,040±685 (6,040±11%)	97±11%	6%	94±11%	1%
8		47,700	24,100	428	3,030	230,000	2	14	8	<0.1	13,033±1,893 (13,033±15%)	98±11%	5%	90±13%	4%
9		156,000	25,300	7,660	10,350	415,000	9	29	8	<0.1	21,550±3,230 (21,550±15%)	94±14%	4%	98±15%	2%

[1]Reference Ra-226 concentrations were measured by gamma spectrometry for 24-72 hours;

[2]Ra-226 recovery was calculated using the mean value of Ra-226 concentration measured by ICP-MS divided by low and high values of Ra-226 concentration measured by gamma spectrometry.

APPENDIX C

SUPPORTING INFORMATION FOR CHAPTER 4

C.1 Derivation of Distribution Coefficient (K_d)

Sulfate-based co-precipitation of radium in a binary system with barium has been previously examined.[1,2,3] Doerner and Hoskins[3] described co-precipitation of Ra-Ba-SO_4 and stipulated that the formation of carrier (M) solids (Equation C.1) happens simultaneously with the replacement reaction (Equation C.2):

$$M^{2+} + SO_4^{2-} \rightarrow MSO_4 \qquad (C.1)$$

$$Ra^{2+} + MSO_4 \rightarrow M^{2+} + RaSO_4 \qquad (C.2)$$

The distribution law is derived assuming that the radium ion and the carrier ion (e.g., Ba^{2+}, Sr^{2+}) precipitation as sulfates is proportional to their concentrations in the solution.[3] The Nernst-Berthelot equation[4] applies to solid solution formation from an aqueous solution of constant composition:

$$\frac{RaSO_4}{MSO_4} = K_d \frac{Ra^{2+}}{M^{2+}} \qquad (C.3)$$

where, K_d is concentration-based effective distribution coefficient, MSO_4 and $RaSO_4$ are relative fractions (or "concentrations") of carrier and radium in solid precipitate that forms and M^{2+} and Ra^{2+} are equilibrium concentrations in solution.

The activity-based equilibrium (K_{eq}) constant for lattice replacement reaction (Equation C.2) can be expressed as:

$$K_{eq} = \left(\frac{\gamma_{M^{2+}} \cdot X_{M^{2+}}}{\gamma_{Ra^{2+}} \cdot X_{Ra^{2+}}}\right) / \left(\frac{\gamma_{MSO4} \cdot X_{MSO4}}{\gamma_{RaSO4} \cdot X_{RaSO4}}\right) \quad \text{(C.4)}$$

where, γ and X are activity coefficient and molar concentration in aqueous or solid phase, respectively.

Combining Equations C.3 and C.4 yields the expression for the theoretical distribution coefficient:

$$K_d = K_{eq} \cdot \frac{\gamma_{Ra^{2+}}}{\gamma_{\square^{2+}}} \cdot \frac{\gamma_{MSO4}}{\gamma_{RaSO4}} \quad \text{(C.5)}$$

The equilibrium constant (K_{eq}) can then be calculated either based on Gibbs free energy of formation (Table C.1) or as the ratio of solubility products:

$$K_{eq} = \frac{K_{sp,RaSO4}}{K_{sp,MSO4}} \quad \text{(C.6)}$$

The activity coefficient (γ) for the solid phase may be calculated using Margules solution model[15] for the binary system consisting of M-Ra-SO_4 as follows:

$$R \cdot T \cdot \ln \gamma_{MSO4} = W \cdot (1 - X_{MSO4})^2 \quad \text{(C.7)}$$

$$R \cdot T \cdot \ln \gamma_{RaSO4} = W \cdot (1 - X_{RaSO4})^2 \quad \text{(C.8)}$$

where, R is the ideal gas constant (8.31446 J/(mol·K)), T is the Kelvin temperature, W is the Margules parameter denoting the energy necessary to interchange one mole of $RaSO_4$ with one mole of MSO_4 in the mixture without changing its composition.[5] The Margules parameter

was derived by Zhu. et al.[6] based on the correlation between the formation energy and volumetric mismatch between the two substituting end-members (Table C.2).

Since the carrier metal dominates the solid phase, activity coefficient of the carrier metal sulfate (γ_{MSO4}) is assumed to be one. The activity coefficient of trace solid component ($RaSO_4$), which accounts for the inconformity of $RaSO_4$ in the carrier lattice, is always larger than 1.

Combining Equations C.5 and C.8, the distribution coefficient can be calculated as follows:

$$\ln K_d = \ln\left(\frac{K_{sp,MSO4}}{K_{sp,RaSO4}}\right) + \ln\left(\frac{\gamma_{Ra^{2+}}}{\gamma_{M^{2+}}}\right) - \frac{W(1-X_{RaSO4})^2}{RT} \qquad (C.9)$$

All terms in Equation C.9 except for the ion activity coefficient ratio are regarded as constant for a fixed solution composition. Therefore, theoretical distribution coefficients for Ra-$BaSO_4$ and Ra-$SrSO_4$ in dilute solutions are:

$$K_{d,Ra-BaSO4} = 1.54 \quad \text{And} \quad K_{d,Ra-SrSO4} = 237$$

It is common to assume that the activity coefficients of similar ions (Ra^{2+} and Ba^{2+}) are identical.[1,2,7] This assumption is valid for dilute solutions but becomes less accurate at higher ionic strength. The dependence of activity coefficients for Ra and Ba on ionic strength can be estimated using Pitzer ion interaction model, which is designed to calculate aqueous phase activity coefficients at ionic strength of up to 6M.[8] The Pitzer parameters ($\beta^{(0)}_{Ra-Cl}$, $\beta^{(1)}_{Ra-Cl}$ and Ra^{ϕ}_{Ra-Cl}) for Ra^{2+}-Cl^- interaction were extrapolated by linear regression of parameters for Ca^{2+}, Mg^{2+}, Sr^{2+} and Ba^{2+} to their 8-fold hydrated ionic radii.[9] Ion activity coefficients were calculated using the geochemical speciation code PHREEQC 2.12.5 (USGS) with Pitzer formalism and are shown in Figure C.1. Theoretical distribution coefficients for Ra-$BaSO_4$ and Ra-$SrSO_4$ as a function of ionic strength were calculated using Equation C.9 and are shown in Figure 4.1.

Table C.1. Standard state thermodynamic properties and molar volumes[17]

Formula	$\Delta G_f^0, J/mol$	logKsp	V^0 cm^3/mol
$RaSO_4$	-1,365,197	-10.38	55.35
$BaSO_4$	-1,362,156	-9.99	52.10
$SrSO_4$	-1,341,809	-6.63	46.37
Ra^{2+}	-561,493	-	-
Ba^{2+}	-555,342	-	-
Sr^{2+}	-559,484	-	-
SO_4^{2-}	-744,459	-	-

Table C.2. Volumetric mismatch ($\Delta V = \frac{(V^0_{RaSO4} - V^0_{MSO4})^2}{V^0_{RaSO4}}$), Margules parameter (W) and activity coefficient of $RaSO_4$ in binary solid-solution

Binary system	ΔV	W (cal/mol)[17]	γ_{RaSO4}
Ra-$BaSO_4$	0.191	1156.87	1.60
Ra-$SrSO_4$	1.457	7826.59	23.59

C.2 Theoretical distribution coefficient under varying ionic strength

Activity coefficient of a species in a mixture is controlled by the ionic strength of the solution. A semi-empirical ion interaction model (Pitzer equation) has been shown to accurately predict activity coefficients at ionic strength up to 6 mol/L and has been adopted in this study to calculate the activity coefficients of divalent cations.[10,11] Geochemical equilibrium model Phreeqc with Pitzer database was used to calculate the activity coefficient ratios for divalent cations of interest in this study shown on Figure C.1. Pitzer parameter that were missing from the Phreeqc database were adopted from previous studies[9,12].

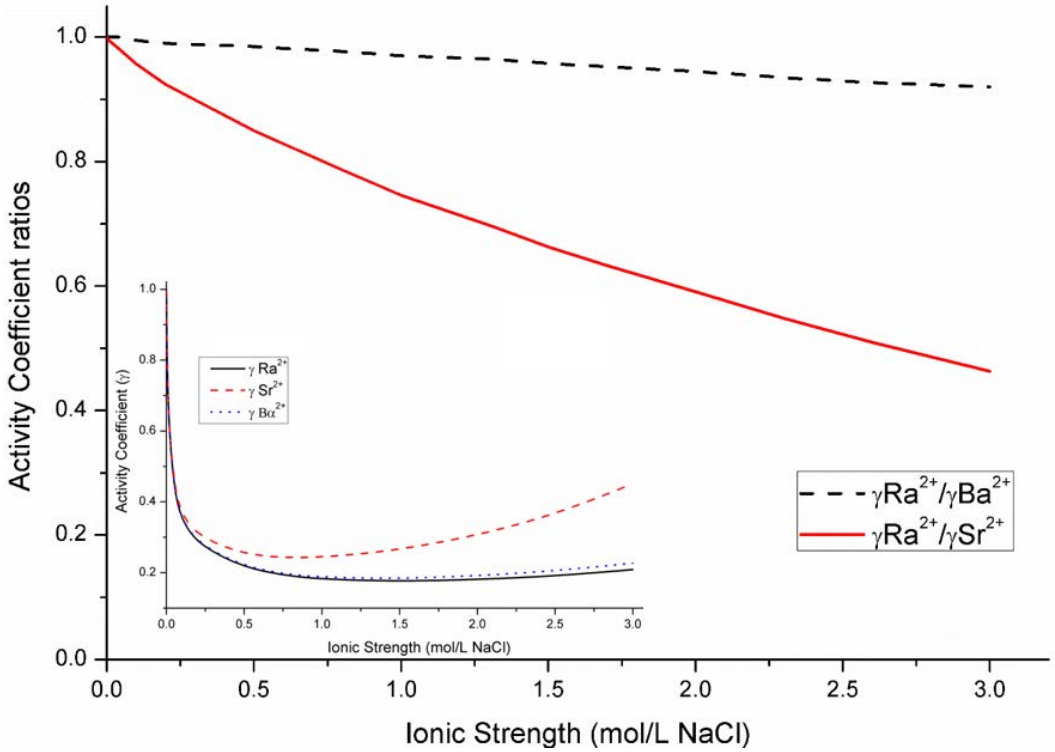

Figure C.1. Theoretical activity coefficient of divalent cations and activity coefficient ratios as a function of ionic strength adjusted with NaCl. Calculations were conducted with geochemical model PhreeqcI using Pitzer ion interaction theory.

BIBLIOGRAPHY

Chapter 1:

1. U.S. Energy Information Admisnistration. Annual Energy Outlook 2014 with projections to 2040, DOE/EIA-0383. U.S. Department Of Energy; Washington DC, 2014.

2. Economides, M. J.; Nolte, K. G. Reservoir stimulation. Chichester, Wiley, 2000.

3. Alexander, T.; Baihly, J.; Boyer, C.; Clark, B.; Waters, G.; Jochen, V.; Calvez J.L.; Lweis. R.; Miler, C.K.; Thaeler, J.; Toleel., B.E. Shale gas revolution. *Oilfield Review*, **2011**, 23(3), 40-55.

4. Holditch, S.; Perry, K.; Lee, J. Unconventional Gas Reservoirs—Tight Gas, Coal Seams, and Shales, Working Document of the National Petroleum Council on Global Oil and Gas Study. National Petroleum Council, 2007.

5. U.S. Energy Information Administration. Annual Energy Outlook 2012. U.S. Department of Energy; Washington, DC, 2012.

6. Vidic, R. D.; Brantley, S. L.; Vandenbossche, J. M.; Yoxtheimer, D.; Abad, J. D. Impact of shale gas development on regional water quality. *Science*, **2013**, 340 (6134): 1235009.

7. Gregory, K. B.; Vidic, R. D.; Dzombak, D. A. Water management challenges associated with the production of shale gas by hydraulic fracturing. *Elements*, **2011**, 7 (3), 181−186.

8. Kargbo, D. M.; Wihelm, R. G.; Campbell, D. J. Natural gas plays in the Marcellus shale: Challenges and potential opportunities. *Environmental Science & Technology*, **2010**, 44 (15), 5679-5684.

9. Swanson, V. E. Geology and geochemistry of uranium in marine black shales: a review. Washington, DC: US Government Printing Office, 1961.

10. Sutton, M.; Burastero, S. R. Uranium (VI) solubility and speciation in simulated elemental human biological fluids. *Chemical research in toxicology*, **2004**, 17 (11), 1468-1480.

11. McDiarmid, M. A.; Gaitens, J. M.; Squibb, K. B. Uranium and thorium. *Patty's toxicology*, **2012**, 42, 769-816.

12. Rowan, E.; Engle, M.; Kirby, C.; Kraemer, T. Radium content of oil-and gas-field produced waters in the Northern Appalachian basin (USA)—Summary and discussion of data. U.S. Geological Survey Scientific Investigations Report 2011-5135, U.S. Geological Survey, 2011.

13. U.S. Nuclear Regulatory Commission, Standards for protection against radiation – Appendix B – Radionuclide Table-Radium-226, **2013**, 10 C.F.R, §20.

14. Norris, W. P.; Kisieleski, W. Comparative metabolism of radium, strontium, and calcium. In Cold Spring Harbor Symposia on Quantitative Biology. Cold Spring Harbor Laboratory Press, Vol. 13, 164-172, 1948.

15. Canu, I. G.; Laurent, O.; Pires, N.; Laurier, D.; Dublineau, I. Health effects of naturally radioactive water ingestion: the need for enhanced studies. *Environ Health Perspect*, **2011**, 119(12), 1676-1680.

Chapter 2:

1. Alexander, T.; Baihly, J.; Boyer, C.; Clark, B.; Waters, G.; Jochen, V.; Calvez J.L.; Lweis. R.; Miler C.K.; Thaeler. J.; Toleel., B.E. Shale gas revolution. *Oilfield Review*, **2011**, 23(3), 40-55.

2. Vidic, R. D.; Brantley, S. L.; Vandenbossche, J. M.; Yoxtheimer, D.; Abad, J. D. Impact of shale gas development on regional water quality. *Science*, **2013**, 340 (6134), 1235009.

3. Gregory, K. B.; Vidic, R. D.; Dzombak, D. A. Water management challenges associated with the production of shale gas by hydraulic fracturing. *Elements*, **2011**, 7(3), 181-186.

4. Barbot, E.; Vidic, N. S.; Gregory, K. B.; Vidic, R. D. Spatial and temporal correlation of water quality parameters of produced waters from Devonian-age shale following hydraulic fracturing. *Environmental Science & Technology*, **2013**, 47(6), 2562-2569.

5. Rowan, E.; Engle, M.; Kirby, C.; Kraemer, T. Radium content of oil-and gas-field produced waters in the Northern Appalachian basin (USA)—Summary and discussion of data. U.S. Geological Survey Scientific Investigations Report 2011-5135, U.S. Geological Survey, 2011.

6. Johnston, A.; Martin, P. Rapid analysis of ^{226}Ra in waters by γ-ray spectrometry. *Applied radiation and isotopes*, **1997**, 48(5), 631-638.

7. Murray, A. S.; Marten, R.; Johnston, A.; Martin, P. Analysis for naturally occurring radionuclides at environmental concentrations by gamma spectrometry. *Journal of Radioanalytical and Nuclear Chemistry*, **1987**, 115(2), 263-288.

8. New York State Department of Environmental Conservation (NYSDEC), 2009. Draft Supplemental Generic Environmental Impact Statement (SGEIS) on the oil, gas, and solution mining regulatory program: Well permit issuance for horizontal drilling and high-volume hydraulic fracturing to develop the Marcellus Shale and other low-permeability gas reservoirs: New York State Department of Environmental Conservation, Division of Mineral Resources, Bureau of Oil and Gas Regulation, Appendix 13, NYS Marcellus radiological data from production brine, accessed July 14, 2011, Full document: http://www.dec.ny.gov/energy/58440.html

9. PADEP BOGM, Bureau of Oil and Gas Management. Frac and flowback water analytical data, Radioisotopes, spreadsheet. Available at http://www.bfenvironmental.com/pdfs/PADEP_Frac_Flow_Back_Water_Study_Presence_of_Radioisotopes.pdf

10. Carpenter, A. B. Origin and chemical evolution of brines in sedimentary basins. SPE Annual Fall Technical Conference and Exhibition, Society of Petroleum Engineers, 1978.

11. Dresel, P. E.; Rose, A. W. Chemistry and origin of oil and gas well brines in western Pennsylvania. Pennsylvania Geological Survey, 4th series Open-File Oil and Gas Report: 10-01, 2010.

12. Sonney, R.; Vuataz, F. D.; Cattin, S. Use of Cl/Br ratio to decipher the origin of dissolved mineral components in deep fluids from the Alps range and neighbouring areas, 2010.

13. McCaffrey, M. A.; Lazar, B.; Holland, H. D. The evaporation path of seawater and the coprecipitation of Br^- and K^+ with halite. *Journal of Sedimentary Research*, **1987**, 57(5), 928-937.

14. Engle, M. A.; Rowan, E. L. Interpretation of Na–Cl–Br systematics in sedimentary basin brines: comparison of concentration, element ratio, and isometric log-ratio approaches. *Mathematical Geosciences*, **2013**, 45(1), 87-101.

15. Haluszczak, L. O.; Rose, A. W.; Kump, L. R. Geochemical evaluation of flowback brine from Marcellus gas wells in Pennsylvania, USA. *Applied Geochemistry*, **2013**, 28, 55-61.

16. Blauch, M. E.; Myers, R. R.; Moore, T.; Lipinski, B. A.; Houston, N. A. Marcellus Shale Post-Frac Flowback Waters-Where Is All the Salt Coming From and What Are the Implications?. SPE Eastern Regional Meeting. Society of Petroleum Engineers, 2009.

17. Lutz, B. D.; Lewis, A. N.; Doyle, M. W. Generation, transport, and disposal of wastewater associated with Marcellus Shale gas development. *Water Resources Research*, **2013**, 49(2), 647-656.

18. Bibby, K. J.; Brantley, S. L.; Reible, D. D.; Linden, K. G.; Mouser, P. J.; Gregory, K. B.; Brian R. E.; Vidic, R. D. Suggested Reporting Parameters for Investigations of Wastewater from Unconventional Shale Gas Extraction. *Environmental Science & Technology*, **2013**, 47(23), 13220-13221.

19. Balashov, V. N.; Engelder, T.; Gu, X.; Fantle, M. S.; Brantley, S. L. A model describing flowback chemistry changes with time after Marcellus Shale hydraulic fracturing. *AAPG Bulletin*, **2014**, 20 (140), 143-154.

20. Goswami, A.; Acharya, A.; Pandey, A. K. Study of self-diffusion of monovalent and divalent cations in Nafion-117 ion-exchange membrane. *The Journal of Physical Chemistry B*, **2001**, 105 (38), 9196-9201.

21. Resnikoff, M.; Alexandrova, E.; Travers, J. Radioactivity in marcellus shale. Report Prepared for Residents of for the Preservation of Lowman and Chemung (RFPLC), 2010.

22. Wiegand, J. W., Sebastian, F. Origin of radium in high-mineralized waters. 2002

23. Heaton, B.; Lambley, J. TENORM in the oil, gas and mineral mining industry. *Applied radiation and isotopes*, **1995**, 46(6), 577-581.

24. Zhang, T.; Gregory, K.; Hammack, R. W.; Vidic, R. D. Co-precipitation of Radium with Barium and Strontium Sulfate and Its Impact on the Fate of Radium during Treatment of Produced Water from Unconventional Gas Extraction. *Environmental Science & Technology*, **2014**, 48(8), 4596-4603.

25. Zielinski, R. A.; Otton, J. K.; Budahn, J. R. Use of radium isotopes to determine the age and origin of radioactive barite at oil-field production sites. *Environmental Pollution*, **2001**, 113(3), 299-309.

26. Zhang, L.; Zhang, J.; Swarzenski, P. W.; Liu, Z. Radium Isotope Tracers to Evaluate Coastal Ocean Mixing and Residence Times. Handbook of Environmental Isotope Geochemistry. Springer Berlin Heidelberg, 2012, 331-343.

27. Chapman, E. C.; Capo, R. C.; Stewart, B. W.; Kirby, C. S.; Hammack, R. W.; Schroeder, K. T.; Edenborn, H. M. Geochemical and strontium isotope characterization of produced waters from Marcellus Shale natural gas extraction. *Environmental Science & Technology*, **2012**, 46(6), 3545-3553.

28. Bank, T. Uranium Geochemistry in the Marcellus Shale: Effects on Metal Mobilization. GSA Denver Annual Meeting, 2010.

29. Loveland, W. D.; Morrissey, D. J.; Seaborg, G. T. Modern nuclear chemistry. John Wiley & Sons, 2005.

30. Bateman, H. The solution of a system of differential equations occurring in the theory of radioactive transformations. Proc. *Cambridge Philos. Soc.*, **1910**, 15, 423-427.

31. McKee, B. A.; DeMaster, D. J.; Nittrouer, C. A. The use of $^{234}Th/^{238}U$ disequilibrium to examine the fate of particle-reactive species on the Yangtze continental shelf. *Earth and Planetary Science Letters*, **1984**, 68(3), 431-442.

32. Broecker, W. S.; Kaufman, A.; Trier, R. M. The residence time of thorium in surface sea water and its implications regarding the rate of reactive pollutants. *Earth and Planetary Science Letters*, **1973**, 20(1), 35-44.

33. Ivanovich, Miro, Russell S. Harmon, eds. Uranium series disequilibrium: applications to environmental problems. Oxford University Press, USA, 1982.

Chapter 3:

1. Vidic, R. D.; Brantley, S. L.; Vandenbossche, J. M.; Yoxtheimer, D.; Abad, J. D. Impact of shale gas development on regional water quality. *Science*, **2013**, 340 (6134), 1235009.

2. Barbot, E.; Vidic, N. S.; Gregory, K. B.; Vidic, R. D. Spatial and Temporal Correlation of Water Quality Parameters of Produced Waters from Devonian-Age Shale following Hydraulic Fracturing. *Environmental Science & Technology*, **2013**, 47 (6), 2562-2569.

3. Gregory, K. B.; Vidic, R. D.; Dzombak, D. A. Water management challenges associated with the production of shale gas by hydraulic fracturing. *Elements*, **2011**, 7 (3), 181-186.

4. Warner, N. R.; Christie, C. A.; Jackson, R. B.; Vengosh, A. Impacts of shale gas wastewater disposal on water quality in Western Pennsylvania. *Environmental Science & Technology*, 47 (20), **2013**, 11849-11857.

5. Rowan, E.; Engle, M.; Kirby, C.; Kraemer, T. Radium content of oil-and gas-field produced waters in the Northern Appalachian basin (USA)—Summary and discussion of data. U.S. Geological Survey Scientific Investigations Report 2011-5135, *U.S. Geological Survey*, **2011**.

6. Brantley, S. L; Dave Y.; Sina. A.; Paul G.; Radisav V.; Jon P.; Garth T. L.; Jorge A.; Cesar S. Water Resource Impacts during Unconventional Shale Gas Development: the Pennsylvania Experience. *International Journal of Coal Geology*, **2014**, 126, 140-156.

7. U.S. Environmental Protection Agency. Method 903.0. Alpha-Emitting Radium Isotopes in Drinking Water.

8. U.S. Environmental Protection Agency. Method 903.1. Radium-226 in Drinking Water Radon Emanation Technique.

9. U.S. Environmental Protection Agency. Method 901.1. Gamma Emitting Radionuclides in Drinking Water.

10. Nelson, A. W.; May, D.; Knight, A. W.; Eitrheim, E. S.; Mehrhoff, M.; Shannon, R.; Litman, R.; Schultz M. K. Matrix complications in the determination of radium levels in hydraulic-fracturing flowback water from Marcellus Shale. *Environmental Science & Technology Letters*, **2014**, 1 (3), 204-208.

11. Köhler, M.; W. Preube, B; Gleisberg, I. Schäfer; T. Heinrich; B. Knobus. Comparison of methods for the analysis of ^{226}Ra in water samples. *Applied Radiation and Isotopes*, **2002**, 56 (1), 387-392.

12. Harvey, David. Modern analytical chemistry. Boston: McGraw-Hill, 2000.

13. Lawrie, W. C.; Desmond, J. A.; Spence, D.; Anderson, S.; Edmondson, C. Determination of radium-226 in environmental and personal monitoring samples. *Applied Radiation and Isotopes*, **2000**, 53 (1), 133-137.

14. Gómez Escobar, V.; Vera Tomé, F; Lozano, J. C.; Martin Sanchez. A. Determination of ^{222}Rn and ^{226}Ra in aqueous samples using a low-level liquid scintillation counter. *Applied radiation and isotopes*, **1996**, 47 (9), 861-867.

15. Hancock, G. J;P. Martin. Determination of Ra in environmental samples by α-particle spectrometry. *International Journal of Radiation Applications and Instrumentation. Part A. Applied Radiation and Isotopes*, **1991**, 42 (1), 63-69.

16. Keisch, B.; Arnold, S. L. Sample preparation for low-level, alpha-particle spectrometry of radium-226. *Analytical Chemistry*, **1966**, 38 (13), 1969-1970.

17. Joannon, S.; Pin, C. Ultra-trace determination of ^{226}Ra in thermal waters by high sensitivity quadrupole ICP-mass spectrometry following selective extraction and concentration using radium-specific membrane disks. *Journal of Analytical Atomic Spectrometry*, **2001**, 16 (1), 32-36.

18. Horwitz, E. P.; Eietz, M. L.; Chiarizia, R. The application of novel extraction chromatographic materials to the characterization of radioactive waste solutions. *Journal of Radioanalytical and nuclear chemistry*, **1992**, 161 (2), 575-583.

19. Leermakers, M.; Gao, Y.; Navez, J.; Poffijn, A.; Croes, K.; Baeyens, W. Radium analysis by sector field ICP-MS in combination with the Diffusive Gradients in Thin Films (DGT) technique. *Journal of Analytical Atomic Spectrometry*, **2009**, 24 (8), 1115-1117.

20. Varga, Z. Preparation and characterization of manganese dioxide impregnated resin for radionuclide pre-Concentration. *Applied Radiation and Isotopes*, **2007**, 65 (10), 1095-1100.

21. Larivière, D.; Epov, V. N.; Reiber, K. M.; Cornett, R. J.; Evans, R. D. Micro-extraction procedures for the determination of Ra-226 in well waters by SF-ICP-MS. *Analytica Chimica Acta*, **2005**, 528 (2), 175-182.

22. Moldovan, M.; Krupp, Eva M.; Holliday, Alison E.; Donard, Olivier F. X. High resolution sector field ICP-MS and multicollector ICP-MS as tools for trace metal speciation in environmental studies: a review. *Journal of Analytical Atomic Spectrometry*, **2004**, 19 (7), 815-822.

23. Larivière, D., Epov, V. N.; Evans, R. D.; Cornett, R. J. Determination of radium-226 in environmental samples by inductively coupled plasma mass spectrometry after sequential selective extraction. *Journal of Analytical Atomic Spectrometry*, **2003**, 18 (4), 338-343.

24. Park, Chang J; Oh, Pil J.; Kim, Hae Y.; Lee, Dong S. Determination of ^{226}Ra in mineral waters by high-resolution Inductively Coupled Plasma Mass Spectrometry after sample preparation by cation exchange. *Journal of Analytical Atomic Spectrometry*, **1999**, 14 (2), 223-227.

25. Hsieh, Yu-Te; Gideon M. H. Precise measurement of ^{228}Ra/^{226}Ra ratios and Ra concentration in seawater samples by multi-collector ICP Mass Spectrometry. *Journal of Analytical Atomic Spectrometry*, **2011**, 27 (7), 1338-1346.

26. Ghaleb, B; Pons-Branchu, E; Deschamps, P. Improved method for radium extraction from environmental samples and its analysis by thermal ionization mass spectrometry. *Journal of Analytical Atomic Spectrometry*, **2004**, 19 (7), 906-910.

27. De Muynck, D.; Huelga-Suarez, G.; Van Heghe, L.; Degryse, P.; Vanhaecke, F. Systematic evaluation of a strontium-specific extraction chromatographic resin for obtaining a purified Sr fraction with quantitative recovery from complex and Ca-rich matrices. *Journal of Analytical Atomic Spectrometry*, **2009**, 24 (11), 1498-1510.

28. Blackburn, R.; Al-Masri, M. S. Determination of radium-226 in aqueous samples using liquid scintillation counting. *Analyst*, **1992**, 117 (12), 1949-1951.

29. Horrocks, Donald, ed. Applications of liquid scintillation counting. Academic Press, 1974.

30. Mizuike, A. Enrichment techniques for inorganic trace analysis, Springer-verlag, 1983.

31. Zhang, T.; Gregory, K.; Hammack R. W.; Vidic, R. D. Co-precipitation of Radium with Barium and Strontium Sulfate and Its Impact on the Fate of Radium during Treatment of Produced Water from Unconventional Gas Extraction. *Environmental Science & Technology*, **2014**, 48 (8), 4596-4603.

32. Decaillon, J-G.; Bickel, M.; Hill, C.; Alzitzoglou, T. Validation of methods for the determination of radium in waters and soil. *Applied radiation and isotopes*, **2004**, 61 (2), 409-413.

33. Blackburn, R.; Al-Masri. M. S. Determination of radon-222 and radium-226 in water samples by Cerenkov counting. *Analyst*, **1993**, 118 (7), 873-876.

34. Ayranov, M.; Krähenbühl, U; Schneider, U. Fast determination of uranium and radium in waters of variable composition. *Czechoslovak Journal of Physics*, **2006**, 56 (4), 219-227.

35. Dietz, M. L.; Chiarizia, R.; Horwitz, E. P.; Bartsch, R. A.; Talanov, V. Effect of crown ethers on the ion-exchange behavior of alkaline earth metals. Toward improved ion-exchange methods for the separation and preconcentration of radium. *Analytical chemistry*, **1997**, *69* (15), 3028-3037.

36. Horwitz, P. E.; Chiarizia, R.; Dietz, M. L. A novel strontium-selective extraction chromatographic resin. *Solvent extraction and ion exchange*, **1992**, *10* (2), 313-336.

37. Chabaux, F.; Othman, D. B.; Birck, J. L. A new Ra-Ba chromatographic separation and its application to Ra mass-spectrometric measurement in volcanic rocks. *Chemical Geology*, **1994**, 114 (3), 191-197.

38. Olivares, J. A.; Houk, R. S. Suppression of analyte signal by various concomitant salts in inductively coupled plasma mass spectrometry. *Analytical Chemistry*, **1986**, 58 (1), 20-25.

39. Tan, S. H.; Horlick, G. Background spectral features in inductively coupled plasma/mass spectrometry. *Applied Spectroscopy*, **1986**, *40* (4), 445-460.

40. Olesik, J. W. Elemental Analysis Using ICP-OES and ICP-MS. *Analytical Chemistry*, **1991**, 63 (1), 12A-21A.

41. Makishima, A.; Nakamura, E. Suppression of Matrix Effects in ICP-MS by High Power Operation of ICP: Application to Precise Determination of Rb, Sr, Y, Cs, Ba, REE, Pb, Th and U at ng g^{-1} Levels in Milligram Silicate Samples. *Geostandards Newsletter*, **1997**, 21 (2), 307-319.

Chapter 4:

1. Rowan, E.; Engle, M.; Kirby, C.; Kraemer, T. Radium content of oil-and gas-field produced waters in the Northern Appalachian basin (USA)—Summary and discussion of data. U.S. Geological Survey Scientific Investigations Report 2011-5135, U.S. Geological Survey 2011.

2. Vidic, R. D.; Brantley, S. L.; Vandenbossche, J. M., Yoxtheimer, D.; Abad, J. D. Impact of Shale Gas Development on Regional Water Quality, *Science*, **2013**, 340 (6134), 1235009.

3. Grundl, T.; Cape, M. Geochemical factors controlling radium activity in a sandstone aquifer. *Ground Water*, **2006**, 44 (4), 518-527.

4. U.S. Nuclear Regulatory Commission, Standards for protection against radiation – Appendix B – Radionuclide Table-Radium-226, 2013, 10 C.F.R, §20.

5. Gregory, K. B.; Vidic, R. D.; Dzombak, D. A. Water management challenges associated with the production of shale gas by hydraulic fracturing. *Elements*, **2011**, 7 (3), 181-186.

6. Gordon, L.; Rowley, K. Coprecipitation of radium with barium sulfate. *Analytical Chemistry*, **1957**, 29 (1), 34-37.

7. Barbot, E.; Vidic, N. S.; Gregory, K. B.; Vidic, R. D. Spatial and Temporal Correlation of Water Quality Parameters of Produced Waters from Devonian-Age Shale following Hydraulic Fracturing. *Environmental Science & Technology*, **2013**, 47 (6), 2562-2569.

8. Fakhru'l-Razi, A.; Pendashteh, A.; Abdullah, L. C.; Biak, D. R. A.; Madaeni, S. S.; Abidin, Z. Z. Review of technologies for oil and gas produced water treatment. *Journal of Hazardous Materials*, **2009**, 170 (2), 530-551.

9. Langmuir, D.; Riese, A. C. The thermodynamic properties of radium. *Geochimica et Cosmochimica Acta*, **1985**, 49 (7), 1593-1601.

10. Li, M. Removal of Divalent Cations from Marcellus Shale Flowback Water through Chemical Precipitation. Master Dissertation, University of Pittsburgh, Pittsburgh, PA, 2011.

11. Prieto, M. Thermodynamics of solid solution-aqueous solution systems. *Reviews in Mineralogy and Geochemistry*, **2009**, 70 (1), 47-85.

12. Doerner, H. A.; Hoskins, W. M. Co-precipitation of Radium and Barium Sulfates. *Journal of the American Chemical Society*, **1925**, 47 (3), 662-675.

13. Risthaus, P.; Bosbach, D.; Becker, U.; Putnis, A. Barite scale formation and dissolution at high ionic strength studied with atomic force microscopy. *Colloids and Surfaces A: Physicochemical and Engineering Aspects*, **2001**, 191 (3), 201-214.

14. Gordon, L.; Reimer, C. C.; Burtt, B. P. Distribution of strontium within barium sulfate precipitated from homogeneous solution. *Analytical Chemistry*, **1954**, 26 (5), 842-846.

15. Kudryavskii, Y. P.; Rakhimova, O. V. Coprecipitation of radium with barium sulfate from salt solutions. *Radiochemistry*, **2007**, 49 (5), 541-544.

16. Harvey, D. Modern Analytical Chemistry. Boston: McGraw-Hill, 2000.

17. Nichols, M. L.; Smith, E. C. Coprecipitation with Barium Sulfate. *The Journal of Physical Chemistry*, **1941**, 45 (3), 411-421.

18. Schneider, F.; Rieman III, W. The Mechanism of Coprecipitation of Anions by Barium Sulfate1. *Journal of the American Chemical Society*, **1937**, 59 (2), 354-357.

19. Blackburn, R.; Al-Masri, M. S. Determination of radium-226 in aqueous samples using liquid scintillation counting. *Analyst*, **1992**, 117 (12), 1949-1951.

20. Horrocks, D., Eds. *Applications of liquid scintillation counting*. Academic Press, 1974.

21. Johnston, A.; Martin, P. Rapid Analysis of ^{226}Ra in waters by Gamma-Ray Spectrometry. *Applied Radiation and Isotopes*, **1997**, 48 (5): 631-639.

22. Rosenberg, Y. O.; Metz V.; Ganor J. Co-precipitation of radium in high ionic strength systems: 1. Thermodynamic properties of the Na–Ra–Cl–SO_4–H_2O system – Estimating Pitzer parameters for $RaCl_2$. *Geochimica et Cosmochimica Acta*, **2011**, 75 (19): 5389-5402.

23. Bokern, D. G.; Hunter, K. A.; McGrath, K. M. Charged barite-aqueous solution interface: Surface potential and atomically resolved visualization. *Langmuir*, **2003**, 19 (24), 10019-10027.

24. Meissner, H. P.; Tester, J. W. Activity Coefficients of Strong Electrolytes in Aqueous Solutions. *Industrial & Engineering Chemistry Process Design and Development*, **1972**, 11 (1), 128-133.

25. Fernandez-Diaz, L.; Putnis, A.; Cumberbatch, T. J. Barite nucleation kinetics and the effect of additives. *European Journal of Mineralogy*, **1990**, 2 (4), 495-501.

26. Nielsen, A. E.; Toft, J. M. Electrolyte crystal growth kinetics. *Journal of Crystal Growth*, **1984**, 67 (2), 278-288.

27. He, S.; Oddo, J. E.; Tomson, M. B. The nucleation kinetics of barium sulfate in NaCl solutions up to 6 m and 90 °C. *Journal of colloid and interface science*, **1995**, 174 (2), 319-326.

28. Anderson, G. M.; Crerar, D. A. *Thermodynamics of geochemistry: The equilibrium model*. Vol. 588. New York: Oxford University Press, 1993.

29. Risthaus, P.; Bosbach, D.; Becker, U.; Putnis, A. Barite scale formation and dissolution at high ionic strength studied with atomic force microscopy. *Colloids and Surfaces A: Physicochemical and Engineering Aspects*, **2001**, 191 (3), 201-214.

30. Hang, J. Z.; Zhang, Y. F.; Shi, L. Y.; Feng, X. Electrokinetic properties of barite nanoparticles suspensions in different electrolyte media. *Journal of Materials Science*, **2007**, 42 (23): 9611-9616.

31. Zhu, C. Coprecipitation in the barite isostructural family: 1. binary mixing properties. *Geochimica et Cosmochimica Acta*, **2004**, 68 (16), 3327-3337.

32. He, C.; Li, M.; Liu, W.; Barbot, E.; Vidic, R. D. Kinetics and Equilibrium of barium and strontium sulfate formation in Marcellus Shale flowback water. *Journal of Environmental Engineering*, **2014**, 140 (5).

33. Ceccarello, S.; Black, S.; Read, D.; Hodson, M. E. Industrial radioactive barite scale: suppression of radium uptake by introduction of competing ions. *Minerals engineering*, **2004**, 17 (2), 323-330.

34. Brower, E. Synthesis of barite, celestite and barium-strontium sulfate solid solution crystals. *Geochimica et Cosmochimica Acta*, **1973**, 37 (1), 155-158.

35. Kargbo, D. M.; Wilhelm, R. G.; Campbell, D. J. Natural gas plays in the Marcellus shale: Challenges and potential opportunities. *Environmental Science & Technology*, **2010**, 44 (15), 5679-5684.

36. Maloney, K. O.; Yoxtheimer, D. A. Production and disposal of waste materials from gas and oil extraction from the Marcellus Shale play in Pennsylvania. *Environmental Practice*, **2012**, 14 (4), 278-287.

37. Lutz, B. D.; Lewis, A. N.; Doyle, M. W. Generation, transport, and disposal of wastewater associated with Marcellus Shale gas development. *Water Resources Research*, **2013**, 49 (2), 647-656.

38. Warner, N. R.; Christie, C. A.; Jackson, R. B.; Vengosh, A. Impacts of Shale Gas Wastewater Disposal on Water Quality in Western Pennsylvania. *Environmental Science & Technology*, **2013**, 47 (20), 11849-11857.

39. PA Department of Environmental Protection. Final Guidance Document on Radioactivity Monitoring at Solid Waste Processing and Disposal Facilities, 2004, available at http://www.elibrary.dep.state.pa.us/dsweb/Get/Document-48337/250-3100-001.pdf.

40. RPSEA. Produced water treatment for water recovery and salt production. 2012, 08122-36-final report.

41. Oakley, D.; Cullum, D. Advanced technology makes new use of age-old drilling fluid agent. Drilling Contractor, May/June 2007, from http://www.drillingcontractor.org/dcpi/dc-mayjune07/DC_May07_MISWACO.pdf

42. Smith, K. P.; Arnish, J. J.; Williams, G. P.; Blunt, D. L. Assessment of the disposal of radioactive petroleum industry waste in nonhazardous landfills using risk-based modeling. *Environmental science & technology*, **2003**, 37 (10), 2060-2066.

43. U.S. Environmental Protection Agency. Method 1311. Toxicity Characteristic Leaching Procedure, 1992, available at http://www.epa.gov/osw/hazard/testmethods/sw846/pdfs/1311.pdf.

Chapter 5:

1. Rowan, E.; Engle, M.; Kirby, C.; Kraemer, T. Radium content of oil-and gas-field produced waters in the Northern Appalachian basin (USA)—Summary and discussion of data. U.S. Geological Survey Scientific Investigations Report 2011-5135, U.S. Geological Survey, 2011.

2. Grundl, T.; Cape, M. Geochemical factors controlling radium activity in a sandstone aquifer. *Ground Water*, **2006**, 44 (4), 518-527.

3. Lutz, B. D.; Lewis, A. N.; Doyle, M. W. Generation, transport, and disposal of wastewater associated with Marcellus Shale gas development. *Water Resources Research*, **2013**, 49 (2), 647-656.

4. McCurdy, R. Underground Injection Wells For Produced Water Disposal. In Proceedings of the Technical Workshops for the Hydraulic Fracturing Study: Water Resources Management. EPA. 2011.

5. Warner, N. R.; Christie, C. A.; Jackson, R. B.; Vengosh, A. Impacts of shale gas wastewater disposal on water quality in western Pennsylvania. *Environmental Science & Technology*, **2013**, 47(20), 11849-11857.

6. Bibby, K. J.; Brantley, S. L.; Reible, D. D.; Linden, K. G.; Mouser, P. J.; Gregory, K. B.; Ellis, B. R.; Vidic, R. D. Suggested Reporting Parameters for Investigations of Wastewater from Unconventional Shale Gas Extraction. *Environmental Science & Technology*, **2013**, 47(23), 13220-13221.

7. Tetra Tech. Evaluation of high TDS Concentrations in the Monongahela River Rep., 126pp., Tetra Tech, Inc., Pittsburgh, PA.

8. Vidic, R. D.; Brantley, S. L.; Vandenbossche, J. M.; Yoxtheimer, D.; Abad, J. D. Impact of shale gas development on regional water quality. *Science*, **2013**, 340 (6134), 1235009.

9. Tessier, A.; Campbell, P. G.; Bisson, M. Sequential extraction procedure for the speciation of particulate trace metals. *Analytical Chemistry*, **1979**, 51 (7), 844-851.

10. U.S. Environmental Protection Agency. Method 1311. Toxicity Characteristic Leaching Procedure, 1992, available at http://www.epa.gov/osw/hazard/testmethods/sw846/pdfs/1311.pdf.

11. U.S. Environmental Protection Agency. Method 901.1. Gamma Emitting Radionuclides in Drinking Water, available at http://www.epa.gov/ogwdw000/radionuclides/training/resources/EPA_Method_901.1.pdf

12. Nelson, A. W.; May, D.; Knight, A. W.; Eitrheim, E. S.; Mehrhoff, M.; Shannon, R.; Litman, R.; Schultz M. K. Matrix complications in the determination of radium levels in hydraulic-fracturing

flowback water from Marcellus Shale. *Environmental Science & Technology Letters*, **2014**, 1(3), 204-208.

13. Barbot, E.; Vidic, N. S.; Gregory, K. B.; Vidic, R. D. Spatial and temporal correlation of water quality parameters of produced waters from devonian-age shale following hydraulic fracturing. *Environmental science & technology*, **2013**, 47 (6), 2562-2569.

14. Murali Mohan, A.; Hartsock, A.; Bibby, K. J.; Hammack, R. W.; Vidic, R. D.; Gregory, K. B. Microbial community changes in hydraulic fracturing fluids and produced water from shale gas extraction. *Environmental Science & Technology*, **2013**, 47 (22), 13141-13150.

15. Zhang, T.; Gregory, K.; Hammack, R. W.; Vidic, R. D. Co-precipitation of Radium with Barium and Strontium Sulfate and Its Impact on the Fate of Radium during Treatment of Produced Water from Unconventional Gas Extraction. *Environmental Science & Technology*, **2014**, 48 (8), 4596-4603.

16. He, C.; Zhang, T.; Zheng, X.; Li, Y.; Vidic, R. D. Management of Marcellus Shale Produced Water in Pennsylvania: A Review of Current Strategies and Perspectives. *Energy Technology*, **2014**.

17. Chau, N. D.; Chruściel, E. Leaching of technologically enhanced naturally occurring radioactive materials. *Applied Radiation and Isotopes*, **2007**, 65 (8), 968-974.

18. Nirdosh, I.; Trembley, W. B.; Johnson, C. R. Adsorption-desorption studies on the ^{226}Ra-hydrated metal oxide systems. *Hydrometallurgy*, **1990**, 24 (2), 237-248.

19. U.S. Environmental Protection Agency. Solid Wastes- Identification and Listing of Hazardous Waste. 2012, 40 C.F.R, §261, Subpart-C.

20. Phillips, E. J., Landa, E. R., Kraemer, T., Zielinski, R. Sulfate-reducing bacteria release barium and radium from naturally occurring radioactive material in oil-field barite. *Geomicrobiology Journal*, **2001**, 18 (2), 167-182.

21. U.S. Nuclear Regulatory Commission. Standards for protection against radiation – Appendix B – Radionuclide Table-Radium-226, 2013, 10 C.F.R, §20.

22. Renou, S., Givaudan, J. G., Poulain, S., Dirassouyan, F., Moulin, P. Landfill leachate treatment: Review and opportunity. *Journal of Hazardous Materials*, **2008**, 150(3), 468-493.

23. Subramanian, K. S., Sastri, V. S. Reverse osmosis separation of radium from dilute aqueous solutions. *Separation Science and Technology*, 1980, 15(2), 145-152.

24. U.S. Environmental Protection Agency. A System's Guide to the Management of Radioactive Residual from Drinking Water Treatment Technologies. EPA 816-F-06-012. August, 2006.

25. Research Partnership to Secure Energy for America (RPSEA). Produced Water Treatment for Water Recovery and Salt Production; RPSEA: Sugar Land, TX, 2012; 08122-36-Final Report.

26. U.S. Environmental Protection Agency. Storage, Treatment, Transportation, and Disposal of Mixed Waste. 2001, 40 C.F.R, §266.

27. PA Department of Environmental Protection. Final Guidance Document on Radioactivity Monitoring at Solid Waste Processing and Disposal Facilities, 2004, available at http://www.elibrary.dep.state.pa.us/dsweb/Get/Document-48337/250-3100-001.pdf.

Chapter 6:

1. National Council on Radiation Protection and Measurements. Sources and magnitude of occupational and public exposures from nuclear medicine procedure. Bethesda, MD: National Council on Radiation Protection and Measurement; NCRP Report 124, 1996.

2. U.S. Department of Energy. Radiation Protection of the Public and the Environment. DOE Order 5400.5. U.S. Department of Energy, Washington, D.C. February, 1990.

3. Pennsylvania Department of Environmental Protection. Technologically Enhanced Naturally Occurring Radioactive Materials (TENORM) Study Report. Perma-Fix Environmental Services. January, 2015; available at: http://www.elibrary.dep.state.pa.us/dsweb/Get/Document-105822/PA-DEP-TENORM-Study_Report_Rev._0_01-15-2015.pdf

4. Brooks, A. L. Chromosome damage in liver cells from low dose rate alpha, beta, and gamma irradiation: Derivation of RBE. *Science*, **1975**, 190 (4219), 1090-1092.

5. PA Department of Environmental Protection. Final Guidance Document on Radioactivity Monitoring at Solid Waste Processing and Disposal Facilities, 2004, available at http://www.elibrary.dep.state.pa.us/dsweb/Get/Document-48337/250-3100-001.pdf.

6. Yu, C.; Zielen, A. J.; Cheng, J. J.; LePoire, D. J.; Gnanapragasam, E.; Kamboj, S. A.; Wallo, A. I.; Williams, W. A.; Peterson, H. User's manual for RESRAD version 6 (No. ANL/EAD-4). Argonne National Lab., IL (US), 2001, available at http://www.ipd.anl.gov/anlpubs/2001/07/40176.pdf.

7. USA Nuclear Regulatory Commission. Part 20: Standards for Protection Against Radiation, 1995.

8. U.S. Department of Energy. Radiation Protection of the Public and the Environment. DOE Order 5400.5. U.S. Department of Energy, Washington, D.C. February, 1990.

9. Rowan, E.; Engle, M.; Kirby, C.; Kraemer, T. Radium content of oil-and gas-field produced waters in the Northern Appalachian basin (USA)—Summary and discussion of data. U.S. Geological Survey Scientific Investigations Report 2011-5135, U.S. Geological Survey, 2011.

10. International Commission on Radiological Protection. Recommendations of the International Commission on Radiological Protection, Publication 60. 1991. Pergamon Press: Oxford, United Kingdom.

11. Kocher, D. C., Hoffman, F. O. Regulating environmental carcinogens: where do we draw the line?. *Environmental Science & Technology*, **1991**, 25 (12), 1986-1989.

12. Smith, K. P.; Arnish, J. J.; Williams, G. P.; Blunt, D. L. Assessment of the disposal of radioactive petroleum industry waste in nonhazardous landfills using risk-based modeling. *Environmental Science & Technology*, **2003**, 37 (10), 2060-2066.

13. Bank, T. Uranium Geochemistry in the Marcellus Shale: Effects on Metal Mobilization. GSA Denver Annual Meeting, 2010.

14. White, G. J., Rood, A. S. Radon emanation from NORM-contaminated pipe scale and soil at petroleum industry sites. *Journal of environmental radioactivity*, **2001**, 54(3), 401-413.

15. Greeman, D. J., Rose, A. W. Factors controlling the emanation of radon and thoron in soils of the eastern USA. *Chemical Geology*, **1996**, 129(1), 1-14.

16. Zhang, T.; Gregory, K.; Hammack, R. W.; Vidic, R. D. Co-precipitation of Radium with Barium and Strontium Sulfate and Its Impact on the Fate of Radium during Treatment of Produced Water from Unconventional Gas Extraction. *Environmental Science & Technology*, **2014**, 48(8), 4596-4603.

Appendix B:

1. Blackburn, R.; Al-Masri, M. S. Determination of radium-226 in aqueous samples using liquid scintillation counting. *Analyst*, **1992**, 117 (12), 1949-1951.

2. U.S. Environmental Protection Agency. Method 903.0. Alpha-Emitting Radium Isotopes in Drinking Water.

3. Nelson, A. W.; May, D.; Knight, A. W.; Eitrheim, E. S.; Mehrhoff, M.; Shannon, R.; Litman, R.; Schultz M. K. Matrix complications in the determination of radium levels in hydraulic-fracturing flowback water from Marcellus Shale. *Environmental Science & Technology Letters*, **2014**, 1 (3), 204-208.

4. Johnston, A.; Martin, P. Rapid analysis of ^{226}Ra in waters by γ-ray spectrometry. *Applied radiation and isotopes*, **1997**, 48 (5), 631-638.

Appendix C:

1. Gordon, L.; Rowley, K. Coprecipitation of radium with barium sulfate. *Analytical Chemistry*, **1957,** 29 (1), 34-37.

2. Langmuir, D.; Riese, A. C. The thermodynamic properties of radium. *Geochimica et Cosmochimica Acta*, **1985**, 49 (7), 1593-1601.

3. Doerner, H. A.; Hoskins, W. M. Co-precipitation of Radium and Barium Sulfates. *Journal of the American Chemical Society*, **1925**, 47 (3), 662-675.

4. Ganguly, J., Saxena, S. K. *Mixtures and Mineral Reactions*. Berlin: Springer-Verlag, 1987.

5. Anderson, G. M., Crerar, D. A. *Thermodynamics of geochemistry: The equilibrium model*. Vol. 588. New York: Oxford University Press, 1993.

6. Zhu, C. Coprecipitation in the barite isostructural family: 1. binary mixing properties. *Geochimica et Cosmochimica Acta*, **2004**, 68 (16), 3327-3337.

7. Ceccarello, S.; Black, S.; Read, D.; Hodson, M. E. Industrial radioactive barite scale: suppression of radium uptake by introduction of competing ions. *Minerals engineering*, **2004**, 17 (2), 323-330.

8. Aniceto, J. P.; Cardoso, S. P.; Faria, T. L.; Lito, P. F.; Silva, C. M. Modeling ion exchange equilibrium: Analysis of exchanger phase non-ideality. *Desalination*, **2012**, 290, 43-53.

9. Rosenberg, Y. O.; Metz V.; Ganor J. Co-precipitation of radium in high ionic strength systems: 1. Thermodynamic properties of the Na–Ra–Cl–SO_4–H_2O system – Estimating Pitzer parameters for $RaCl_2$. *Geochimica et Cosmochimica Acta*, **2011**, 75 (19): 5389-5402.

10. Burkin, A. R. Chemical hydrometallurgy: theory and principles (Vol. 1). World Scientific, 2001.

11. Pitzer, K. S. Thermodynamics of electrolytes. I. Theoretical basis and general equations. *The Journal of Physical Chemistry*, **1973**, 77 (2), 268-277.

12. He, C.; Li, M.; Liu, W.; Barbot, E.; Vidic, R. D. Kinetics and Equilibrium of barium and strontium sulfate formation in Marcellus Shale flowback water. *Journal of Environmental Engineering*, **2014**, 14 (5).